APPENDIX IV

Groundwater Concentrations
and
Drinking Water Doses with Uncertainty

Commercial Low-Level Radioactive Waste Disposal Site

Richland, Washington

K-Spar Inc. *Scientific Consulting*
493 N 4154 E, Rigby, Idaho 83442 (208) 745-1288 email asr@srv.net

FINAL REPORT

Groundwater Concentrations and Drinking Water Doses with Uncertainty for the U.S. Ecology Low-Level Radioactive Waste Disposal Facility, Richland Washington

Date March 2003
Revised February, 2004

Arthur S. Rood

Submitted to Washington State Department of Health
in partial fulfillment of contract No. N10996

K-Spar Inc. ***Scientific Consulting***
493 N 4154 E, Rigby, Idaho 83442 (208) 745-1288 email asr@srv.net

EXECUTIVE SUMMARY

US Ecology Incorporated operates a low-level radioactive waste disposal facility on leased land from the U.S. Department of Energy's Hanford Reservation located near Richland Washington. The Washington State Department of Health (WDOH) is currently developing an Environmental Impact Statement (EIS) for the site. Part of the EIS involves the evaluation of impacts to groundwater of various closure options for the site. A Draft Environmental Impact Statement (DEIS) was completed in 2000 which included an assessment of the groundwater pathway. Recent environmental monitoring data have detected radionuclides in the subsurface below the facility. Because of the way the original transport model was constructed, evaluation of radionuclide concentrations in the unsaturated zone was not possible. Additional information regarding waste disposal history, the effects of open trenches on water infiltration, and evolution of ideas regarding the site conceptual model led WDOH to revisit the groundwater assessment performed for the DEIS.

A new model for radionuclide transport in the unsaturated zone was constructed that incorporated effects of transient infiltration and historical waste disposal rates. Radionuclide inventories were re-evaluated and important radionuclides identified through a two-phase screening approach. Fifteen radionuclides were identified as being important in terms of their potential for groundwater ingestion dose: C-14, Cl-36, H-3, I-129, Pu-238,-239,-240,-242, Ra-226, Tc-99, Th-230, Th-232, U-234, U-235, and U-238. Nickel-63 and Sr-90 were removed from consideration during the screening process, but were retained for model calibration because these radionuclides were detected in measurable quantities in the unsaturated zone beneath trench 5. Assumptions regarding partition coefficients and cover longevity were revisited and modified accordingly.

Radionuclide release rates from the trenches and their transport in the unsaturated zone were calibrated to measured concentrations taken in boreholes beneath trench 5. Measured radionuclide concentration profiles of relatively immobile radionuclides beneath trench 5 could not be explained by dissolved-phase transport, and a colloidal transport model was proposed as an alternative. The colloidal transport model assumes a fraction of the radionuclide inventory (hereafter referred to as the mobile fraction) moves by colloidal transport. We assumed colloidal transport to be represented by a dissolved-phase transport model with no sorption; therefore, radionuclides move with the velocity of water. Calibrated radionuclide mobile fractions ranged from 6.2×10^{-4} to 4.6×10^{-6} for Ni-63, U-238, Sr-90, and Pu-239 and 0.047 for Tc-99. The higher mobile fraction value for Tc-99 reflects its dissolved-phase mobility. For Tc-99, it was necessary to limit the radionuclide release rate from the trenches so that model-predicted radionuclide inventories below the trenches matched inventories extrapolated from the borehole data. Conservative estimates of drinking water dose from the mobile fractions of Ni-63 and Sr-90 were less than 4 mrem yr^{-1}. Therefore, no further evaluation of these radionuclides was warranted beyond model calibration.

The revised transport model also incorporated a cover lifetime of 500 years and partition coefficients that reflect sorption only on the fine material in the rock matrix. Aquifer concentrations and drinking water ingestion doses were calculated as a function of time for five cover design/closure option scenarios. Three cover designs were included in the analysis; a site soils cover which had an infiltration to 20 mm yr^{-1}, an enhanced cover that limited infiltration to

0.5 mm yr^{-1}, and the US Ecology proposed cover that limited infiltration to 2 mm yr^{-1}. Background infiltration was assumed to be 5 mm yr^{-1} after the cover failed.

A parametric uncertainty analysis was performed to evaluate the variability in the model-predicted concentrations and doses. Monte Carlo sampling coupled with simple random sampling was used to propagate sampled parameters values through the transport model yielding distributions of predicted groundwater concentrations and doses at specified output times. The design-based infiltration rates of the covers, calibrated mobile release fractions, exposure scenario parameters (drinking water ingestion rate), and dose conversion factors were not treated stochastically, rather, these parameters were fixed at their deterministic value. Additionally, the fractional release rates from waste to soil were conservatively assumed to be instantaneous because data was lacking on waste form and the corresponding release rate, and the lifetime of waste containment vessels. Parameter distributions were based on analyst interpretation of relevant data. When relevant field data were lacking, a distribution was assumed. Although Monte Carlo methods were used to analyze parametric uncertainty, the analysis was not a probabilistic risk assessment. The output distribution represents the variability in the calculated concentrations and doses resulting from variability in the input parameters that were considered stochastically. A parametric uncertainty analysis makes no assessment of accuracy of the model or model bias. Only by comparing model predictions to measured values can the accuracy of the model be assessed.

The parametric uncertainty analysis presented here was not intended to be comprehensive because time and resources limited what could be accomplished in an uncertainty analysis for this project. Nevertheless, the analysis lays the framework for uncertainty analysis that can be refined later with revised parameter distributions and assumptions.

Groundwater concentrations were both higher and lower compared to results in the original DEIS. Higher concentrations were attributed to a) enhanced infiltration through the site during active disposal, b) an assumed cover failure time 500 years after placement, and c) uranium solubility. Lower concentrations were attributed to lower leaching rate constants for Tc-99 and Cl-36 based on model calibration below trench 5. Deterministic drinking water doses were dominated by four of the five DEIS radionuclides (I-129, Tc-99, U-235, and U-238) plus H-3, C-14, and the mobile fractions of U-234, U-238, and Pu-239. Total deterministic drinking water doses for the enhanced cover were less than 5 mrem yr^{-1} 100 years after the start of facility operations in the year1965. Doses were1 mrem yr^{-1} between 100 and 1,000 years after 1965, and around 2 mrem yr^{-1} 10,000 years after 1965. The mobile fraction of U-238 dominated the dose 1,000 years after closure, while I-129 and C-14 dominated the doses 10,000 years after closure. Tritium dominated the dose in the 0- to100-year time frame. No credit was taken for dilution of I-129 in the iodine pool in drinking water or the total diet. Doses for the enhanced and proposed cover *while* the cover remained intact were about one order of magnitude lower that those of the site soils cover.

Parametric uncertainty analysis was performed for the enhanced cover only for closure in 2056. The range of the distribution of total drinking water dose (2.5% to 97.5%) was roughly a factor of 22 at times less than 100 years after the start of facility operations (1965), and increases to over three orders-of-magnitude for times greater than 100 years. Results are summarized in terms of the percentiles of the output distribution for selected times in Table ES-1

Table ES-1 Summary of Distributions of Predicted Total Drinking Water Dose at the Receptor Well for the Enhanced Cover for Closure in year 2056

	Year of dose (years from start of simulation in 1965)				
	Year 2,025 (60 years)	Year 2,465 (500 years)	Year 2,965 (1,000 years)	Year 4,465 (2,500 years)	Year 9,965 (8,000 years)
Percentile	Dose (mrem)	Dose (mrem)	Dose (mrem)	Dose (mrem)	Dose (mrem)
2.5th	0.77	0.0091	0.045	0.018	0.0057
5th	1.0	0.012	0.066	0.024	0.0095
25th	2.2	0.026	0.27	0.056	0.052
50th	3.6	0.043	0.57	0.10	0.55
75th	6.4	0.077	1.2	0.25	2.6
95th	14	0.18	3.6	2.8	13
97.5th	17	0.22	4.6	6.8	28

The uncertainty analysis provides a measure of the precision of the transport model and should not be interpreted as the probability of any real or actual exposure occurring. It simply provides a measure of the variability in the predicted quantity given the limitations and assumptions inherent in the model, and the interpretation of relevant data that formed the basis for model parameter values.

Overall, the assessment integrates natural processes that govern the transport radionuclides in the subsurface, with known waste disposal histories, past operational practices, and future closure plans of the site into a transport model that estimates both past and future radionuclide migration from the US Ecology low-level radioactive waste site. Conservative assumptions were made where uncertainty exists and therefore, these results should be viewed as conservative estimates of radionuclide concentrations and drinking water doses.

CONTENTS

FIGURES

TABLES

INTRODUCTION

US Ecology Incorporated operates a low-level radioactive waste disposal facility on leased land from the U.S. Department of Energy's Hanford Reservation located near Richland Washington. The Washington State Department of Health (WDOH) is currently developing an Environmental Impact Statement (EIS) for the site. Part of the EIS involves the evaluation of impacts to groundwater of various closure options for the site. A Draft Environmental Impact Statement (DEIS) was completed in 2000. The groundwater pathway analysis was documented in Dunkelman (2000). Radionuclide transport in the unsaturated zone and aquifer was evaluated in a separate document (Rood 2000a) which was later integrated with the DEIS. Groundwater concentrations were calculated for a single cover design and aquifer concentration included estimates of parametric uncertainty. A later document (Rood 2000b) expanded the deterministic analysis to three cover designs. Recent environmental monitoring data (US Ecology 1999) have detected radionuclides in the subsurface. Because of the way the original transport model in Rood (2000a) and Rood (2000b) was constructed, evaluation of radionuclide concentrations in the unsaturated zone was not possible. Additional information regarding waste disposal history, the effects of open trenches on water infiltration, and evolution of ideas regarding the site conceptual model led WDOH to revisit the groundwater assessment performed for the DEIS.

This report documents a reassessment of groundwater concentration estimates including an uncertainty analysis, for radionuclides disposed at the US Ecology low-level radioactive waste disposal facility. This assessment includes an evaluation of three cover designs and several closure dates. The simulations incorporate recent field data taken at the site, along with a conceptual model that includes both historical and future waste disposals. The primary objective of this work was to provide estimates of groundwater concentrations as a function of time for radionuclides disposed at the US Ecology site and to reconcile radionuclide measurements in the unsaturated zone with model estimates. These estimates were intended to error on the side of conservatism. The transport models used in this assessment are relatively simple, but incorporate the major processes that govern the release and transport of radionuclides from the disposal trenches to the aquifer. Estimates of radiation dose from the consumption of drinking water were also made. This work was funded by the WDOH under contract number N08344.

FACILITY DESCRIPTION AND HISTORY

This section provides a brief description of the US Ecology site, its historical operations, and the geology, hydrology, and climate of the Hanford area. It focuses only on the salient features that are pertinent to this assessment. A more detailed description can be found in Kincaid et al. (1998), and US Ecology (1994).

The US Ecology site is located on the Hanford Reservation in Eastern Washington State near the city of Richland. The site is located between the Department of Energy (DOE) 200 Area West and 200 Area East facilities, near the southwest corner of 200 Area East (Figure1). The US Ecology disposal site began operation in 1965 with the opening of Trench Number 1 (Figure 2, Table 1) followed by 19 other trenches. The early trenches were left open as they were filled with soil being placed over the trench as a new trench was excavated to receive waste shipments. A separate trench was set aside to receive chemical waste. Three yet-to-be-dug trenches have been

proposed to receive future waste (Trenches 17, 19, and 20) and three trenches are currently open (12-A, 15, 18).

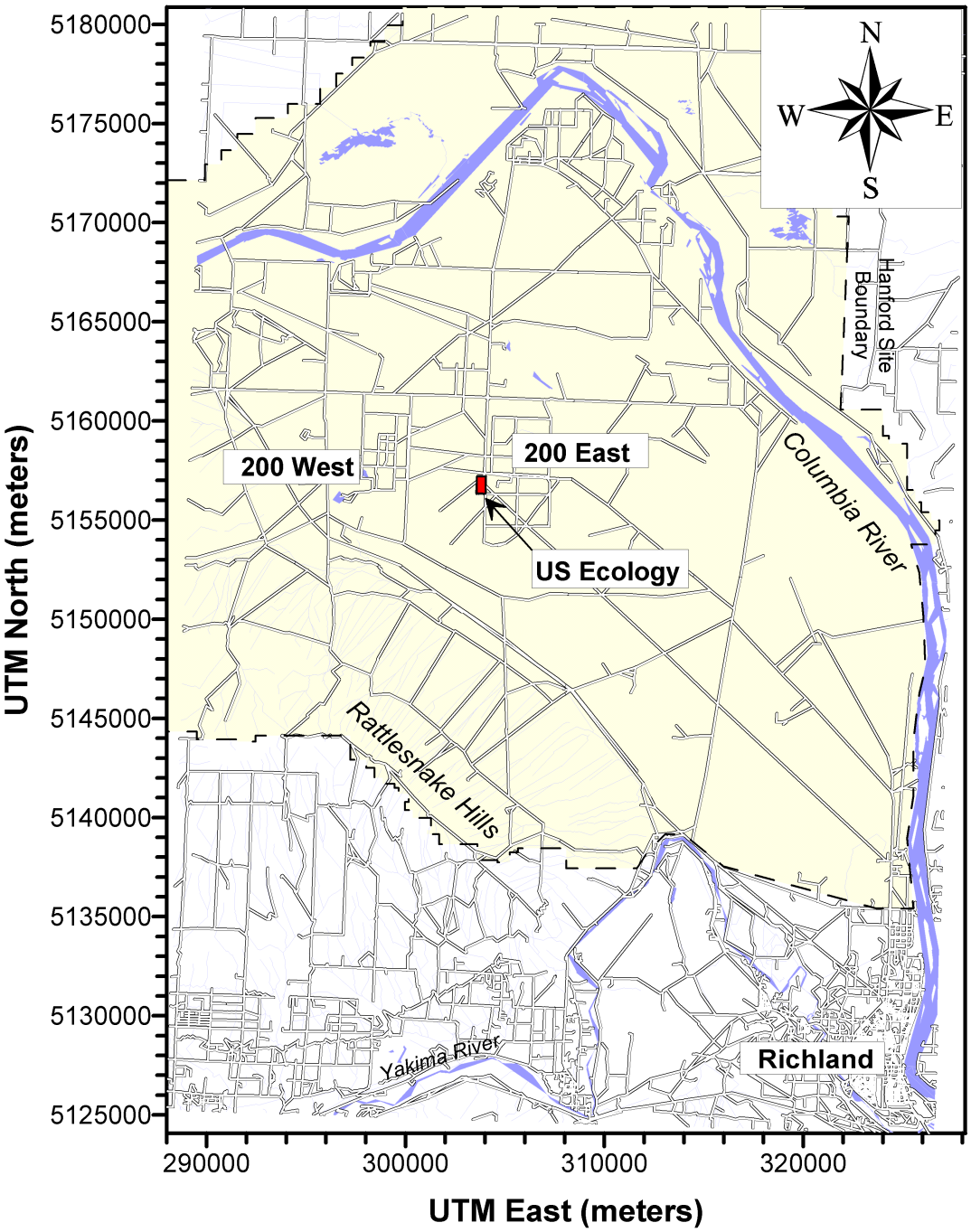

Figure 1. Location of the US Ecology site within the Hanford Reservation in eastern Washington State. The 200 East and 200 West area, the Columbia and Yakima Rivers, and north Richland are also shown. Groundwater flow is generally to the north and east from the Rattlesnake Hills toward the Columbia River. The coordinate system used in the map is the Universal Transverse Mercator (UTM).

In 1999, a comprehensive facility investigation was completed for the US Ecology site (US Ecology 1999). Data obtained from this investigation included concentrations of radionuclides in soil borings taken below Trench 5. These measurements were used to calibrate the unsaturated transport model.

Geology, Hydrology, and Climate

The Hanford Site lies within the Pasco Basin, a structural depression that has accumulated a relatively thick sequence of fluvial, lacustrine, and glacio-fluvial sediments (Kincaid et al. 1998). Underlying the fluvial and lacustrine sediments of the Ringold formation and the glacio-fluvial Hanford formation, are a thick sequence of basalts known as the Columbia River Basalt group. Together, the Hanford and Ringold formation host an unconfined aquifer system. The unconfined system is greater than 61 m in some locations, but its thickness decreases near the flanks of basalt ridges that lie to the west of the site. Groundwater flow is generally from recharge areas in the west toward the Columbia River to the north and east. Transmissivity in the aquifer varies from ~100 m^2 d^{-1} up to 92,900 m^2 d^{-1} (Figure 4.18 in Kincaid et al. 1998). Near the US Ecology site, transmissivity ranged from ~465 to 12,500 m^2 d^{-1}. The unconfined aquifer system is the point of compliance for this assessment.

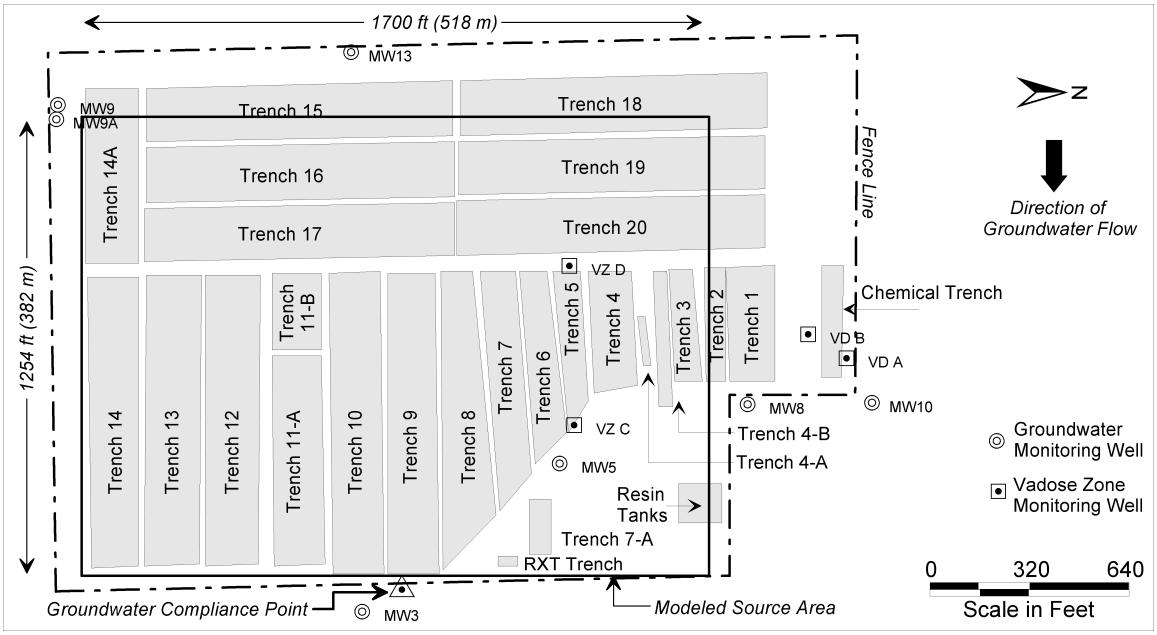

Figure 2. Map of US Ecology facility showing trench locations, property boundaries, monitoring wells points, modeled source area, and the groundwater compliance point (redrawn from Figure 1 in US Ecology 1999).

Soils in the 200 Area of Hanford are predominately course-textured alluvial sands, covered by a variable thick mantel of wind-borne fine sands (Gee at al. 1992). Gravel contents range from 2 to 43% (Kincaid et al. 1998). The soils have potentially high infiltration capacities. The 79-year annual average precipitation at the Hanford site is 16.2 cm yr^{-1} (Gee et al. 1992). Winters are

typically cool and wet while hot and dry conditions persist during summer months. Consequently, most of the water available for recharge comes from winter precipitation when evapotranspiration rates are low. Annual recharge rates range from near zero to about 100-mm yr^{-1} (Gee et al. 1992) and are highly dependent on soil type and vegetative cover. Recent estimates of infiltration for course sediments on a vegetation-free surface are around 7.5 cm yr^{-1} and 0.5 cm yr^{-1} for a vegetated surface (Kincaid et al. 1998).

Table 1. Trench Open and Close Dates for the US Ecology Site (Data provided by WDOH)

Trench Identification	Open Date	Close Date
1	Sep-65	Sep-66
2	Aug-66	Nov-71
3	Dec-71	Mar-75
4	Apr-75	Aug-78
4-A	Apr-82	Jun-82
4-B	Jul-84	Aug-85
5	Apr-78	Sep-79
6	Aug-79	Jun-80
7	Oct-82	Oct-83
7-A	Jun-85	Jul-85
8	May-80	May-81
9	Sep-83	Nov-84
10	May-81	Dec-82
11-A	Oct-84	Jan-86
11-B	Oct-84	Open
12-A	Aug-99	Sep-99
13	Jul-85	Mar-95
14	Feb-87	Open
15	Proposed	Proposed
16	Jan-92	Jun-99
17	Proposed	Proposed
18	Nov-95	Open
19	Proposed	Proposed
20	Proposed	Proposed

RADIONUCLIDE INVENTORIES

Radionuclide inventories were provided by WDOH in two Microsoft Excel® spreadsheets and one Microsoft Word® Document. The primary source term data were obtained from the spreadsheet "sourceterm.xls" and included data on 26 radionuclides plus naturally occurring uranium, naturally occurring thorium, and depleted uranium for disposals from 1965 to 2002. Disposals during the 1965-2002 were segregated into 12 time periods; 1965-1981, 1982-1987, 1988-1993, 1994, 1995, 1996, 1997, 1998, 1999, 2000, 2001, and 2002. These values were supplemented with data from the Microsoft Word® file, "potential additional isotopes for gw modeling.doc". Nineteen radionuclides were listed in this document, but some were already

included in "sourceterm.xls". Additional isotopes were listed by total disposal inventories from 1965 to 2002 and were not segregated into annual disposal amounts. The future projected annual disposals for 21 radionuclides were provided in the spreadsheet "Source Term projections for Art 101302.xls".

Table 2 shows the estimated radionuclide inventory disposed of in the US Ecology site for the time periods, 1965-2002, 1965-2056, and 1965-2215. The values are not decay corrected, but represent the total activity disposed for these time periods. Additionally, values have been rounded to two significant digits, so the sum of the proposed and 1965-2002 inventory may not exactly add up to the values listed in Total column in Table 2. The time periods represent the three closure options considered by WDOH; that is, closure in year 2003, closure in year 2056, and closure in year 2215. Time-variable disposal rates are presented in a later section and were considered in the detailed modeling for those radionuclides that were not removed from consideration through a screening process that is explained in the next section.

Inventory values for the uranium isotopes (U-238, U-235, and U-234) from 1965 to 2002 were later revised by WDOH[1] from the original values provided in the spreadsheet "sourceterm.xls". Originally, uranium was segregated into the three primary isotopes (U-234, U-235, and U-238) plus natural uranium, and depleted uranium. The revised uranium numbers provided in the spreadsheet, "Recommended uranium values for USE.xls" were only segregated by uranium isotope. Estimates of future disposals of U-235 and U-234 were also revised from the original values provided by WDOH in the spreadsheet "sourceterm.xls" because the U-235 activity exceeded that of U-238 and no U-234 values were provided. The projected activity disposal rates for U-235 and U-234 were calculated by multiplying the U-238 proposed activity disposal rate by the ratio of the 1965–2002 activity disposed for U-235 and U-234 respectively to the corresponding U-238 value.

Table 2. Radioactive Inventories for the U.S. Ecology Low-Level Waste Site (Data provided by WDOH)

Radionuclide	Inventory 1965-2002 (mCi)[a]	Additional Isotopes 1965-2002 (mCi)[b]	Proposed (mCi yr^{-1})[c]	Total 1965-2056 (mCi)	Total 1965-2215 (mCi)
Ac-227	6.01E+00			6.01E+00	6.01E+00
Am-241	4.64E+05		5.59E+01	4.67E+05	4.76E+05
Ba-133		6.68E+03		6.68E+03	6.68E+03
Bi-207		1.17E+03		1.17E+03	1.17E+03
C-14	3.97E+06		2.07E+04	5.09E+06	8.37E+06
Cd-113		2.94E+03		2.94E+03	2.94E+03
Cl-36	3.12E+03		2.05E+00	3.23E+03	3.55E+03
Cm-244		2.08E+05		2.08E+05	2.08E+05
Co-60	1.53E+09			1.53E+09	1.53E+09
Cs-134		1.59E+07		1.59E+07	1.59E+07
Cs-137		1.21E+08		1.21E+08	1.21E+08
Eu-152		2.52E+06		2.52E+06	2.52E+06

[1] Revised uranium inventory numbers were provided by Drew Thatcher (WDOH), January 7, 2003 in the spreadsheet, "Recommended uranium values for USE.xls".

Table 2. Radioactive Inventories for the U.S. Ecology Low-Level Waste Site (Data provided by WDOH)

Radionuclide	Inventory 1965-2002 (mCi)[a]	Additional Isotopes 1965-2002 (mCi)[b]	Proposed (mCi yr^{-1})[c]	Total 1965-2056 (mCi)	Total 1965-2215 (mCi)
Eu-154		2.14E+06		2.14E+06	2.14E+06
Eu-155		4.48E+04		4.48E+04	4.48E+04
Fe-55		2.78E+08		2.78E+08	2.78E+08
H-3	7.99E+08		1.12E+06	8.60E+08	1.04E+09
Hf-182		1.56E+03		1.56E+03	1.56E+03
I-129	5.63E+03		6.35E+00	5.98E+03	6.99E+03
K-40	4.76E+03			4.76E+03	4.76E+03
Kr-85		5.89E+07		5.89E+07	5.89E+07
Na-22		3.47E+04		3.47E+04	3.47E+04
Nb-94	7.09E+03		5.95E+01	1.03E+04	1.98E+04
Ni-59	1.17E+06		1.94E+04	2.22E+06	5.30E+06
Ni-59 (activated metal)	3.04E+02			3.04E+02	3.04E+02
Ni-63	1.92E+08		3.22E+06	3.66E+08	8.78E+08
Ni-63 (activated metal)	5.40E+06			5.40E+06	5.40E+06
Pa-231	1.31E+00			1.31E+00	1.31E+00
Pb-210	1.92E+04			1.92E+04	1.92E+04
Pm-147		2.94E+08		2.94E+08	2.94E+08
Pu-238	1.06E+07		1.41E+02	1.06E+07	1.06E+07
Pu-239	4.50E+06		1.54E+02	4.51E+06	4.53E+06
Pu-240	1.95E+06		3.67E-03	1.95E+06	1.95E+06
Pu-241	2.48E+07		9.44E+03	2.53E+07	2.68E+07
Pu-242	2.39E+05		1.73E+00	2.39E+05	2.40E+05
Ra-226	2.33E+05		1.67E+03	3.23E+05	5.89E+05
Sb-125		4.17E+06		4.17E+06	4.17E+06
Sm-151		3.19E+03		3.19E+03	3.19E+03
Sr-90	4.44E+07		9.98E+04	4.98E+07	6.57E+07
Tc-99	5.01E+04		9.27E+01	5.51E+04	6.98E+04
Th-230	1.95E+03			1.95E+03	1.95E+03
Th-232	1.16E+04		1.04E+01	1.22E+04	1.38E+04
Th-natural	1.98E+05			1.98E+05	1.98E+05
Tl-204		6.12E+03		6.12E+03	6.12E+03
U-232		1.34E+03		1.34E+03	1.34E+03
U-234	2.79E+05		1.62E+01	2.79E+05	2.82E+05
U-235	3.05E+04		1.77E+00	3.06E+04	3.09E+04
U-238	1.51E+06		8.74E+01	1.51E+06	1.52E+06

a. From "sourceterm.xls" spreadsheet. Values for U-238, U-235, and U-234 were later revised in the spreadsheet "Recommended uranium values for USE.xls".

b. From the document, "Potential additional isotopes for gw modeling.doc"

c. From the spreadsheet "Source term projections for Art 101302.xls". Value for U-234 and U-235 were modified as discussed in text.

Radionuclide Screening

Screening is defined here as an assessment of the potential for a radionuclide to contribute significantly to the overall dose via the groundwater pathway. The purpose of screening is to remove from consideration those radionuclides that do not have the potential to contribute significantly to the overall dose, and thereby focus resources on those radionuclides that are truly important. Screening calculations should be relatively simple, conservative estimates of the dose-potential of a radionuclide. Conservative is defined here as an upper-bound estimate that is intended to overstate the potential for dose. A radionuclide is termed "screened" if it has been removed from the list of important radionuclides following a screening calculation. A radionuclide is termed "not screened" if it has not been removed from the list of important radionuclides following a screening calculation.

Screening Methods

Screening was performed in two phases. In the first phase, a conservative estimate of the water travel time from the disposal site to the aquifer was compared with the radionuclide half-life. If the half-life was less than or equal to $1/10^{th}$ the conservatively estimated water travel time, then the nuclide was screened or removed from further consideration. The $1/10^{th}$ value of the water travel time was chosen because this would assure that all nuclides that were screened (i.e., had half-lives less than $1/10^{th}$ the water travel time) would have gone through a minimum of 10 half-lives before reaching the aquifer, and therefore only $\exp(-\ln(2) \times 10) = 9.7656 \times 10^{-4}$ of their initial inventory would reach the aquifer.

The second phase of screening used the GWSCREEN code (Rood 1999) with conservative transport parameters to estimate the peak annual groundwater ingestion dose to a persons who's drinking water source is an aquifer well immediately down gradient from the US Ecology facility. The peak dose is compared to a dose limit of 4 mrem yr^{-1} committed effective dose equivalent (CEDE) assuming 2 liters of water are ingested per day for 365 days per year. The 4 mrem yr^{-1} CEDE limit is based on the maximum contaminant limit (MCL) of 4 mrem yr^{-1} committed dose equivalent (CDE) for beta-gamma radionuclides as stated in the Code of Federal Regulation 40 CFR 141. Those radionuclides with doses less than 4 mrem yr^{-1} CEDE were removed from further consideration. Drinking water ingestion doses were calculated using the highest dose conversion factor reported by International Commission on Radiation Protection (ICRP) in their CD version of the ICRP database of dose coefficients (ICRP 1998) which is based on the methodology presented in ICRP-67. (ICRP 1993). However, the MCL is based on the committed dose equivalent using data from National Bureau of Standards Handbook 69 which is derived from methodology developed in ICRP 2 (ICRP 1958). The two dose estimates are not entirely comparable and result in different values for the MCL. However, the use of 4 mrem yr^{-1} CEDE as a screening cutoff is still applicable because annual dose limits for low-level waste performance are also based on the CEDE. Therefore, we have adopted the 4 mrem yr^{-1} CEDE as our screening cutoff. To address possible cumulative impacts from nuclides that have doses less than 4 mrem yr^{-1}, the percent contribution to the total dose was also computed. The total dose was computed by summing the maximum dose regardless of the time of maximum. If a screened radionuclide (i.e., a radionuclide with a screening dose of < 4 mrem yr^{-1}) contributed more than 0.1% to the total dose, then it was removed from the screened list and retained for further consideration.

Phase I Screening

Phase I screening required a conservative estimate of the mean unsaturated water travel time and compared this value to the radionuclide half-lives. The mean unsaturated water travel time is given by

$$T_{unsat} = \frac{x\theta}{I} \quad (1)$$

where

T_{unsat} = mean unsaturated water travel time (yr)
x = depth to the aquifer (m)
θ = moisture content in the unsaturated zone ($m^3\ m^{-3}$)
I = infiltration rate ($m\ yr^{-1}$)

A conservative estimate of the site-specific infiltration rate at the US Ecology site was chosen to be 10 cm yr^{-1} based on the observations and measurements in Gee et al. (1992). The depth to the aquifer of 82.3 m was taken from the original DEIS groundwater assessment (Rood 2000a). The moisture content of 0.0606 $m^3\ m^{-3}$ was calculated for 10-cm yr^{-1} infiltration using the moisture characteristic curve presented in Rood (2000a). Using these values in Equation (1) yields a mean unsaturated water travel time of 49.87 yr. One-tenth this value (4.987 yr) was compared to the radionuclide half-life ($T_{1/2}$). If $T_{1/2} \leq T_{unsat}/10$ then the radionuclide was removed from further consideration. That is, if the half-life was less than one-tenth the conservative estimate of the unsaturated *water* travel time, then the radionuclide was eliminated from further consideration or screened. Results of this screening are presented in Table 3.

The radionuclides Cd-113, Hf-182, and Kr-85 were eliminated from consideration because ingestion dose conversion factors were not available. Lack of an ingestion dose conversion factor for a radionuclide indicates ingestion doses are inconsequential or improbable.

Table 3. Phase I Screening Results for the U.S. Ecology Site

Radionuclide	Half-Life (yr)	$T_{1/2} \leq 4.987$ yr?	Radionuclide	Half-Life (yr)	$T_{1/2} \leq 4.987$ yr?
Ac-227	21.773	No	Ni-63AM	100.1	No
Am-241	432.7	No	Pa-231	3.28E+04	No
Ba-133	10.52	No	Pb-210	22.3	No
Bi-207	32.2	No	Pm-147	2.6234	Yes
C-14	5730	No	Pu-238	87.4	No
Cd-113	9.30E+15	No	PU-239	24119	No
Cl-36	3.01E+05	No	Pu-240	6563	No
Cm-244	18.1	No	Pu-241	14.35	No
Co-60	5.2714	No	Pu-242	3.73E+05	No
Cs-134	2.062	Yes	Ra-226	1600	No
Cs-137	30.1	No	Sb-125	2.73	Yes
Eu-152	13.542	No	Sm-151	90	No
Eu-154	8.592	No	Sr-90	29.1	No
Eu-155	4.68	Yes	Tc-99	2.11E+05	No
Fe-55	2.73	Yes	Th-230	7.54E+04	No
H-3	12.33	No	Th-232	1.41E+10	No
Hf-182	9.00E+06	No	Th-nat	1.41E+10	No
I-129	1.57E+07	No	Tl-204	3.78	Yes
K-40	1.28E+09	No	U-232	68.9	No
Kr-85	10.756	No	U-234	2.45E+05	No
Na-22	2.6088	Yes	U-235	7.04E+08	No
Nb-94	2.03E+04	No	U-238	4.47E+09	No
Ni-59	7.50E+04	No	U-dep	4.47E+09	No
Ni-59AM	7.50E+04	No	U-DEP	4.47E+09	No
Ni-63	100.1	No	U-nat	4.47E+09	No

Phase II Screening

The radionuclides that were not screened in Phase I were evaluated in Phase II. As was done in Phase I screening, a conservative infiltration rate of 10-cm yr^{-1} was assumed. Partition coefficient values (K_d) were taken from Kincaid et al. (1998). Most other parameters (Table 4) were taken from Rood (2000a). The partitioning coefficient values that were used represented the most conservative values for source areas (i.e. areas where radionuclides were disposed or discharged into the soil) and unsaturated/aquifer materials as reported in Kincaid et al. (1998). Source-area partition coefficients were assumed to represent a highly mobile environment and in many cases, were near zero. Partition coefficients were not available in Kincaid et al. (1998) for all radionuclides considered. For the radionuclides not available in Kincaid et al. (1998), a K_d value of 0 mL g^{-1} was assumed for the source and the lowest K_d value reported in Sheppard and Thibault (1990) was used for unsaturated/aquifer materials. Partition coefficient values were then corrected for the percent gravel composition in the unsaturated zone and aquifer (see Equation 12

and Table 10). The simulation did not consider waste emplacement rates over time. Instead, the entire inventory was assumed to be placed in the trenches at the start of the simulation. This assumption provides the most conservative estimate of the maximum mass flux from the source area to the aquifer.

Table 4. Parameter used in the Phase II Screening Analysis using GWSCREEN

Parameter name (units)	Value
Source length (m)	518
Source width (m)	382
Percolation (m yr^{-1})	0.1
Source thickness (m)	10.6
Bulk density of source (g cm^{-3})	1.26
Moisture content in source zone (m^{-3} m^{-3})[a]	0.0606
Unsaturated zone thickness (m)	82.3
Bulk density of unsaturated zone (g cm^{-3})	1.6
Unsaturated zone dispersivity (m)	0
Percent gravel in unsaturated zone and aquifer	41.7%
Moisture content in unsaturated zone (m^{-3} m^{-3})[a]	0.0606
Longitudinal dispersivity in aquifer (m)	27.5
Transverse dispersivity in aquifer (m)	5.0
Bulk density of aquifer (g cm^{-3})	1.6
Aquifer porosity (m^{-3} m^{-3})	0.1
Darcy velocity in aquifer (m y^{-1})	32.9
Receptor distance (m)[b]	275

a. Calculated using van Genuchten fitting parameters in Rood 2000a: $\alpha = 7.51$ m^{-1}, $n = 2.298$, $K_{sat} = 1710$ m y^{-1}, $\theta_{sat} = 0.2724$, $\theta_{residual} = 0.0321$

b. Measured from the center of the source. Transverse distance = 0 m.

Ingrowth of radioactive progeny was also considered for actinides. For some actinides that are relatively immobile, have short-half lives relative to their transit time in the unsaturated zone, and have long-lived mobile progeny, transport of the progeny was modeled instead of that of the parent. Nuclides that fall into this category include Am-241→Np-237, Cm-244→Pu-240, Pu-238→U-234, and Pu-241→Am-241→Np-237. In these cases, the parent activity was conservatively converted into the equivalent mobile progeny activity by multiplying the parent activity by the ratio of the progeny/parent half-lives.

For actinides with relatively short-lived progeny (≤ 1 year), parent and progeny were assumed to be in secular equilibrium and the dose conversion factors were summed as shown in Table 5.

Table 5. ICRP Dose Conversion Factors for Actinide Decay Chains[a]

Parent	Progeny	Progeny Included	Subtotals (rem Ci^{-1})	Total (rem Ci^{-1})	Total (mrem pCi^{-1})
Pu-242			8.88E+05	8.88E+05	8.88E-04
	U-238		1.67E+05		
		Th-234	1.26E+04		
		Pa-234	1.89E+03		

Table 5. ICRP Dose Conversion Factors for Actinide Decay Chains[a]

Parent	Progeny	Progeny Included	Subtotals (rem Ci^{-1})	Total (rem Ci^{-1})	Total (mrem pCi^{-1})
		Total	1.81E+05	1.81E+05	1.81E-04
	U-234		1.81E+05	1.81E+05	1.81E-04
	Th-230		7.77E+05	7.77E+05	7.77E-04
	Ra-226		1.04E+06		
		Pb-214	5.18E+02		
		Bi-214	4.07E+02		
		Total	1.04E+06	1.04E+06	1.04E-03
	Pb-210		2.55E+06		
		Bi-210	4.81E+03		
		Po-210	4.44E+06		
		Total	7.00E+06	7.00E+06	7.00E-03
Pu-241			1.78E+04	1.78E+04	1.78E-05
	Am-241		7.40E+05	7.40E+05	7.40E-04
	Np-237		4.07E+05		
		Pa-233	3.22E+03		
		Total	4.10E+05	4.10E+05	4.10E-04
	U-233		1.89E+05	1.89E+05	1.89E-04
	Th-229		1.81E+06		
		Ra-225	3.66E+05		
		Ac-225	8.88E+04		
		Bi-213	7.40E+02		
		Total	2.27E+06	2.27E+06	2.27E-03
Pu-240			9.25E+05	9.25E+05	9.25E-04
	U-236		1.74E+05	1.74E+05	1.74E-04
	Th-232		8.51E+05	8.51E+05	8.51E-04
	Ra-228		2.55E+06		
		Ac-228	1.59E+03		
		Total	2.55E+06	2.55E+06	2.55E-03
	Th-228		2.66E+05		
		Ra-224	2.41E+05		
		Pb-212	2.22E+04		
		Bi-212	9.62E+02		
		Total	5.30E+05	5.30E+05	5.30E-04
Pu-239			9.25E+05	9.25E+05	9.25E-04
	U-235		1.74E+05		
		Th-231	1.26E+03		
		Total	1.75E+05	1.75E+05	1.75E-04
	Pa-231		2.63E+06	2.63E+06	2.63E-03
	Ac-227		4.07E+06		
		Th-227	3.26E+04		
		Fr-223	8.88E+03		
		Ra-223	3.70E+05		
		Pb-211	6.66E+02		
		Total	4.48E+06	4.48E+06	4.48E-03

a. From the ICRP Database of Dose Coefficients, version 1.0 (ICRP 1998). Original units were Sv Bq^{-1} and were converted to rem Ci^{-1} and mrem pCi^{-1}.

For Ni-59 and Ni-63, WDOH segregated activated metal waste forms from the remainder of the inventory. The activated metal inventory was about two orders of magnitude lower than that

of the other inventory for these nuclides presented in Table 1, and therefore were considered insignificant in terms of the overall inventory for screening purposes.

Phase II screening results are presented in Table 6. Those radionuclides that are retained for the final analysis are shaded. Fifteen radionuclides (compared to 5 in the original analysis) were not screened and retained for further evaluation: C-14, Cl-36, H-3, I-129, Pu-238,-239,-240,-242, Ra-226, Tc-99, Th-230, Th-232, U-234, U-235, and U-238. Strontium-90 and Ni-63 were screened from radionuclide inventory but were retained because these radionuclides had detectable concentrations in the unsaturated zone below trench 5.

Table 6. Results of Phase II Screening
(Shaded radionuclides were not screened and retained for further evaluation)

Radionuclide/ Progeny[a]	Number of progeny	Half-Life (yr)[b]	DCF (mrem pCi^{-1})[c]	Source K_d (mL g^{-1})[d]	Unsaturated/ aquifer K_d (mL g^{-1})[e]	Total Dose (mrem yr^{-1})[f]	Is Dose<4 mrem yr^{-1} ?	% of total
Ac-227	0	2.18E+01	4.48E-03	0	100	0.00E+00	Yes	0.000%
Am-241[Np]	2	2.14E+06	4.10E-04	0.1	10	1.19E+00	Yes	0.002%
U-233	na	1.59E+05	1.89E-04	0	0.6			
Th-229	na	7.43E+03	2.27E-03	0	40			
Ba-133	0	1.05E+01	5.55E-06	0	60	0.00E+00	Yes	0.000%
Bi-207	0	3.22E+01	4.81E-06	0	100	0.00E+00	Yes	0.000%
C-14	0	5.73E+03	2.15E-06	0	0	8.44E+03	No	12.937%
Cl-36	0	3.01E+05	3.44E-06	0	0	5.77E+00	No	0.009%
Cm-244(Pu)	4	6.56E+03	9.25E-04	0.1	80	1.12E-02	Yes	0.000%
U-236	0	2.34E+07	1.74E-04	0	0.6			
Th-232	0	1.41E+10	8.51E-04	0	40			
Ra-228	0	5.75E+00	2.55E-03	0	8			
Th-228	0	1.91E+00	5.30E-04	0	40			
Co-60	0	5.27E+00	1.26E-05	0	1200	0.00E+00	Yes	0.000%
Cs-137	0	3.01E+01	4.81E-05	5	540	0.00E+00	Yes	0.000%
Eu-152	0	1.35E+01	5.18E-06	0	100	0.00E+00	Yes	0.000%
Eu-154	0	8.59E+00	7.40E-06	0	100	0.00E+00	Yes	0.000%
H-3	0	1.23E+01	1.55E-07	0	0	3.97E+03	No	6.093%
I-129	0	1.57E+07	4.07E-04	0	0.3	9.09E+02	No	1.393%
K-40	0	1.28E+09	2.29E-05	0	15	1.84E+00	Yes	0.003%
Nb-94	0	2.03E+04	6.29E-06	2	50	1.34E-01	Yes	0.000%
Ni-59	0	7.50E+04	2.33E-07	2	50	3.55E+00	Yes	0.005%
Ni-63[g]	0	1.00E+02	5.55E-07	2	50	0.00E+00	Yes	0.000%
Pa-231	1	3.28E+04	2.63E-03	0.1	10	8.37E-02	Yes	0.000%
Ac-227	na	2.18E+01	4.48E-03	0	100			
Pb-210	0	2.23E+01	2.55E-03	0	2000	0.00E+00	Yes	0.000%
Pu-238[U]	3	2.45E+05	1.81E-04	0.1	0.6	8.75E+01	No	0.134%
Th-230	na	7.54E+04	7.77E-04	0	40			
Ra-226	na	1.60E+03	1.04E-03	0	8			
Pb-210	na	2.23E+01	7.00E-03	0	2000			
Pu-239	3	2.41E+04	9.25E-04	0.1	80	2.22E+03	No	3.402%

Table 6. Results of Phase II Screening
(Shaded radionuclides were not screened and retained for further evaluation)

Radionuclide/ Progeny[a]	Number of progeny	Half-Life (yr)[b]	DCF (mrem pCi^{-1})[c]	Source K_d (mL g^{-1})[d]	Unsaturated/ aquifer K_d (mL g^{-1})[e]	Total Dose (mrem yr^{-1})[f]	Is Dose<4 mrem yr^{-1} ?	% of total
U-235	na	7.04E+08	1.75E-04	0	0.6			
Pa-231	na	3.28E+04	2.63E-03	0	10			
Ac-227	na	2.18E+01	4.48E-03	0	100			
Pu-240	4	6.56E+03	9.25E-04	0.1	80	4.19E+01	No	0.064%
U-236	na	2.34E+07	1.74E-04	0	0.6			
Th-232	na	1.41E+10	8.51E-04	0	40			
Ra-228	na	5.75E+00	2.55E-03	0	8			
Th-228	na	1.91E+00	5.30E-04	0	40			
Pu-241[Np]	2	2.14E+06	4.10E-04	0.1	10	2.23E+00	Yes	0.003%
U-233	na	1.59E+05	1.89E-04	0	0.6			
Th-229	na	7.43E+03	2.27E-03	0	40			
Pu-242	5	3.73E+05	8.88E-04	0.1	80	6.04E+02	No	0.926%
U238	na	4.47E+09	1.81E-04	0	0.6			
U-234	na	2.45E+05	1.81E-04	0	0.6			
Th-230	na	7.54E+04	7.77E-04	0	40			
Ra-226	na	1.60E+03	1.04E-03	0	8			
Pb-210	na	2.23E+01	7.00E-03	0	2000			
Ra-226	1	1.60E+03	1.04E-03	0.1	8	1.21E+03	No	1.856%
Pb-210	na	2.23E+01	7.00E-03	0	2000			
Sm-151	0	9.00E+01	3.63E-07	0	245	0.00E+00	Yes	0.000%
Sr-90[g]	0	2.91E+01	1.04E-04	0.1	8	1.20E-60	Yes	0.000%
Tc-99	0	2.11E+05	2.37E-06	0	0	7.81E+01	No	0.120%
Th-230	2	7.54E+04	7.77E-04	1	40	5.18E+01	No	0.079%
Ra-226	na	1.60E+03	1.04E-03	0	8			
Pb-210	na	2.23E+01	7.00E-03	0	2000			
Th-232	2	1.41E+10	8.51E-04	1	40	1.09E+03	No	1.668%
Ra-228	na	5.75E+00	2.55E-03	0	8			
Th-228	na	1.91E+00	5.30E-04	0	40			
U-232	1	6.89E+01	1.22E-03	0.1	0.6	1.04E+00	Yes	0.002%
Th-228	na	1.91E+00	5.30E-04	0	40			
U-234	3	2.45E+05	1.81E-04	0.1	0.6	6.23E+02	No	0.956%
Th-230	na	7.54E+04	7.77E-04	0	40			
Ra-226	na	1.60E+03	1.04E-03	0	8			
Pb-210	na	2.23E+01	7.00E-03	0	2000			
U-235	2	7.04E+08	1.75E-04	0.1	0.6	4.82E+03	No	7.387%
Pa-231	na	3.28E+04	2.63E-03	0	10			
Ac-227	na	2.18E+01	4.48E-03	0	100			
U-238	4	4.47E+09	1.81E-04	0.1	0.6	4.11E+04	No	62.960%
U-234	na	2.45E+05	1.81E-04	0	0.6			
Th-230	na	7.54E+04	7.77E-04	0	40			

Table 6. Results of Phase II Screening
(Shaded radionuclides were not screened and retained for further evaluation)

Radionuclide/ Progeny[a]	Number of progeny	Half-Life (yr)[b]	DCF (mrem pCi^{-1})[c]	Source K_d (mL g^{-1})[d]	Unsaturated/ aquifer K_d (mL g^{-1})[e]	Total Dose (mrem yr^{-1})[f]	Is Dose<4 mrem yr^{-1} ?	% of total
Ra-226	na	1.60E+03	1.04E-03	0	8			
Pb-210	na	2.23E+01	7.00E-03	0	2000			
Total						7.24E+04		

a. Radioactive progeny that are included in the dose estimate are right justified. Radionuclides followed by another radionuclide in brackets (e.g., Am-241[Np-237]) indicates that the radionuclide in brackets was the radionuclide modeled.

b. From Tuli (1990).

c. From ICRP (1998). Contributions from radioactive progeny in secular equilibrium are included in the dose estimate.

d. Partition coefficients for the following elements were obtained from Kincaid et al., 1998: H, Cl, Tc, Ac, Am, Cm, Eu, C, Co, Cs, I, Ni, Sn, Nb, Np, Pa, Pb, Pu, Ra, Sr, Ru, Se, Th, Zr, and U. Source K_d values represent the conservative estimate for Source Term Category A in Table E.5 of Kincaid et al. (1998). Elements not represented in Kincaid et al. (1998) were assumed to be zero. Radioactive progeny are assumed to travel with their parent, therefore no source K_d values are presented for radioactive progeny. Partition coefficient values shown are not corrected for the percent gravel component.

e. Partition coefficient values represent the conservative estimate for Source Term Category F in Table E.10. Elements not represented in Kincaid et al. (1998) were from Sheppard and Thibault (1990). Partition coefficient values shown are not corrected for the percent gravel component.

f. The total dose includes all contributions from progeny. The doses from progeny are not shown. These doses should not be interpreted as a realistic estimate of radiological impacts from the site.

g. These radionuclides had screening doses less than 4 mrem yr^{-1} but were retained because they were detected in the unsaturated zone below Trench 5.

CONCEPTUAL MODEL OF FATE AND TRANSPORT

In this section the conceptual model for radionuclide fate and transport is presented for the three primary elements of the transport model: the source term, the unsaturated zone, and the aquifer (Figure 3). The source term represents the release of radionuclides from the waste and transport through the bottom of the trenches and is geometrically represented by the total volume of trenches within the facility. Individual trenches are not modeled; rather, all the trenches are modeled as a single composite trench that represents the entire disposal facility. The area of the composite trench is illustrated in Figure 2 and labeled “modeled source area”. The unsaturated zone represents the area from the bottom of the trenches to the top of the aquifer where the rock matrix is partially saturated and water flow is vertical and downward. The unsaturated zone is composed multiple layers, each having their own unique properties and water fluxes. The aquifer represents a fully saturated media where water flow is essentially horizontal. The three primary elements are linked by radionuclide fluxes across their boundaries. For example, the source term and unsaturated zone are linked by the radionuclide flux from the bottom of the trenches to the top of the unsaturated zone.

Infiltrating water is the primary mechanism of radionuclide transport. Vapor transport is only important for tritium and radon, however tritium is conservatively assumed to move only by aqueous phase transport. Gas-phase radon transport is not considered and radon progeny are assumed to travel with radium. Radionuclides are present in two phases; a sorbed solid phase and a dissolved aqueous phase. Partitioning between the sorbed and aqueous phases is described by the equilibrium partitioning coefficient or K_d. As infiltrating water comes in contact with the waste, radionuclides partition into the aqueous phase according to the K_d and are transported with

the water. Radionuclide pore water concentrations are not allowed to exceed their element-specific solubility limit. Radioactive progeny that form during transport are also accounted for and partition according to their element-specific K_d.

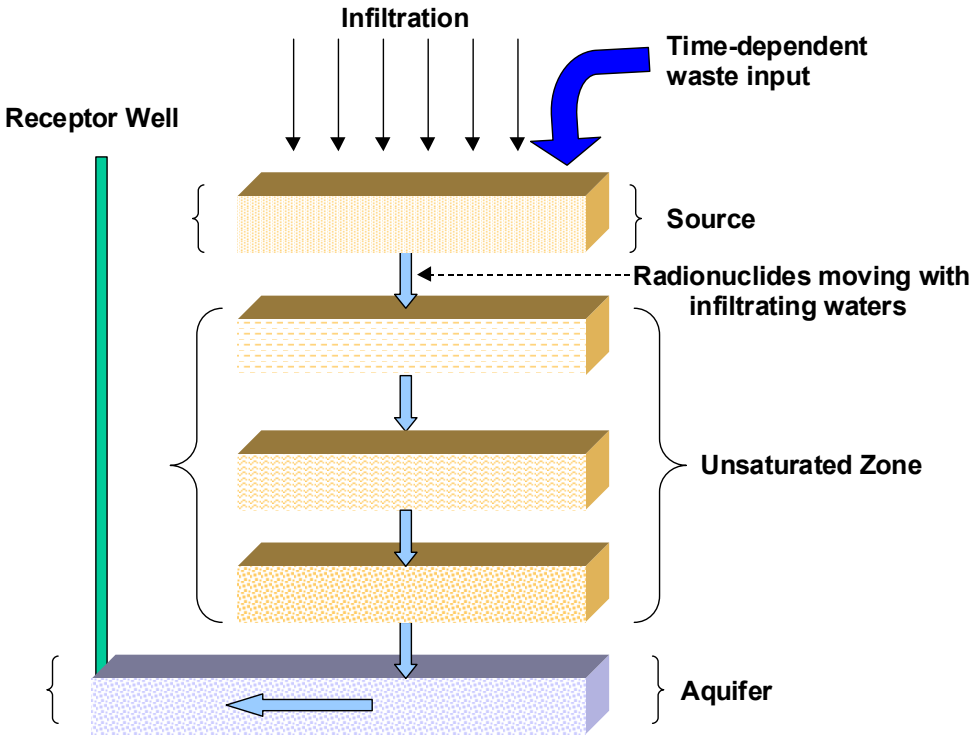

Figure 3. Overall conceptual model for US Ecology LLRW facility showing the three primary elements; source, unsaturated zone, and aquifer. The source is modeled as a separate unit. The unsaturated zone is composed of multiple layers, each having unique properties and water flux.

Source Term and Unsaturated Zone Conceptual Model

The source term conceptual model for the site was segregated into three time periods; pre-cover, cover, and post cover. The pre-cover period begins in 1965 (Figure 4) when the facility started operation and ends when the cover is installed. In all cases, a cover is assumed to be installed in the year 2005. Future operations of the site are assumed to limit infiltration through the active trenches to no more than the designed infiltration rate of the cover. Eventually, water fluxes through the trenches extend vertically down to the aquifer. The temporal histories of waste disposals are accounted for in the model. That is, waste is disposed over time as represented by the disposal history provided by WDOH. While a trench is actively receiving waste, infiltration is enhanced. After the trench is closed (ceases to receive waste), the trench is backfilled with soil. Infiltration through the trench after closure is lower than active disposal, but higher than natural infiltration.

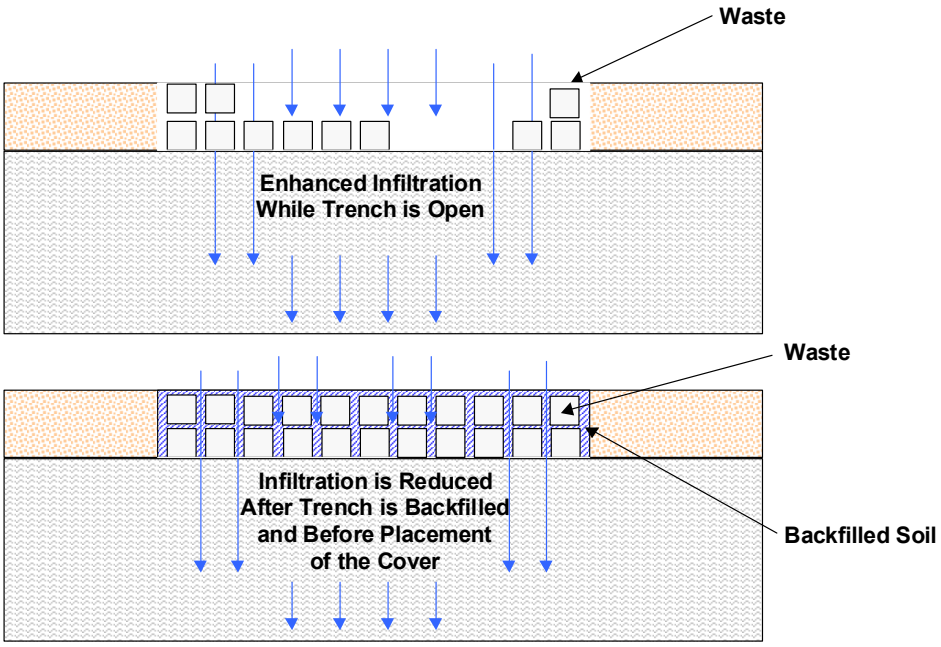

Figure 4. Source term conceptual model of the US Ecology LLRW facility from 1965 to the time of cover placement (2005). Enhanced water infiltration is assumed to occur in the open trench and infiltration slightly enhanced over background occurs after the trench is closed (backfilled with soil) and before placement of the cover.

The cover time period represents the time when the cover is intact and performs according to its design specifications (Figure 5). The cover restricts infiltration through the waste. Some of the precipitation that falls on the cover runs off the sides and infiltrates around the edge of the cover, although this amount is assumed to be minimal. After placement of the cover, soils underneath the facility dry over time. The drying front as it is referred to here advances over time until reaching the aquifer. Once the drying front reaches the aquifer, water fluxes throughout the unsaturated zone are equivalent to the net water infiltration rate through the cover.

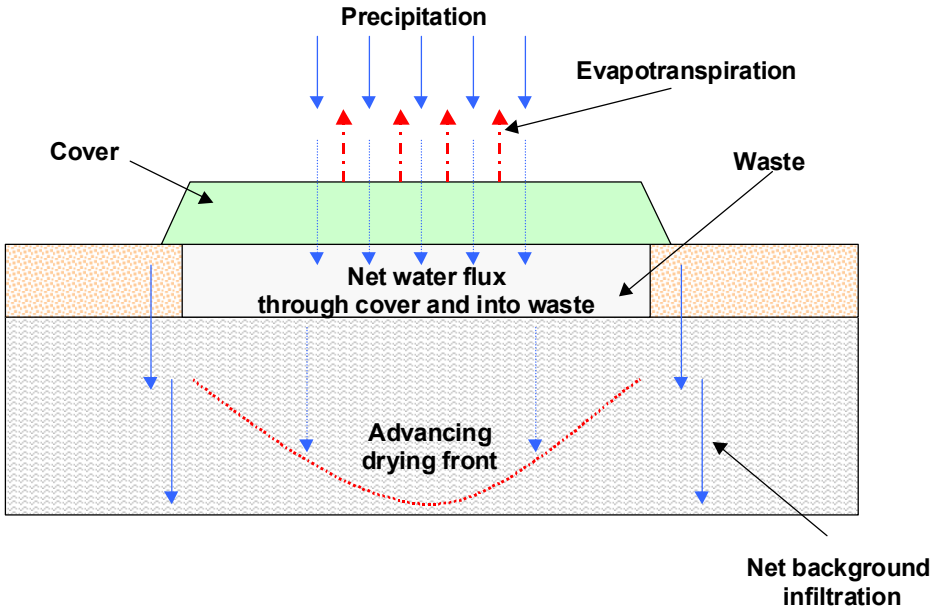

Figure 5. Source term conceptual model of the US Ecology LLRW facility from the time of cover placement (2005) to the time of cover failure. The amount of water that passes through the cover and into the waste is specified by the design of the cover.

The post cover period represents the time when the cover fails and infiltration through the waste returns to natural recharge rates over time (Figure 6). The wetting front advances over time until it reaches the aquifer. Water flux through the cover, waste, and unsaturated zone are assumed to be constant for all future times after the wetting front reaches the aquifer.

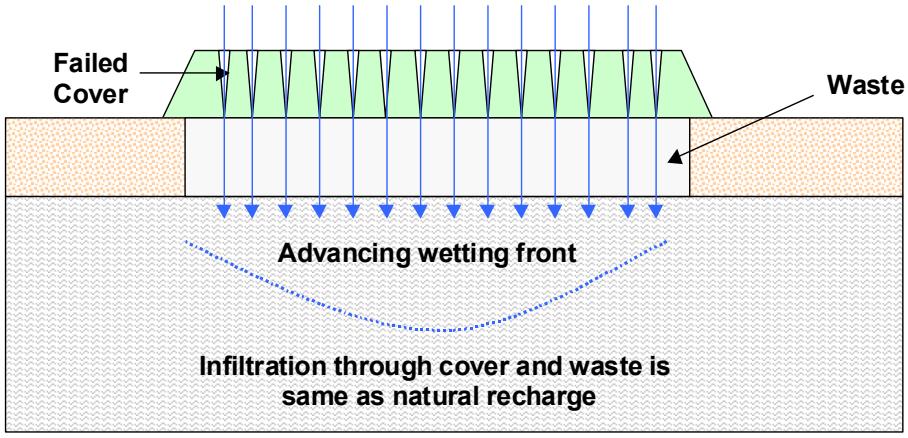

Figure 6. Source term conceptual model of the US Ecology LLRW facility for times after cover failure. Net infiltration through the cover is assumed to be the same as natural recharge.

Waste packaging is assumed to be ineffective in controlling water from coming in contact with the waste. Partitioning between radionuclides in the waste form and infiltrating water, and

between radionuclides in back-filled soil and infiltrating water, is treated as a single process characterized by a single partitioning coefficient.

For modeling purposes, the entire site is represented by a single composite trench as shown in Figure 1. The surface area (identified as "Modeled Source Area" in Figure 1) of the composite trench represents the total surface area of all individual trenches. Infiltration through an open trench is assumed to be greater than infiltration through a closed trench. Therefore, infiltration through the composite trench represents an area-weighted infiltration that is based on the number of open trenches at a given time.

Radionuclides leaving the bottom of the trenches enter the unsaturated zone. The net water flow in the unsaturated zone is assumed to be vertical and downward. Where sufficient data exists, the characteristics of specific lithologic units are accounted for in this model. Radionuclides and radioactive progeny partition between the rock matrix and the infiltrating water according to their element-specific partitioning coefficient. Partitioning was assumed to only occur on the portion of the rock matrix composed of fine material and not on the coarse gravelly components (Kincaid et al. 1998).

Aquifer Conceptual Model

Radionuclides enter the aquifer across an area defined by the footprint of the source as illustrated in Figure 1. The aquifer is assumed to be a homogeneous porous media of infinite lateral extent and finite thickness. Aquifer flow is assumed to be constant and unidirectional, with no appreciable sources or sinks within the footprint of the facility. A drinking water well is assumed to be drilled on the downgradient edge of the facility at the property line. The well is assumed to have a screened interval beginning at the surface of the aquifer and extending 15-m below its surface, the length of a typical well screen. Pumping from the well is assumed to be minimal and have little impact on the overall flow in the aquifer. Ingrowth of radioactive progeny is not considered in the aquifer because transport times from the radionuclide source in the aquifer to the receptor well are relatively short. This simplifying assumption is considered suitable for this analysis where the receptor well is relatively close to the source. However, this assumption is not considered suitable for receptor distances a substantial distance from the source.

IMPLEMENTATION OF THE CONCEPTUAL MODEL

In the first iteration of this assessment (Rood 2000a), the GWSCREEN Version 2.5 code (Rood 1999) was used to implement a simplified version of the conceptual model presented earlier. Although GWSCREEN was suitable for the earlier iteration of this assessment, it lacks the processes necessary to implement the source term and unsaturated conceptual models as outlined in the previous section. Therefore, it was necessary to investigate alternative models for use in this assessment.

Preliminary Modeling with DUST

The Disposal Unit Source Term Model (DUST) code (Sullivan 1996) provided a viable alternative to GWSCREEN for computing the source term and unsaturated transport. DUST is a waste form release model coupled with a one-dimensional finite difference approximation to the advection dispersion equation used to compute transport in the unsaturated zone. DUST allows for time-variable waste disposal rates, container failure rates, and time-variable water fluxes.

Preliminary simulations were performed with DUST for nuclides remaining after Phase II screening. Initial model simulations were satisfactory; however, closer inspection revealed inconsistent mass balance errors ranging from <2% to up to 30% when time-varying waste input rates were considered. Changes in time stepping and finite difference node spacing from their initial values appeared to have little impact on the overall results. However, mass balance errors for initial concentration problems with no time-variable waste input rates were insignificant. Monte Carlo uncertainty analysis was part of this project and it was uncertain whether correct results would be obtained for all model realizations that used time-variable waste input rates. Additionally, implementation of the conceptual model required two iterations of DUST for each radionuclide simulated, further adding to the overall complexity of the simulation. For these reasons, a new model was developed that could implement the conceptual model outlined earlier. For situations where the accuracy of DUST could be assured, it was used as a check on the new model. The GWSCREEN model was retained for radionuclide transport in the aquifer and dose calculation.

Description of the FOLAT Model

The name FOLAT (First Order Leach and Transport) was given to the new model, although non-first order processes may also be included in the model. The FOLAT model treats the source and unsaturated zones as a series of compartments where interchange between the compartments is described by advection-driven first-order or solubility-limited processes. The FOLAT model is conceptually similar to the SESOIL model (Scott and Hetrick 1994) originally developed at Oak Ridge National Laboratory. Details of the FOLAT model are described in a separate document (Rood 2003) and are summarized below.

The conceptual model for FOLAT is relatively simple. The subsurface environment is envisioned to be composed of a series of “compartments”. Within each compartment, radionuclides enter, mix, sorb, decay, and are eventually removed by the downward movement of water. Each compartment may have its own unique qualities that include horizontal and vertical

dimensions, bulk density, porosity, hydraulic conductivity, net water flux through the compartment, and sorptive properties. Water flux through each compartment may change as a function of time. As the water flux changes, so too does the moisture content of the compartment. Radionuclides sorb on to the solid matrix as described by the equilibrium partitioning coefficient or K_d. Sorption retards the overall downward movement of radionuclides. The rate of transport of radioactive decay products or progeny that form during vertical transport of a parent radionuclide are governed by the sorptive properties of the progeny, and not those of the parent.

Radionuclides may be present in each of the compartments at the start of the simulation, or alternatively, the parent member of the decay chain may be placed over time in the uppermost compartment. Concentrations of radionuclides in pore water are not allowed to exceed their solubility limit. Unit gradient conditions are assumed to apply to each compartment.

Ordinary differential equations describe the mass balance of radionuclides in each of the compartments. Radionuclide concentrations in pore water and the radionuclide fluxes from each compartment are determined from the radionuclide inventory within each compartment. The uppermost or first compartment for the first (parent) member of the decay chain is described by

$$\frac{dQ_{1,1}}{dt} = R(t) - F_{1,1}(t) - \lambda_1 Q_{1,1} \tag{2}$$

where

$Q_{1,1}$ = the number of atoms in compartment 1 for decay chain member 1 (atoms)
$R(t)$ = the input rate of decay chain member 1 into compartment 1 (atoms time^{-1})
$F_{1,1}(t)$ = the removal rate (flux) of decay chain member 1 from compartment 1 to compartment 2 (atoms time^{-1})
λ_1 = the decay rate constant for decay chain member 1 (time^{-1}).

For simplicity and clarity, all equations are written in terms of the number of atoms of each decay chain member. The mass balance equation for the remaining compartments is given by

$$\frac{dQ_{i,j}}{dt} = F_{i-1,j}(t) - \lambda_j Q_{i,j} + \lambda_{j-1} Q_{i,j-1} - F_{i,j}(t) \tag{3}$$

where i is the index for the compartment and j is the index for the decay chain member and $i \neq 1$ and $j \neq 1$. Other terms are defined previously. Equation 3 assumes the branching ratio between the parent and radioactive progeny is 1.0 (i.e. 100% of the parent decays to the progeny). When the radionuclide concentration in pore water is less than the solubility limit, the flux term in Equations 2 and 3 is given by

$$F_{i,j}(t) = \left(\kappa_{i,j}(t) + \eta_{i,j}\right) Q_{i,j} \tag{4}$$

where

$\kappa_{i,j}(t)$ = the leach rate constant for compartment i and decay chain member j (time^{-1})
$F_{i,j}(t)$ = the flux of decay chain member j from compartment i into compartment i+1 (atoms time^{-1})

$\eta_{i,j}$ = a fixed removal rate constant for compartment i and decay chain member j (time^{-1}).

In general, only the leach rate constant is used to remove radionuclides from a compartment. However, the user may which to bypass this calculation and calculate a removal rate constant outside the code. We have included $\eta_{i,j}$ for this situation. When the pore water concentration exceeds the solubility limit, then the flux term in Equations 2 and 3 is given by

$$F_{i,j}(t) = S_j \, q_i(t) \, L_i \, W_i \tag{5}$$

where

S_j = the solubility limit of decay chain member j (atoms m^{-3})
$q_i(t)$ = water flux through compartment i as a function of time (m time^{-1})
L_i = length of compartment i (m)
W_i = width of compartment i (m).

In Equations 4 and 5, $i \le n$, where n is the number of compartments in the simulation. Likewise, $j \le m$, where m is the number of decay chain members including the parent. The pore water concentration in compartment i for decay chain member j ($C_{i,j}$) is given by

$$C_{i,j}(t) = \frac{Q_{i,j}(t)}{\theta_i(t) \, L_i \, W_i \, T_i \left(1 + \dfrac{Kd_{i,j} \rho_i}{\theta_i(t)}\right)} \tag{6}$$

where

$\theta_i(t)$ = volumetric moisture content in compartment i as a function of time (m^3 m^{-3})
$Kd_{i,j}$ = equilibrium partition coefficient for compartment i and decay chain member j (mL g^{-1})
ρ_i = bulk density of compartment i (g mL^{-1})
T_i = thickness of compartment i (m)
L_i = length of compartment i (m)
W_i = width of compartment i (m).

The term, $1 + Kd_{i,j} \, \rho_i / \theta(t)_i$ is the retardation coefficient and is 1.0 for a K_d of zero. The leach rate constant is given by Baes and Sharp (1983) as

$$\kappa_{i,j}(t) = \frac{q_i(t)}{\theta_i(t) \, T_i \left(1 + \dfrac{Kd_{i,j} \rho_i}{\theta_i(t)}\right)} \tag{7}$$

and the decay rate constant is given by

$$\lambda_j = \frac{\ln(2)}{T1/2_j} \tag{8}$$

where $T1/2_j$ = half-life of decay chain member j.

Transport of radionuclides in the aquifer was computed using the GWSCREEN code. GWSCREEN takes as input, the time-variable radionuclide fluxes from FOLAT at the top of the aquifer and transports them down gradient from the source using a 2 or 3-dimentional semi-analytical solution to the advection-dispersion equation. The 2-dimensional solution was used in this assessment. GWSCREEN assumes radioactive progeny travel at the same rate as their parent. Because transport times from source to receptor are relatively short, generation of progeny in the aquifer was ignored. Concentrations in the aquifer were vertically averaged from the top of the aquifer to the length of a typical well screen.

ENGINEERED COVERS, CLOSURE SCENARIOS AND COMPLIANCE TIME

Five closure and cover design options were simulated in this assessment (Table 7). Water fluxes through the three engineered cover designs were provided by WDOH along with the three closure scenarios. The engineered covers considered consisted of a site soils cover, the US Ecology proposed cover, and an enhanced cover. Closure options considered included 1) ceasing waste disposal in year 2003, 2) ceasing waste disposal year 2056, and 3) ceasing waste disposal in year 2215. Disposal rates after year 2002 were assumed to be constant and given by the values in Table 2 under the column heading "Proposed". Not all covers were evaluated for each closure option. In all cases, the cover was assumed to be installed in the year 2005 over the existing trenches and infiltration in open trenches for future site operations would be controlled to no more than the cover design. Covers were assumed to begin to fail 500 years after placement in the year 2505 based on the typical cover design lifetime for Hanford Reservation facilities[2]. Cover failure was assumed to occur at this time (500 years after placement) regardless of the closure option considered. The time for the cover to degrade to natural infiltration is assumed to be the lifetime of the cover. That is, if the cover lasts 500 years, then the cover degrades to natural infiltration in 1000 years. This assumption is also based on Hanford facilities[2].

The site soils cover has a design-based infiltration rate greater than natural recharge. In this case, we have assumed that the cover does not fail, but returns to natural infiltration over time. The design-based infiltration is assumed to persist for 500 years. After that, infiltration through the cover decreases over the next 500 years and eventually returns to its natural state (0.005 m yr^{-1}) 1000 years after cover placement.

Table 7. Cover and Closure Options

Cover/closure option	Infiltration through cover (m yr^{-1})
Site soils cover/waste disposal ceasing in 2056	0.02
Enhanced cover/ waste disposal ceasing in 2003	0.0005
Enhanced cover/ waste disposal ceasing in 2056	0.0005
Enhanced cover/ waste disposal ceasing in 2215	0.0005
US Ecology proposed cover/ waste disposal ceasing in 2056	0.002

[2] Personal communication with Michael J. Fayer, Pacific Northwest National Laboratory, Richland Washington January 24, 2003.

The compliance time is defined as the time period over which predicted doses are compared to performance objectives. WDOH issued a compliance time of 10,000 year from present. However, predicted concentrations and doses presented in this report go well beyond 10,000 years. The purpose of extending the calculations beyond 10,000 years was to understand the overall behavior of the release and transport model in light of the great uncertainty that exists in making model predictions so far in the future. Radionuclide fluxes to the aquifer were calculated out to 100,000 years and then set to zero. Radionuclide concentrations in the aquifer were calculated out to 200,000 years.

MODEL INPUT

With the exception of water fluxes and waste input rates, model input was largely taken from Rood (2000a), Rood (2000b), and Kincaid et al. (1998). Model input for radionuclide-independent parameters are presented in Table 8, and in Table 9 for radionuclide-dependent parameters. Parameters that require additional explanation and justification are discussed in separate subsections.

Table 8. Radionuclide Independent Model Input Parameters

Parameter[a]	Nominal value	Reference/Comments
Length of source parallel to groundwater flow (m)	382	Rood (2000a) (see discussion below)
Width of source perpendicular to groundwater flow (m)	518	Rood (2000a) (see discussion below)
Cover longevity (years)	500	Assumed
Source thickness (m)	10.6	Rood (2000a)
Bulk density of source (g cm^{-3})	1.97	Kincaid et al. (1998) (see discussion below)
Saturated hydraulic conductivity for source (m y^{-1})	555	Kincaid et al. (1998) (see discussion below)
van Genuchten fitting parameter α for source (m^{-1})	0.811	Kincaid et al. (1998) (see discussion below)
van Genuchten fitting parameter *n* for source	1.58	Kincaid et al. (1998) (see discussion below)
Residual moisture content for source (m^3 m^{-3})	0.015	Kincaid et al. (1998) (see discussion below)
Total porosity for source (m^3 m^{-3})	0.119	Kincaid et al. (1998) (see discussion below)
Unsaturated thickness (m)	82.3	Rood (2000a)
Number of unsaturated layers (compartments)	13	This report (see discussion below)
Thickness of each unsaturated layer (m)	6.331	This report (see discussion below)
Bulk density of unsaturated layer 1 (g cm^{-3})	1.78	Kincaid et al. (1998) (see discussion below)
Saturated hydraulic conductivity, unsaturated layer 1 (m y^{-1})	3753	Kincaid et al. (1998) (see discussion below)
van Genuchten fitting parameter α for unsaturated layer 1 (m^{-1})	1.3	Kincaid et al. (1998) (see discussion below)
van Genuchten fitting parameter *n* for unsaturated layer 1	2.1	Kincaid et al. (1998) (see discussion below)
Residual moisture content for unsaturated layer 1 (m^3 m^{-3})	0.026	Kincaid et al. (1998) (see discussion below)
Total porosity for unsaturated layer 1 (m^3 m^{-3})	0.337	Kincaid et al. (1998) (see discussion below)
Bulk density of unsaturated layers 2–13 (g cm^{-3})	1.97	Kincaid et al. (1998) (see discussion below)
Saturated hydraulic conductivity for unsaturated layer 2-13 (m y^{-1})	555	Kincaid et al. (1998) (see discussion below)
van Genuchten fitting parameter α for unsaturated layer 2-13 (m^{-1})	0.811	Kincaid et al. (1998) (see discussion below)
van Genuchten fitting parameter *n* for unsaturated layer 2-13	1.58	Kincaid et al. (1998) (see discussion below)
Residual moisture content for unsaturated layer 2-13 (m^3 m^{-3})	0.015	Kincaid et al. (1998) (see discussion below)
Total porosity for unsaturated layer 2-13 (m^3 m^{-3})	0.119	Kincaid et al. (1998) (see discussion below)
Longitudinal dispersivity in aquifer (m)	27.5	Rood (2000a)
Transverse dispersivity in aquifer (m)	5	Rood (2000a)
Well screen thickness (m)	15	Rood (2000a)
Aquifer porosity (m^3 m^{-3})	0.1	Rood (2000a)
Darcy velocity in aquifer (m y^{-1})	32.9	Rood (2000a)
Bulk density of aquifer (g cm^{-3})	1.6	Rood (2000a)

a. Time variable water fluxes and waste input rates are discussed in Water Fluxes in the Unsaturated Zone and Waste Input Rates sections later in the text.

Table 9. Radionuclide Dependent Model Input Parameters

Parameter	Nominal value[a]	Reference/Comments
Carbon K_d (mL g^{-1})	0.5	Kincaid et al. (1998)
Chlorine K_d in source (mL g^{-1})	0.75	see "Integration of Mobile Release Fraction and Partition Coefficients" section
Chlorine K_d in unsaturated zone/aquifer (mL g^{-1})	0	Kincaid et al. (1998)
Hydrogen K_d in all media (mL g^{-1})	0	Kincaid et al. (1998)
Iodine K_d (mL g^{-1})	0.5	Kincaid et al. (1998)
Protactinium K_d (mL g^{-1})	15	Kincaid et al. (1998)
Plutonium K_d (mL g^{-1})	200	Kincaid et al. (1998)
Radium K_d (mL g^{-1})	20	Kincaid et al. (1998)
Technetium K_d in source (mL g^{-1})	0.75	see "Integration of Mobile Release Fraction and Partition Coefficients" section
Technetium K_d in unsaturated zone/aquifer (mL g^{-1})	0	Kincaid et al. (1998)
Thorium K_d (mL g^{-1})	1000	Kincaid et al. (1998)
Uranium K_d (mL g^{-1})	3	Kincaid et al. (1998)
Uranium solubility (mg L^{-1})	25	Rood (2000)

a. The K_d values are for geochemical environment F as described in Kincaid et al. (1998)

Length and Width of Source

The dimensions of the source parallel and perpendicular to groundwater flow were initially taken from Rood (2000a) which had the longer side of the source oriented parallel to groundwater flow. This orientation was presumably chosen in the initial assessment because it provided a more conservative estimate of groundwater concentrations. However, further examination of head elevations presented in Kincaid et al. (1998) for the year 2100 revealed that the source should have been oriented with the long side perpendicular to groundwater flow. Therefore, the dimensions were changed in this assessment to reflect the correct orientation of the source relative to flow in the aquifer.

Length of Well Screen

The well screen length used in this assessment was based on the default value used in screening calculations at the Idaho National Engineering and Environmental Laboratory (DOE 1994). The 200-Area composite analysis (Kincaid et al. 1998) used a numerical three-dimensional aquifer flow and transport model that had vertical grid resolution of 8 m. Therefore, at a minimum, concentrations were averaged across 8 m of the aquifer. The transverse dispersivity used in the 200 Area Composite Analysis was 20 m. Presumably, the transverse dispersivity was also applied to the vertical component of dispersion in the aquifer. Using a value of 20 m for vertical dispersivity in a three-dimensional GWSCREEN simulation resulted in a significant portion of the contaminant plume extending beyond the 15-m well screen. Therefore, using a two-dimensional aquifer solution with a 15-m mixing thickness results in a conservative estimate of aquifer concentrations compared to the more realistic three-dimensional model used in the 200 Area Composite Analysis. Because it was the intent of this assessment to error on the side of

conservatism, the two-dimensional aquifer solution with a 15-m well screen was retained from the previous DEIS work and used in this assessment.

Number of Unsaturated Layers

The number of unsaturated layers or compartments in a FOLAT model simulation influences the amount of plume spreading or dispersion. Assuming a uniform compartment thickness in all compartments except the source, it was shown that a compartment thickness of 0.243 × the standard deviation of the radionuclide plume at the unsaturated-saturated interface would yield about the same amount of plume spreading as estimated by the advection dispersion equation[3]. The standard deviation of the contaminant plume is given by

$$\sigma = \sqrt{2\alpha_L x} \tag{9}$$

where σ = the standard deviation of the contaminant plume at distance, x (m), and α_L = the longitudinal dispersivity in the unsaturated zone (m). Using the median estimated dispersivity value in Rood (2000a) of 4 m and a total unsaturated thickness of 82.3 m, we have an estimated compartment thickness of

$$T = \sqrt{2 \times 4\,\text{m} \times 82.3\,\text{m}} \times 0.243 = 6.23\,\text{m} \tag{10}$$

Dividing this value into the unsaturated thickness then provides an estimate of the number of compartments needed in the simulation (82.3 m/6.23 m = 13.199). The compartment thickness value was modified slightly to 6.331 m because the number of compartments must be a whole number. Figure 7 shows a comparison of the flux predicted by the advection dispersion equation as implemented in GWSCREEN and that produced by FOLAT. Considering the overall uncertainty in any unsaturated transport model, there is virtually no *meaningful* difference between the fluxes generated with FOLAT and GWSCREEN.

[3] Later analysis showed the amount of plume spreading or dispersion is related to the Peclet number (*Pe*) which is given by x/α_L. The number of compartments can be approximated by *Pe*/2.

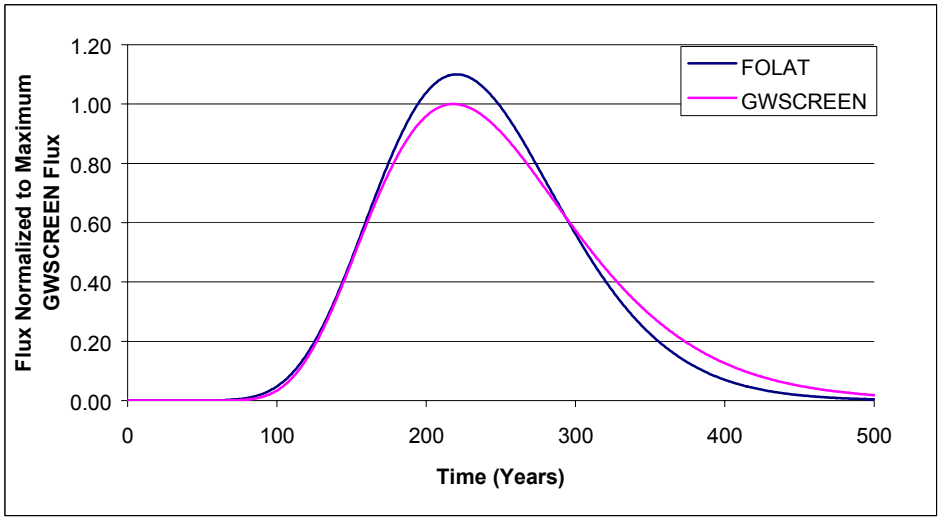

Figure 7. GWSCREEN and FOLAT flux to groundwater normalized to the maximum flux predicted by GWSCREEN for an 82.3 m unsaturated thickness and 4 m dispersivity.

Material Properties of Source and Unsaturated Zone

Material properties included bulk density, saturated hydraulic conductivity, residual moisture content, total porosity and the van Genuchten fitting parameters, α and n. The van Genuchten fitting parameters are used to determine the moisture content for a given water flux. In the original assessment (Rood 2000a), both the source and unsaturated zone had essentially the same properties. The FOLAT model allows for unique material properties assigned to the source and each unsaturated layer. Lithology of the unsaturated zone and surface soils where the trenches are located were provided in Kincaid et al (1998) for the US Ecology site (Table 10) and were used in these simulations without modification. Partition coefficients given in Table 9 are adjusted for the percent gravel content as discussed in the partition coefficient section later in the report. The aquifer was assumed to have the same percent gravel composition as unsaturated layers 2–13.

Table 10. Lithology of the Unsaturated Zone near the US Ecology Site as Described by Kincaid et al. (1998)[a]

Lithology ID	Thickness (m)	FOLAT layer	% Gravel
East Hanford Gravel	10	Source	41.7%
East Hanford Sand	6	Unsaturated 1	17.3%
Lower East Hanford Gravel	91	Unsaturated 2–13	41.7%

[a] Data from Table 4.6 page 4.82. Column ID 299-E19-1 (from Table 4.3).

Water Fluxes in the Unsaturated Zone

Water fluxes in the unsaturated zone were based on data in Gee et al. (1992), Kincaid et al. (1998), and the estimated infiltration rates for the three covers. Natural recharge in the 200 Area was estimated in Kincaid et al. (1998) to be about 0.5 cm yr^{-1}. Gee et al. (1992) estimated natural recharge to range from near zero for vegetated soils containing silt loam, to up to 10 cm yr^{-1} for unvegetated coarse sediment soils. For this assessment, the natural recharge rate is assumed to be 0.5 cm yr^{-1}. The presence of an engineered cover is assumed to limit infiltration through the waste and influence water fluxes through underlying unsaturated layers. During active disposal, a fraction of the site is excavated and water infiltration through open trenches is enhanced. Water infiltration through an open trench was assumed to be 7.5-cm yr^{-1} based on data in Kincaid et al. (1998). Closed trenches within the US Ecology property boundary during operations from 1965 to 2005 are assumed to be disturbed such that infiltration is enhanced over natural background. A value of 3-cm yr^{-1} is assumed for this time period. Because trenches are not individually modeled, infiltration across the modeled source area is area-averaged. The area-averaged infiltration rate as a function of time is given by

$$q_a(t) = q_t\,\varepsilon(t) + q_b\left(1-\varepsilon(t)\right)$$
$$\varepsilon(t) = \frac{A_o(t)}{A_T(t)} \qquad (11)$$

where

$q_a(t)$ = area average infiltration rate as a function of time (m yr^{-1}),
q_t = infiltration rate through an open trench (0.075 m yr^{-1}),
q_b = background infiltration across the site before cover emplacement (0.03 m yr^{-1}),
$\varepsilon(t)$ = the fraction of the total number of trenches that are open at time t,
$A_o(t)$ = area of active trenches at time t (m^2),
$A_T(t)$ = total area of trenches that are open or have closed at time t (m^2).

At the start of the simulation (in year 1965), water fluxes in all layers are initialized at the trench infiltration rate (7.5 cm yr^{-1}). Water fluxes in subsequent years are calculated using a preprocessor to the FOLAT program that calculates the water balance in each layer based on the user-provided water flux at the surface and the hydrologic characteristics of each soil layer. The water flux at the surface is given by Equation 11 for pre-cover times, the design-based cover infiltration rate while the cover is intact, and the background infiltration rate after the cover has failed. The cover is assumed to degrade over a period of time. The water flux through the cover after degradation begins is assumed to linearly increase from the cover designed-based infiltration rate to the natural recharge rate, over the time the cover degrades over.

Once the cover is installed, the unsaturated zone dries over time and eventually moisture contents reach an equilibrium value determined by the amount of infiltration through the cover. After cover failure, the unsaturated zone beneath the trenches is re-wetted and eventually moisture contents reach an equilibrium value determined by the natural recharge. These processes were examined first using a demonstration version of the HYDRUS 2D code (Simunek et al., 1999). The simulation used a simplified homogeneous representation of the unsaturated zone

consisting of sandy loam. Initial conditions were based on the equilibrium water contents assuming a recharge rate of 2 cm yr^{-1}. Boundary conditions included a 200 m long cover in the center of the model domain which limited infiltration to 5×10^{-4} m yr^{-1}. Free drainage was assumed at the base of the unsaturated zone. This simulation was run until water contents equilibrated throughout the domain. Equilibrium conditions were achieved after about 400 years. A second simulation was performed where the equilibrium water contents with the cover in place at 500 years were the initial conditions for the simulation. The cover was assumed to fail instantaneously and therefore, the upper boundary condition was set to a recharge rate of 2 cm yr^{-1}. The results of the two simulations are illustrated in Figure 8. The frames on the left show the advancement of the drying front following placement of the cover. The frames on the right show the advancement of the wetting front after the cover instantaneously fails.

Based on the HYDRUS simulation, the infiltration shadow beneath the composite trench appears to extend vertically down to the aquifer. Drainage from the unsaturated zone also appears to take much longer than re-wetting following cover failure.

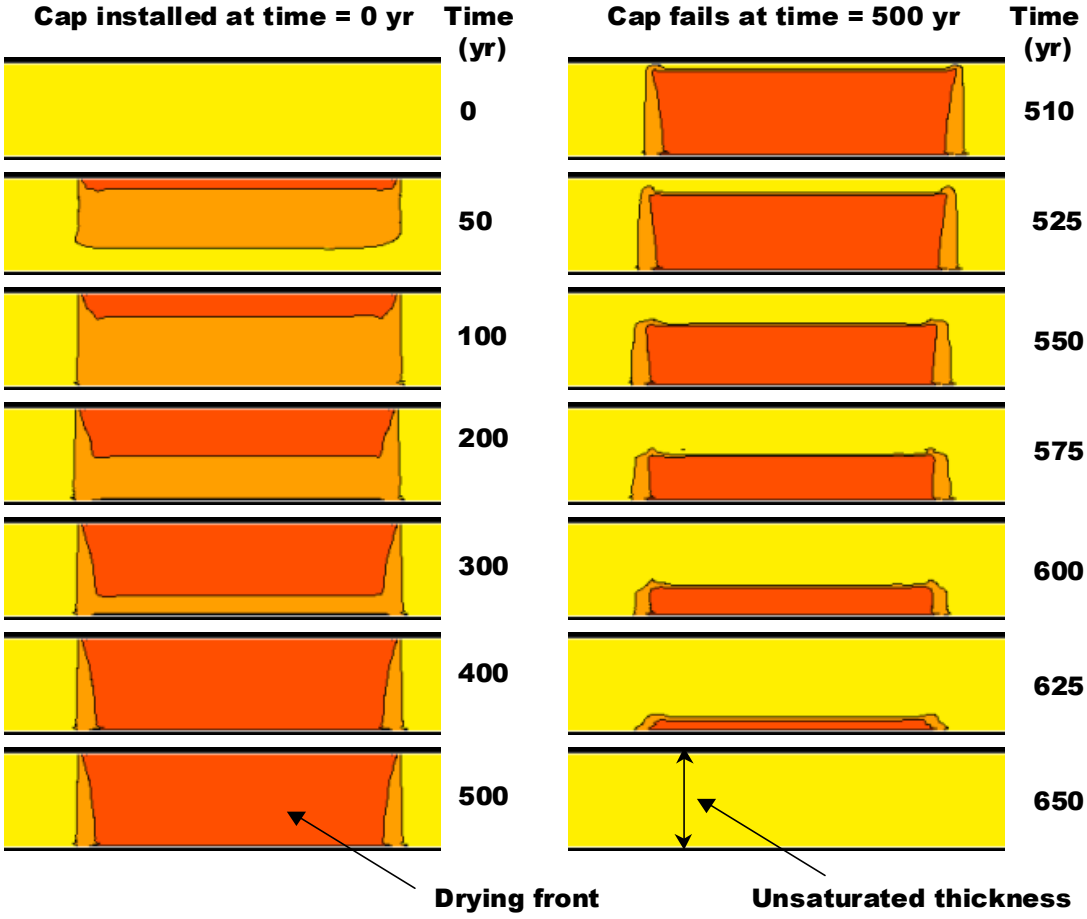

Figure 8. HYDRUS 2D simulation of moisture content profile in the unsaturated zone following cap installation in year zero (left) and cap failure in year 500 (right). Darker shades indicate drier soils. Initially, the moisture content is assumed to be constant throughout the unsaturated zone.

Installation of the cap limits infiltration into the waste and eventually throughout the "infiltration shadow". After cover failure, re-wetting of the unsaturated zone occurs relatively rapidly.

Net water flux at several depths in the unsaturated zone as calculated by the FOLAT preprocessor (FOWL) are illustrated in Figures 9 through 11 for the site soils cover, enhanced cover, and US Ecology proposed cover respectively. Note that the major effects of drying and re-wetting are incorporated into the simulation.

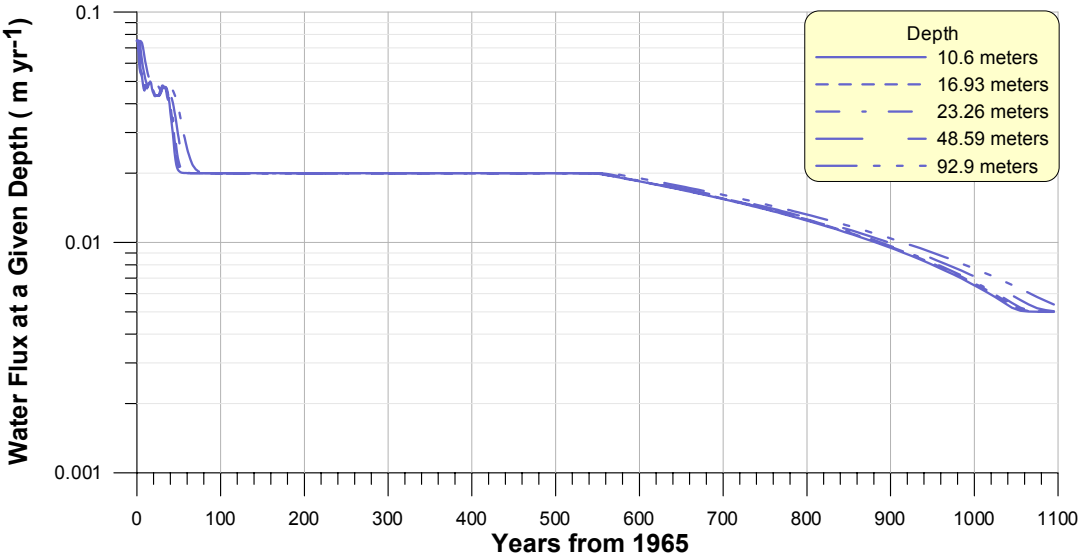

Figure 9. Water flux as a function of time for the site soils cover. Water flux through the site soil cover is 4-times natural recharge. After 500 years, water fluxes begin to return to natural recharge in each unsaturated layer. Water fluxes prior to installation of the cover in the year 2005 are controlled by the fraction of the total trench area that is open during a given year.

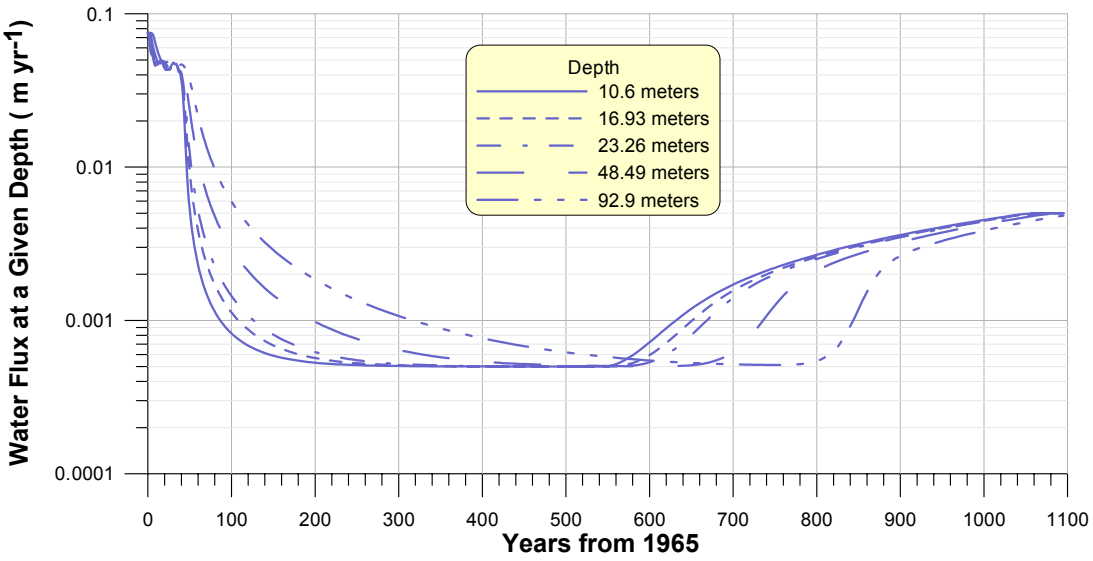

Figure 10. Water flux as a function of time for the enhanced cover. The drying front takes about 800 years to reach the aquifer. Infiltration increases beginning in year 2505, and eventually reaches the natural infiltration rate 1000 years after placement of the cover. Water fluxes prior to installation of the cover in the year 2005 are controlled by the fraction of the total trench area that is open during a given year.

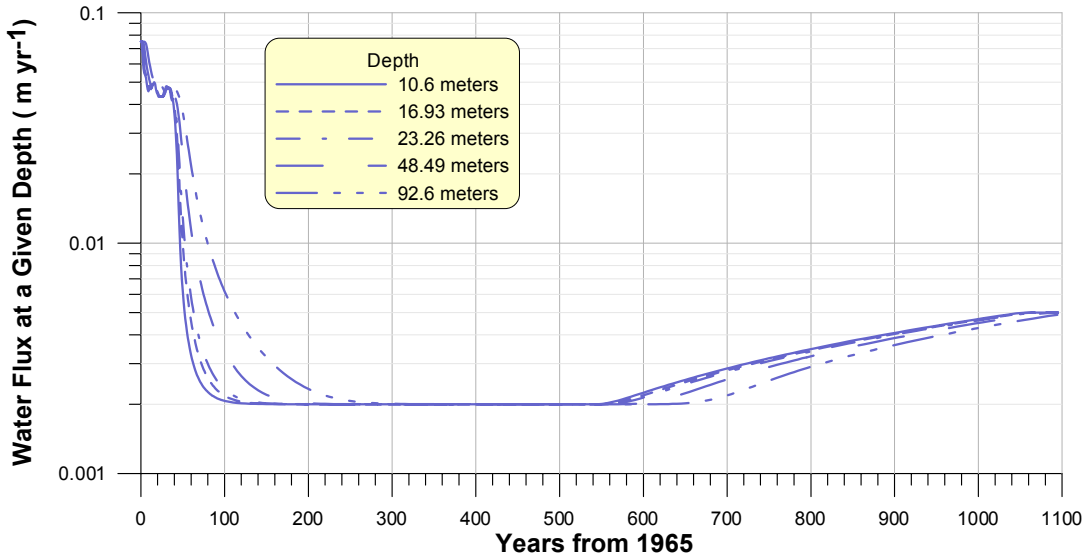

Figure 11. Water flux as a function of time for the US Ecology proposed cover. The drying front takes about 200 years to reach the aquifer. Infiltration increases beginning in year 2505, and eventually reaches the natural infiltration rate at 1000 years after placement of the cover. Water fluxes prior to installation of the cover in the year 2005 are controlled by the fraction of the total trench area that is open during a given year.

Waste Disposal Rates

Time-dependent waste disposal rates were constructed from data provided by WDOH for the radionuclides that had Phase II screening doses greater than 4 mrem yr^{-1}. For scenarios involving operation of the site beyond the year 2003, waste disposal rates were assumed to remain constant for the duration of site operations (year 2056 and year 2215). Figures 12 through 15 illustrate the disposal histories from 1965 to 2002, and the projected waste disposal rate to 2005. Figure 15 includes Ni-63 and Sr-90. Although these radionuclides were previously screened from the analysis, they have been included here because these radionuclides were detected in borehole samples taken at considerable depth below trenches. See the "Evaluation of Borehole Data" section later in this report for more details.

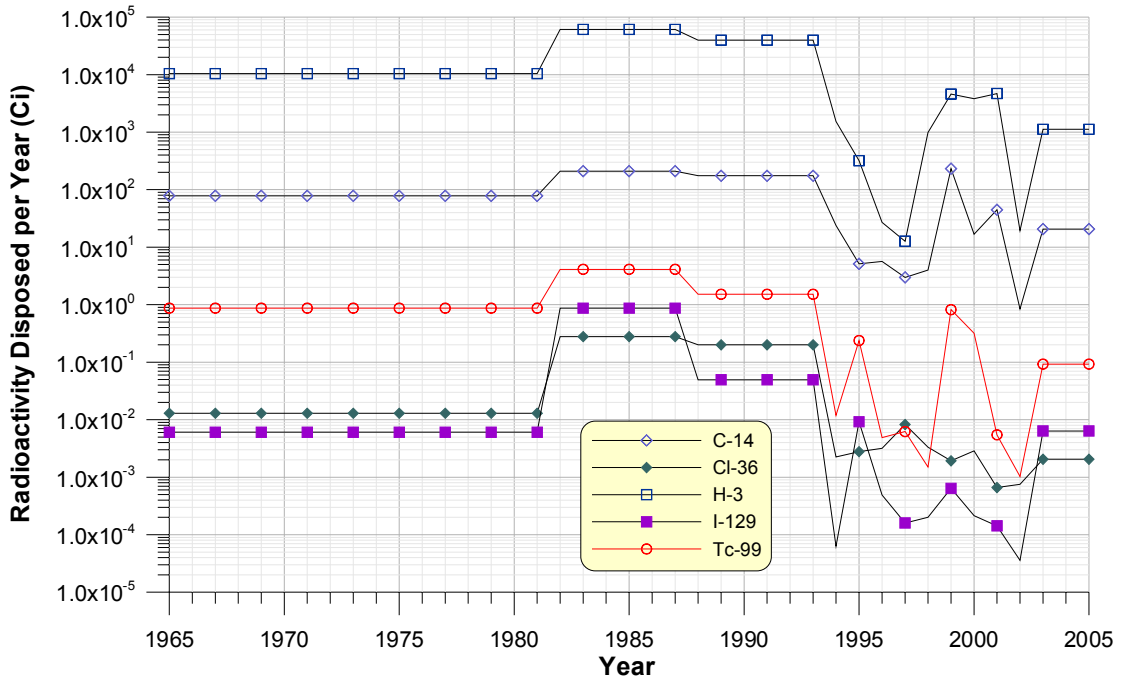

Figure 12. Radioactivity disposed in the US Ecology LLRW facility as a function of time for C-14, Cl-36, H-3, I-129, and Tc-99.

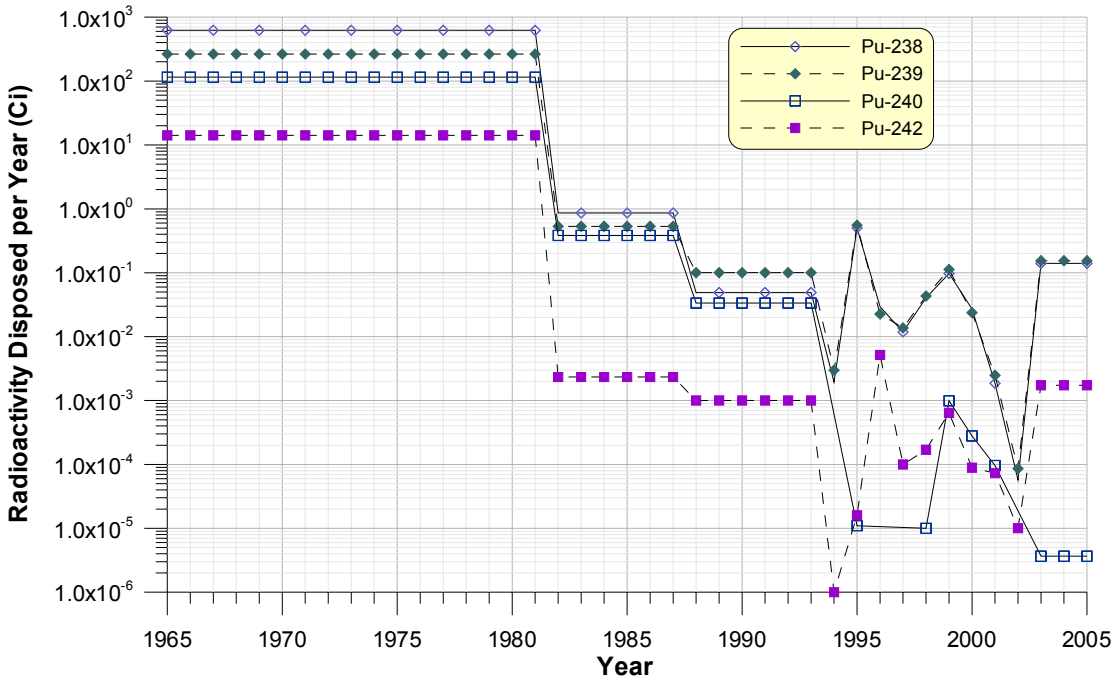

Figure 13. Radioactivity disposed in the US Ecology LLRW facility as a function of time for Pu-238, Pu-239, Pu-240, and Pu-242.

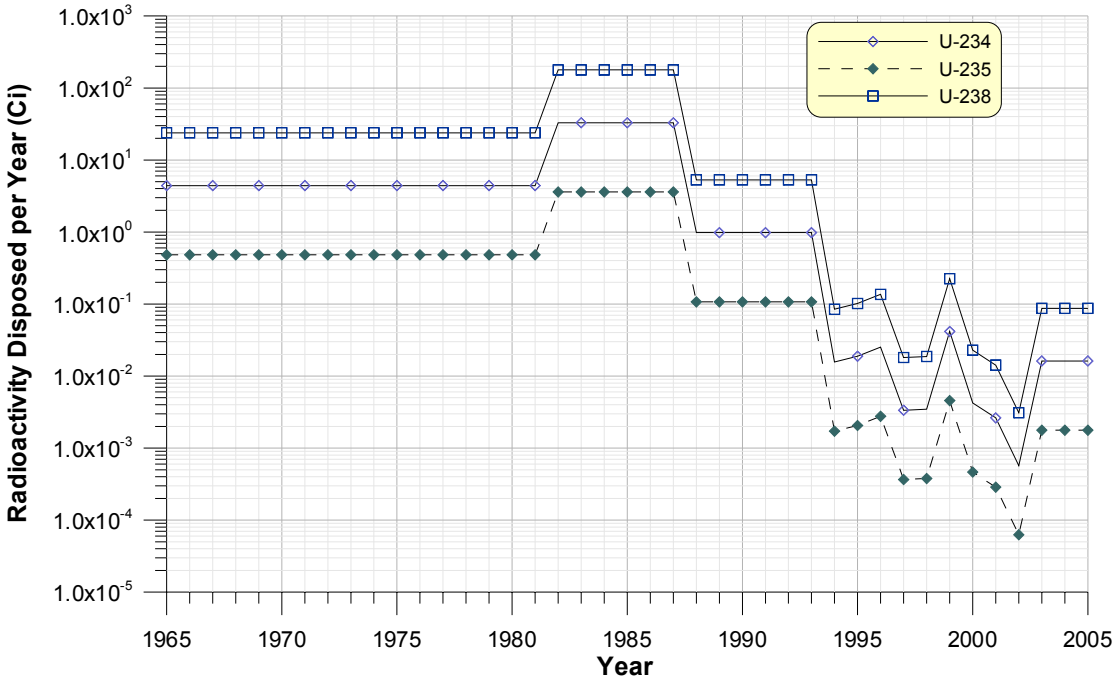

Figure 14. Radioactivity disposed in the US Ecology LLRW facility as a function of time for U-234, U-235, and U-238.

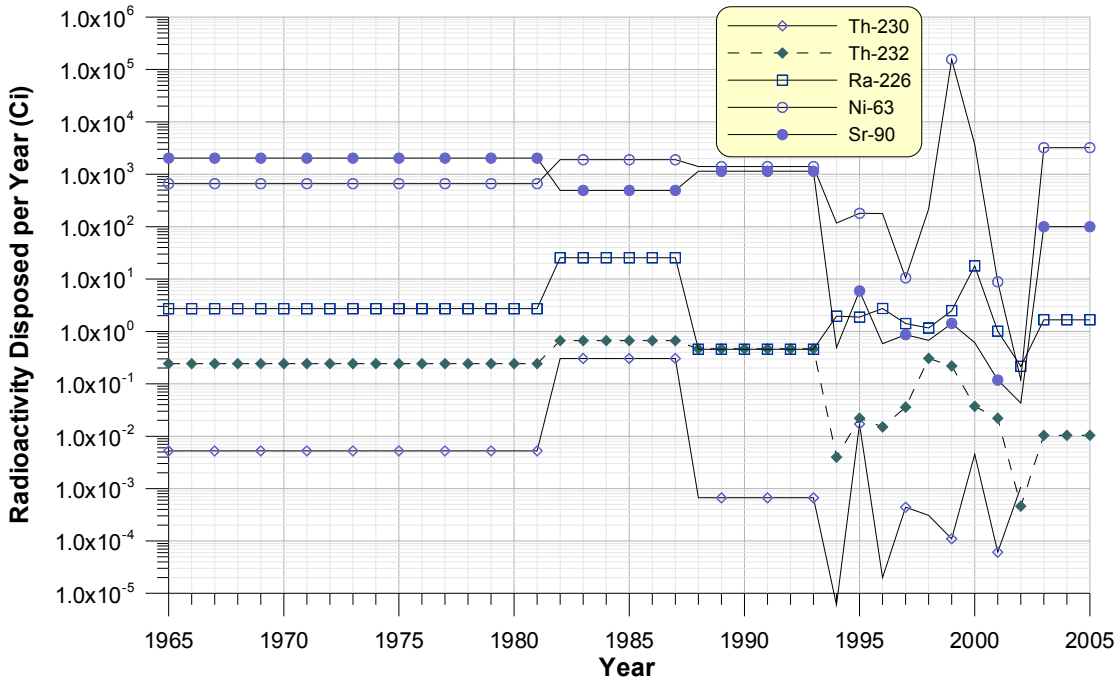

Figure 15. Radioactivity disposed in the US Ecology facility as a function of time for Th-230, Th-232, Ra-226, Ni-63, and Sr-90.

Discussion of Partitioning Coefficients

In this section, we first review the partitioning coefficients that were used in the 200 Area Composite Analysis (Kincaid et al 1998). We then qualitatively evaluate the partitioning coefficients used for the US Ecology site in the 200 Area Composite Analysis (Kincaid et al. 1998) in light of recent measurements of radionuclides in boreholes beneath trench 5 and introduce a transport model that may explain the radionuclide measurements below trench 5.

The 200 Area Composite Analysis (Kincaid et al. 1998) provided estimates of element-specific K_d values for six different geochemical environments identified as A through F. In general, the A environment (described as high organic and very acidic) had the lowest K_d values and the F environment (described as low organic, low salt, and near neutral) had the highest K_d values. Geochemical environments were then assigned to three zone categories; high impact, intermediate impact, and low impact/groundwater.

The high impact zone category was defined as the area in the unsaturated zone near the source that is impacted by the chemical composition of the waste, particularly any contaminated liquids that were disposed. Organic compounds, pH, and salt, when present in the source may affect the K_d values. The high impact zone category has the lowest K_d values

The intermediate impact zone category was assigned to the unsaturated zone where the excessive acidic or basic nature of the waste has been neutralized by the buffering capacity of the natural soil and no pH effects of the plume remain.

The low impact/groundwater zone category was defined in the unsaturated zone and unconfined aquifer where K_d values are not affected by the chemical composition of the

contaminant plume. The chemical properties of the waste are assumed to be so greatly diluted that they do not affect the K_d value. The groundwater zone category has the highest K_d values.

In the 200 Area composite analysis (Kincaid et al. 1998), the US Ecology site was assigned a geochemical environment described as low organic/low salt/near neutral (geochemical environment F) for all soils in the unsaturated zone and aquifer. Consequently, the same K_d values were assigned to all geologic media (although K_d values were modified for the percent gravel in the lithology).

The K_d values used for the US Ecology site in the 200 Area Composite Analysis (Kincaid et al. 1998) are relatively high; for example, the nickel K_d was estimated to be 300 mL g^{-1}. A K_d of this magnitude for nickel would result in little present-day migration of nickel to the unsaturated zone and is at odds with recent measurements of Ni-63 in boreholes beneath Trench 5.

It is beyond the scope of this assessment to fully investigate the mobility of each radionuclide of interest. Radionuclide transport may be a function of many other processes such as colloid transport, presence of complexing agents, and preferential flow paths. In the next section, we examine the borehole data and propose a mobile-fraction transport model that may explain the observed distributions of radioactivity with depth for the radionuclides detected. The mobile-fraction transport model separates radionuclide inventories into a mobile and immobile fraction. The mobile fraction is then calibrated to the measured borehole data for the radionuclides where measurements are available. For the immobile fraction, we have used the K_d values reported in Kincaid et al. (1998) for geochemical environment F without modification. Partition coefficients reported in Table 9 were later modified by the percent gravel in the rock matrix because sorption was assumed to take place only on the fine material and not the course gravel component. The partition coefficient adjusted for gravel content is given by

$$K_d(adjusted) = K_d \times (1 - f_g) \tag{12}$$

where f_g is the fraction of gravel in the rock matrix.

Evaluation of Borehole Data

In 1999, US Ecology conducted a comprehensive facility investigation (US. Ecology 1999). Part of the investigation was to examine radionuclide migration from the disposal trenches, which entailed the drilling of four boreholes to a depth of about 21.3 m (70 feet) below the trench bottom. Two boreholes were drilled adjacent trench 5 (borehole C and D) and two adjacent the chemical disposal trench (borehole A and B). Radionuclides were measured as a function of depth below the boreholes and included Ni-63, Sr-90, Tc-99, Pu-238,239/240, U-234,235,238, Th-230,232, and Ra-226 (Appendix A).

Nickel-63 and Sr-90 had soils concentrations above the minimum detectable concentration (MDC) in almost all the samples and showed relatively uniform concentration with depth. These results included the samples taken beneath chemical trench, which presumably received no radionuclides. This distribution reflects relatively rapid transit times in the unsaturated zone. In fact, to produce the observed depth distribution, the radionuclides would have to been traveling with infiltrating water with essentially no sorption on the rock matrix, which is at odds with laboratory data on the mobility of strontium and nickel.

Plutonium had several samples with plutonium concentrations at or above the MDC. These occurred only in samples taken below the chemical disposal trench.

Uranium, thorium and radium isotopes all had soil concentrations above the MDC. Minor (2001) reviewed these data and concluded "*...the analytical results of nine vadose zone samples agree well with local background concentrations and/or represent data whose quality appear to be reliable—potassium-40; 226- and 228-radium; 228-, 230-, and 232-thorium; and 234-, 235-, and 238-uranium.*" Analysis of uranium isotopic ratios in the borehole samples however suggested that the some of the uranium detected was anthropogenic in nature. If the uranium measured in the boreholes represented naturally occurring uranium in soils, then we would expect the relative proportions of U-238, U-235, and U-234 to be close to their natural abundance (Table 11). However, the mean U-235 weight percent in borehole samples (Table 12) was substantially higher than that for natural uranium, and in fact, was closer to that of enriched uranium. (see Appendix A). Assuming a U-235 enrichment of 3% by weight, the weight percent of U-234 also increases from 0.0054% to 0.017% based on the empirical relationship proved in Bowman and Suto (1996). Although the measured U-235 weight percent appears to suggest an enriched source of uranium, the U-234 weight percent is close to what would be expected from natural uranium. Of the 37 samples analyzed for U-235, 26 were above the MDC (compared to all U-238 and U-234 samples), suggesting greater uncertainty in the U-235 measurement. It is unknown whether a systematic positive bias existed in the U-235 sample analysis. Another interesting observation is that U-238 concentrations in borehole B are substantially lower than those in the other boreholes. If the uranium were from natural sources, then we would expect uranium concentrations in all boreholes to be about the same. It is beyond the scope of this assessment to examine this issue any further. For the purpose of model calibration, we have assumed the U-238 detected in borehole B represents natural sources and subtracted the depth-averaged value (0.048 pCi g^{-1}) from values in boreholes C and D. The net U-238 concentrations were then assumed to be derived entirely from the waste disposed. Calibration was not performed for U-235 and U-234.

Table 11. Properties of Uranium-234, -235, and -238 for One Mole of Natural Uranium.

Isotope	Specific Activity (Ci g^{-1})	% isotopic abundance	Mass (g)	Activity (Ci)	% weight abundance
U-238	3.35172E-07	99.2745%	236.27	7.9192E-05	99.2836%
U-235	1.90291E-06	0.7200%	1.692	3.2197E-06	0.7110%
U-234	6.24393E-03	0.0055%	0.01287	8.0359E-05	0.0054%

Table 12. Statistics of the Distribution of U-238, U-235 and U-234 Percent Weight Abundance in Bore Hole Samples

Statistic	U-238 % weight abundance	U-235 % weight abundance	U-234 % weight abundance
Mean	95.9209%	4.0734%	0.0057%
Standard Deviation	2.6592%	2.6590%	0.0014%
Minimum	90.3091%	1.0347%	0.0042%
Maximum	98.9591%	9.6862%	0.0106%
Number of observations	26	26	26

Release and Transport Model Simulations of Trench 5

The measured concentrations in boreholes C and D (taken below trench 5) and the estimated radioactivity disposed of in trench 5 provide the necessary data to construct a release and transport model of the trench. The chemical trench presumably received no radionuclides and therefore, there is no estimate of the amount of radioactivity that the trench received. For this reason the chemical trench was not modeled. The model considers radioactive waste disposed in the trench in the years 1978–1979. During active disposal, the trench is open and there is no runoff. An infiltration rate of 7.5 cm yr^{-1} is assumed during active disposal, consistent with the estimate of Kincaid et al (1998). During the period the trench was open (April 1978 to September 1979), 22.9 cm of precipitation was recorded at Pasco according to precipitation records obtained from the National Climatic Data Center, so the assumed infiltration rate during this period is reasonable. After closure of the trench, infiltration is assumed to be reduced to 3 cm yr^{-1}. Radionuclide concentration profiles below the trench suggest the radionuclides are moving with the infiltrating water with little or no sorption. To account for the observed radionuclide distribution in soil, the proposed model assumes that there is a small, but mobile fraction of radionuclides in the waste. This fraction, referred to as the mobile fraction hereafter, is easily leached and moves with the infiltrating water. The mechanism for movement could be colloidal transport or chemical complexation with chemicals that may have been disposed of in the trench. However, the model is empirical in nature and does not attempt address the mechanisms of release or transport.

The viability of the proposed model is evaluated by comparing the activity below the trench to the estimated activity in the trench. Assuming the soil concentrations are horizontally uniform across the area beneath the trench, the amount of activity that is below the trench (to a depth of 21.3 m below the bottom of the trench) can be estimated by numeric integration. The integrated activity is given by

$$Q = A\,\rho \int_0^b C(x)\,dx \tag{13}$$

where

Q = integrated activity from the bottom of the trench to depth b (Ci)
A = area of the trench (m^2)
$C(x)$ = soil concentration as a function of depth (Ci g^{-1})
ρ = bulk density of soil (1.9×10^6 g m^{-3})
b = depth below trench (m)

The function, $C(x)$ was generated by averaging the soil concentrations in borehole C and D at each depth. The activity disposed of in trench 5 was estimated from the total radioactivity disposed from 1965 to 1981 reported by WDOH (Table 13). It was assumed that each trench that was open during the 1965 to 1981 time frame received an equal amount of radioactivity. Seven trenches were operating during this time, therefore, the estimated activity disposed in trench 5 was the total 1965 to 1981 disposed radioactivity divided by seven. Measured concentrations of Pu-239 and Pu-240 were not segregated and reported as single value because it is almost

impossible to resolve the two isotopes using alpha spectroscopy. The primary alpha decay energy for Pu-239 is 5.156 MeV (73.1%) and 5.168 MeV (73%) for Pu-240. Therefore, inventories of Pu-239 and Pu-240 were summed.

Table 13. Estimated Radionuclide Inventories Disposed in Trench 5 and Integrated Radionuclide Radioactivity below Trench 5 to a Depth of 21.3 m Below the Bottom of the Trench

	Ni-63	Sr-90	Tc-99	Pu-239/240	U-238	Pu-240	Pu-239
Total 1965-81 inventory (Ci)	1.127E+04	3.462E+04	1.481E+01	6.444E+03	4.054E+02	1.949E+03	4.494E+03
Estimated inventory in trench 5 (Ci)	1.610E+03	4.946E+03	2.116E+00	9.205E+02	5.791E+01	2.785E+02	6.420E+02
Integrated radioactivity to 21.3 m below trench 5 (Ci)	4.932E-01	3.428E-02	6.322E-02	2.379E-03	1.162E-02	n/a	n/a

The integrated radioactivity below the trench may not represent the total radioactivity released from the trench. The mobile-fraction model was used to determine the total activity released from the trench by calibrating the mobile fraction inventory to the distribution of soil concentrations below the trench.

The objective of the calibration was to match radionuclide concentrations in the borehole samples taken below trench 5 to the model-estimated concentrations in unsaturated layers 1–3 which lie at a depth between 10.6 m to 29.5 m (35 ft to 96.8 ft) below ground surface. Measured concentrations were averaged across the thickness of each unsaturated layer. The three unsaturated layers correspond to following depths below the ground surface: 10.6 to 16.9 m for unsaturated layer 1, 16.9 to 23.26 m for unsaturated layer 2, and 23.26 to 29.6 m for unsaturated layer 3. Measured concentrations that were below the minimum detectable concentration (MDC) were assumed to be equivalent to the MDC for this calculation, which provides a conservative estimate of the radioactivity below the trench. The FOLAT model outputs radionuclide pore water concentrations and moisture contents in each layer as a function of time. Radionuclide pore water concentrations in each layer were converted to radioactivity per unit mass (pCi g^{-1}) using

$$C_m = \frac{\theta C_w \left(1 + \frac{K_d \rho}{\theta}\right)}{\rho} \tag{14}$$

where

C_m = radionuclide concentration per unit mass of soil (pCi g^{-1})
C_w = radionuclide concentration in pore water (pCi cm^{-3})
θ = moisture content (cm^3 cm^{-3})
ρ = bulk density of soil (g cm^{-3}).

For comparison, the DUST model (Sullivan 1996) was also run in parallel with FOLAT. The DUST model uses a finite-difference approximation to the advection-dispersion equation to solve for concentrations in the unsaturated zone and provides a verification of the FOLAT model output. Additionally, DUST outputs concentrations on a finer scale than FOLAT, which was important for illustrating the relative migration of the mobile and immobile fraction in the

unsaturated zone. However, the finer scale was not important for calculating flux to the aquifer and for this and other reasons stated earlier, DUST was not utilized in the overall assessment model.

The primary calibration objective was to minimize the bias in the average predicted concentrations over the sampling depth, although a slight positive bias (indicating model overprediction) was considered acceptable. A second calibration objective was to minimize the residuals between the predicted and observed concentrations. Calibration objectives were achieved by adjusting the fraction of the radionuclide inventory that is considered mobile until the calibration objective was met. Model calibration was based only on the FOLAT simulations.

The metrics used to evaluate model calibration incorporate several performance measures commonly used in evaluation of atmospheric transport models (Fox 1981; EPA 1988; Cox and Tikvart 1990). These measures were the fractional bias (*FB*) and normalized mean square error (*NMSE*). The *FB* was given by

$$FB = \frac{2\left(\overline{C_o} - \overline{C_p}\right)}{\left(\overline{C_o} + \overline{C_p}\right)} \tag{15}$$

where C_p and C_o were the predicted and observed concentrations, respectively. Overbars indicated averages over the sample. The *NMSE* was given by

$$NMSE = \frac{\overline{\left(C_o - C_p\right)^2}}{\overline{C_o}\,\overline{C_p}} \tag{16}$$

The *FB* is a measure of the mean bias. A *FB* of 0.67 is equivalent to model under prediction by a factor of 2. A negative value indicates model over prediction. A *FB* value of ±0.3 indicates model bias is roughly ±25%. That is, model predictions are either over- or under predicted by factor of 1.35.

The *NMSE* is a measure of model variance. A *NMSE* value of 1.0 indicates that the typical difference between predictions and observations is approximately equal to the mean. A perfect model would have a *FB* and *NMSE* of zero. Our calibration targets for *FB* and *NMSE* were abs(*FB*) ≤ 0.1 and *NMSE* ≤ 0.1, although these targets were not met in all cases. Excursions of abs(*FB*) above 0.1 were acceptable is the *FB* was negative, indicating model over prediction.

Results of the calibration (Table 14) indicate that all calibration objectives were met. Figures 16 and 17 illustrate the measured and model predicted concentrations as a function of depth below the trench for Ni-63 and Sr-90. The measured data shown are the average concentration in borehole C and D at each sampling depth. The DUST simulation includes both the mobile and immobile fractions. The immobile fraction only migrates about a meter below the bottom of the trench whereas the mobile fraction extends beneath the 21.3 m sampling depth from the bottom of the trench. The measured data in Table 14 are the layer-averaged concentrations. Release fractions were also calculated and are consistent with what we might expect. Technetium-99 had the highest release fraction, which might be expected because it has a low capacity for sorption and is relatively mobile in the environment. It is suspected that the Tc-99 concentrations probably reflect some dissolved-phase transport with some partitioning occurring

in the waste form. However, it is important to note that if we assumed the *entire* Tc-99 inventory moved with the infiltrating water, then the model-predicted concentrations in the unsaturated zone would be much greater than what was observed.

Table 14. Results of Model Calibration to Trench 5 Measurement Data using FOLAT

	Ni-63	Sr-90	Tc-99	Pu-239/240	U-238[d]
Measured concentration in unsaturated layer 1 (pCi g^{-1})[a]	5.48E+00	1.60E-01	5.67E-01	2.45E-02	9.50E-02
Measured concentration in unsaturated layer 2 (pCi g^{-1})[b]	4.73E+00	8.65E-02	6.12E-01	2.53E-02	9.15E-02
Measured concentration in unsaturated layer 3 (pCi g^{-1})[c]	5.07E+00	1.44E-01	5.72E-01	2.33E-02	1.22E-01
Predicted concentration in unsaturated layer 1 (pCi g^{-1})	6.60E+00	1.65E-01	7.58E-01	3.18E-02	1.02E-01
Predicted concentration in unsaturated layer 2 (pCi g^{-1})	5.30E+00	1.32E-01	6.09E-01	2.55E-02	1.06E-01
Predicted concentration in unsaturated layer 3 (pCi g^{-1})	3.94E+00	9.85E-02	4.53E-01	1.90E-02	1.07E-01
Fractional bias	-3.59E-02	-1.22E-02	-3.81E-02	-4.51E-02	-2.17E-02
Normalized mean square error	3.51E-02	8.16E-02	4.77E-02	3.84E-02	1.47E-02
Calibrated mobile release quantity (Ci)	1.00E+00	3.50E-02	1.00E-01	4.20E-03	2.00E-02
Calibrated mobile fraction	6.21E-04	7.08E-06	4.73E-02	4.56E-06	3.45E-04

a. Average of samples taken between 0, 2.4, and 5.2 m below bottom of trench.

b. Average of samples taken between 7.9 and 10.7 m below bottom of trench

c. Average of samples taken between 13.4 and 21.3 m below bottom of trench

d. A background value of 0.048 pCi g^{-1} was subtracted from the measured concentration.

The other radionuclide (Ni-63, Sr-90, Pu-239/240, and U-238) exhibit much lower release fractions. These nuclides are known to sorb and would move little in the 20-year period (1979–1999) if only dissolved-phase transport were considered. The presence of organic matter and acidic conditions may enhance dissolved-phase transport; however, total organic carbon measurements below the trench were typically less than 1000 mg kg^{-1} or <0.1% by weight, which is on the lower end of the distribution of organic carbon contents observed in soils (Lyman et al. 1982). Release fractions for plutonium and strontium were similar, but uranium and nickel were about 2 orders of magnitude greater. The release fraction calculation is sensitive to the estimated initial inventory. Evaluation of the uncertainty in the inventory estimate was beyond the scope of this project, but is recommended for future work.

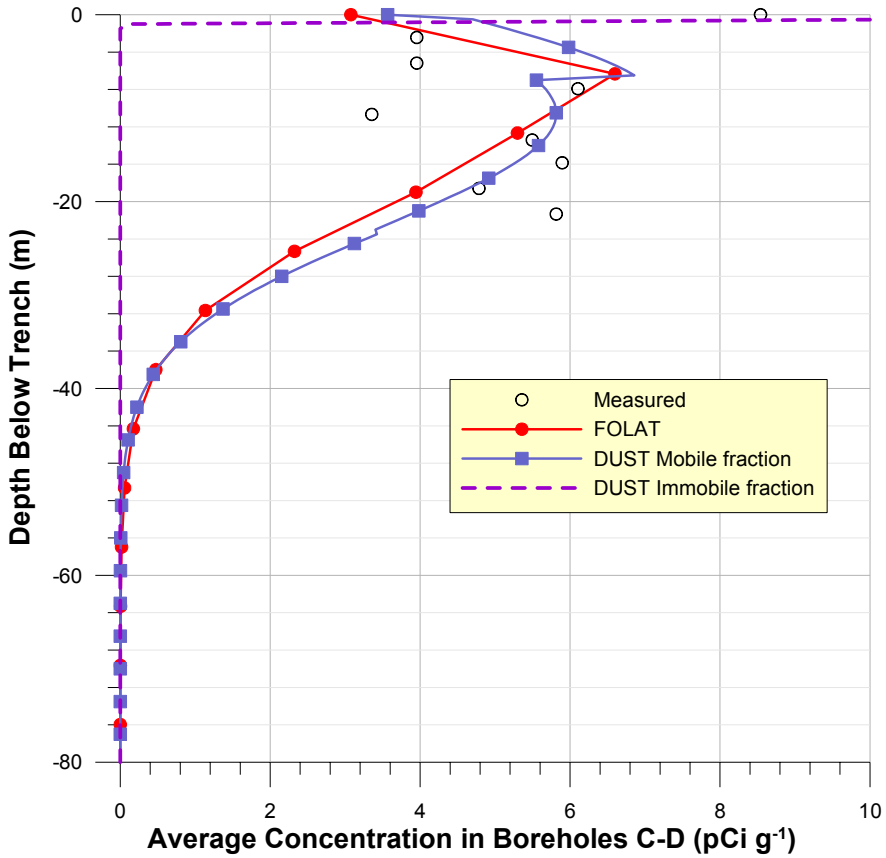

Figure 16. Predicted and observed Ni-63 soil concentrations below trench 5. The concentrations predicted with DUST include the mobile and immobile fraction. The immobile fraction was calculated using the K_d values for geochemical environment F as described in Kincaid et al. (1998). Measured concentrations represent the average between boreholes C and D at each sampling depth.

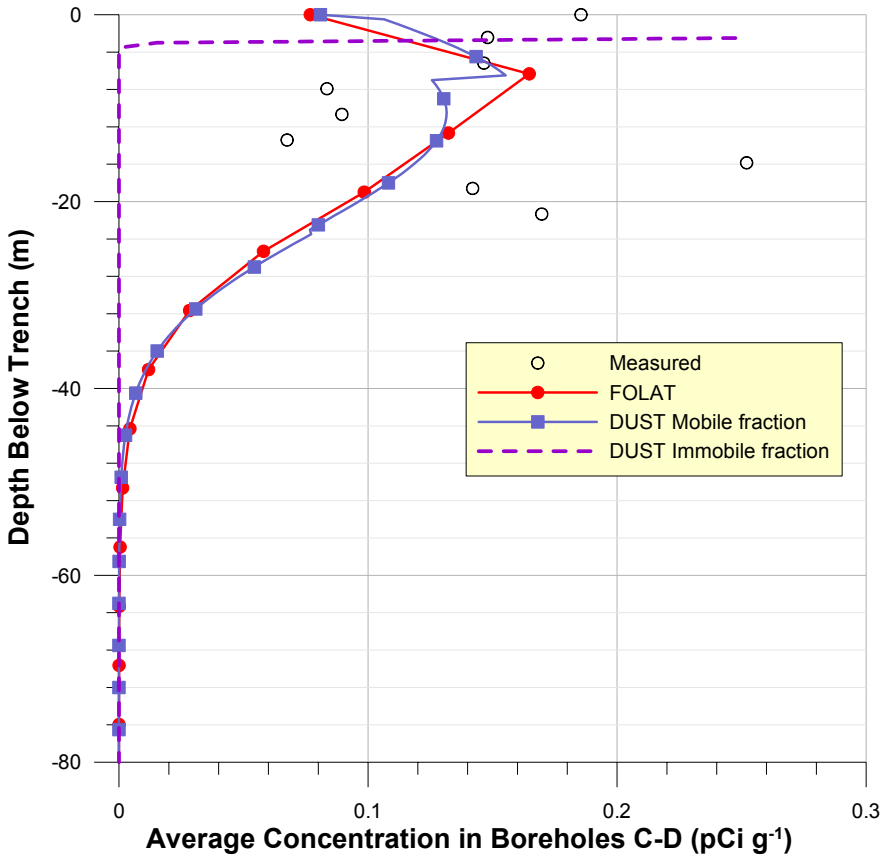

Figure 17. Predicted and observed Sr-90 soil concentrations below trench 5. The concentrations predicted with DUST include the mobile and immobile fraction. The immobile fraction was calculated using the K_d values for geochemical environment F as described in Kincaid et al. (1998). Measured concentrations represent the average between boreholes C and D at each sampling depth.

Colloid transport appears to be a viable mechanism to explain the observed distribution of radionuclides with depth below the trench. This mechanism involves either the physical movement of colloid-sized (0.1 – 1 μm) particles of the radionuclide itself, or physical movement of a radionuclide attached to a colloidal-sized soil particle. Colloids will move with the infiltrating water until they are physically trapped within the rock matrix. Additionally, water fluxes may need to reach some minimum threshold in order for the colloid to move. For this assessment, we have assumed that colloids behave as a dissolved substance with no sorption and move with the velocity of infiltrating water. This assumption provides a conservative estimate of radionuclide flux to the aquifer because colloids are assumed to never be physically trapped within the rock matrix, and there is no water flux threshold for their movement. Colloid transport is currently an area of ongoing research and it is beyond the scope of this assessment to investigate this transport mechanism any further. However, the mobile-fraction model employed provides radionuclide concentrations in the unsaturated zone that are consistent with measured data and provides conservative estimates of radionuclide fluxes to the groundwater.

Integration of the Mobile Release Fraction and Partition Coefficients

Based on the results of the mobile-fraction model calibration, a fraction of each radionuclide in the inventory (except H-3, Tc-99 and Cl-36) was assumed to be mobile. The fraction was only applied to the 1965-2002 inventory. Future disposals were assumed to be controlled so as to minimize mobile-fraction releases. The mobile fraction was based on assumed similarity to other isotopes and/or sorption characteristics. Mobile release fractions were assigned as follows

- A mobile release fraction of 3.45×10^{-4} was assigned to all uranium isotopes
- A mobile release fraction of 6.21×10^{-4} was assigned to I-129 and C-14
- A mobile release fraction of 4.56×10^{-6} was assigned to all plutonium, thorium and radium isotopes
- A mobile release fraction of 1.0 was assigned to tritium

Iodine-129 and C-14 were assumed to have the same mobile release fraction as Ni-63 not because these radionuclides are chemically similar to nickel, but because nickel had the highest mobile release fraction (with the exception of Tc-99, see discussion in next paragraph). Tritium can move both in a dissolved phase and vapor phase. Vapor phase transport would likely result in a substantial quantity of H-3 released to the atmosphere. For this groundwater assessment, we have conservatively assumed all the tritium moves down with infiltrating water.

A mobile release fraction for Tc-99 is more complicated, because some of the Tc-99 detected in the unsaturated zone was probably from dissolved-phase transport. For Tc-99 and the other mobile radionuclide (Cl-36) an "effective" K_d in the source was calculated by calibrating the predicted Tc-99 integrated activity from the bottom of the trench to a depth of 21.3 m below the trench to the corresponding integrated measured activity using the *total* activity disposed of in trench 5. This "effective" K_d represents partitioning from the waste form into infiltrating water. If we were to apply the nominal K_d value of 0 mg L^{-1} to the entire Tc-99 inventory in the trench, then concentrations in the unsaturated zone would be grossly overpredicted. Recall that only 4.73% of the Tc-99 inventory was estimated to have left trench 5. Because the nominal K_d value in the unsaturated zone is zero for Tc-99 and Cl-36, transport times will be the same as the mobile release fractions.

For the remainder of the radionuclides (excluding Tc-99, Cl-36, and H-3), immobile fraction leaching from the trench and transport in the unsaturated zone and aquifer used partition coefficients for geochemical environment F provided in Kincaid et al. (1998).

Both Ni-63 and Sr-90 were eliminated from further consideration in the Phase II screening. To evaluate the radiological dose potential for the mobile fraction of these radionuclides, an additional screening exercise was performed. The Ni-63 and Sr-90 mobile fraction was multiplied by the 1965–2215 inventory (877,535 Ci for Ni-63 and 65,688 Ci for Sr-90) and the entire mobile fraction inventory was assumed to be placed instantaneously in trench 5. A GWSCREEN simulation was run using the Phase II screening infiltration and transport parameters. A receptor well was placed on the downgradient edge of the trench. The maximum doses for Ni-63 and Sr-90 were 0.037 mrem yr^{-1} and 0.021 mrem yr^{-1} respectively. Because these doses were below the screening cutoff of 4 mrem yr^{-1}, further consideration of the nuclides was not warranted.

DETERMINISTIC AQUIFER FLUXES, CONCENTRATIONS, AND DOSES

In this section, integrated radionuclide fluxes to the aquifer, aquifer concentrations, and drinking water doses are presented. Drinking water doses are calculated assuming 2 liters of water are ingested per day for 365 days per year and using the ICRP ingestion dose conversion factors presented earlier in Table 6. Because of the large volume of output generated by the transport model, integrated radionuclide fluxes to the aquifer and groundwater concentrations are only summarized in tables. Detailed output is available electronically via Microsoft Excel spreadsheets and the raw ASCII output for each of the radionuclides analyzed. Doses are presented graphically for each cover/closure scenario. Results are presented on a time scale that begins in the year 1965, the year the US Ecology began operations.

Radionuclide Fluxes to the Aquifer

Radionuclide fluxes to the aquifer were numerically integrated from zero to 10,000 years using a Simpson Rule integration routine (Press et al. 1992) and the unsaturated-saturated radionuclide fluxes generated by the FOLAT model (Table 15). Each FOLAT simulation was truncated at 100,000 years and radionuclide fluxes to the groundwater were set to zero after this time. The integrated fluxes provide a measure of the overall source-unsaturated zone mass balance and the relative merits of each of the cover designs.

Cover design had a minor impact on the integrated radionuclide flux to the aquifer for long-lived mobile radionuclides (Cl-36, Tc-99) and the mobile fraction of relatively immobile radionuclides. However, groundwater concentrations are also influenced by the rate of radionuclide release, which is a function of the infiltration rate through cover. Higher infiltration rates result in higher radionuclide fluxes to the aquifer and higher radionuclide concentrations in the aquifer. The integrated flux to the groundwater may be the same for low and high infiltration rates.

Integrated radionuclide fluxes to the aquifer for relatively short-lived radionuclides (C-14 and H-3) exhibit greater sensitivity to cover design. For example, there is factor of 2.6 decrease in the integrated H-3 flux between the enhanced cover and site soils cover. Cover design influences the 0–10,000 year integrated radionuclide aquifer flux for the immobile actinide fraction primarily by delaying the arrival time in the aquifer. For some of the shorter-lived plutonium and thorium isotopes (Pu-238 and Th-230) and Ra-226, little of the total immobile radionuclide inventory ever reaches the aquifer because of radioactive decay.

There appears to be a discrepancy in the fraction released to groundwater for the immobile fraction of the uranium isotopes. The fraction released to groundwater for the U-234 and U-235 immobile fractions are about the same, but the corresponding U-238 value is substantially smaller. The reason for this is the U-238 release is solubility limited whereas U-234 and U-235 releases are not. Because the specific activity of U-238 is much smaller than U-234 or U-235, and there is much more U-238 disposed, the uranium solubility controls the release of U-238 from the source.

Table 15. Zero to 10,000 year Integrated Groundwater Fluxes for the Three Cover Designs and Year 2056 Closure Date

Radionuclide[a]	Site soils cover (Ci)	Fraction released to aquifer	Enhanced cover (Ci)	Fraction released to aquifer	Proposed cover (Ci)	Fraction released to aquifer
H-3	1.82E+03	2.12E-03	7.00E+02	8.14E-04	7.12E+02	8.28E-04
C-14	1.56E+03	3.07E-01	5.42E+02	1.07E-01	6.09E+02	1.20E-01
C-14MF	2.45E+00	9.80E-01	2.19E+00	7.86E-01	2.26E+00	8.11E-01
Cl-36	3.22E+00	9.98E-01	3.08E+00	9.55E-01	3.10E+00	9.60E-01
I-129	4.22E+00	7.07E-01	1.76E+00	2.95E-01	1.96E+00	3.28E-01
I-129MF	3.51E-03	1.00E+00	3.51E-03	9.93E-01	3.51E-03	9.93E-01
Tc-99	5.36E+01	9.73E-01	5.12E+01	9.30E-01	5.15E+01	9.35E-01
U-238	1.23E-04	8.14E-08	3.80E-06	2.52E-09	5.22E-06	3.46E-09
U-238MF	5.17E-01	1.00E+00	5.16E-01	9.89E-01	5.16E-01	9.90E-01
U-235	4.63E-05	1.51E-06	1.40E-06	4.59E-08	1.93E-06	6.31E-08
U-235MF	1.05E-02	1.00E+00	1.05E-02	9.90E-01	1.05E-02	9.90E-01
U-234	4.13E-04	1.48E-06	1.25E-05	4.47E-08	1.72E-05	6.15E-08
U-234MF	9.56E-02	1.00E+00	9.53E-02	9.87E-01	9.54E-02	9.88E-01
Th-230	2.03E-40	1.04E-40	3.09E-42	1.58E-42	4.48E-42	2.30E-42
Th-230MF	8.87E-06	9.99E-01	8.79E-06	9.76E-01	8.82E-06	9.79E-01
Ra-226	2.67E-16	8.26E-19	3.99E-18	1.23E-20	5.80E-18	1.79E-20
Ra-226MF	9.86E-04	9.31E-01	6.62E-04	5.49E-01	7.40E-04	6.13E-01
Pu-238	2.71E-37	2.55E-41	3.96E-45	3.73E-49	2.15E-44	2.03E-48
Pu-238MF	1.56E-02	3.33E-01	3.00E-03	6.20E-02	3.53E-03	7.31E-02
Pu-239	2.42E-27	5.36E-31	3.84E-29	8.53E-33	5.55E-29	1.23E-32
Pu-239MF	1.98E-02	9.96E-01	1.94E-02	9.44E-01	1.95E-02	9.51E-01
Pu-240	5.20E-28	2.66E-31	8.14E-30	4.17E-33	1.18E-29	6.03E-33
Pu-240MF	8.51E-03	9.84E-01	7.84E-03	8.80E-01	8.04E-03	9.03E-01
Pu-242	1.64E-28	6.86E-31	2.63E-30	1.10E-32	3.79E-30	1.58E-32
Pu-242MF	1.06E-03	1.00E+00	1.06E-03	9.69E-01	1.06E-03	9.69E-01
Th-232	1.39E-39	1.15E-40	2.14E-41	1.76E-42	3.11E-41	2.55E-42
Th-232MF	5.34E-05	1.00E+00	5.34E-05	1.00E+00	5.34E-05	1.00E+00

[a.] The "MF" designation refers to the mobile fraction

Aquifer Concentrations

Groundwater concentrations for the five closure scenarios are presented in Tables 16 through 20. Radioactive progeny were only computed for the actinide immobile fractions, with the exception of Pu-238. Unsaturated transit times of the immobile fractions were short enough such that little progeny generation would occur. However, the half-life of Pu-238 is relatively short and its progeny (U-234) may be important, and was therefore included in the Pu-238 mobile fraction dose. In general, the enhanced cover provides the greatest protection (i.e., lowest groundwater concentrations) while the cover remains intact. The main impact the engineered covers have over

the site soils cover is that they prevent further migration of the relatively mobile radionuclides and thereby, reduce concentrations and dose while the cover is intact. Following cover failure, groundwater concentrations of the less mobile actinides are almost the same for each closure scenario.

Some of the results in Table 16 may seem counterintuitive. For example, the maximum U-238MF concentration of for the enhanced cover is greater than that of the proposed cover, despite the fact that the enhanced cover has a lower infiltration rate. Figure 18 shows the U-238MF groundwater concentrations as a function of time for the two covers. For the enhanced cover, U-238 activity builds up in the unsaturated zone while the cover is intact. When failure occurs, the activity built up in the unsaturated zone releases in a relatively short period of time. For the proposed cover, releases to the aquifer are higher than the enhanced cover while the cover is intact. When the cover fails, there is less activity released to the aquifer compared the enhanced cover, and therefore the *maximum* concentration is less.

Table 16. Groundwater Concentrations for the Site Soils Cover for Closure in 2056

Radionuclide[a]	Progeny	Maximum 0-250 yr (Ci m^{-3})	Maximum 250-500 yr (Ci m^{-3})	Maximum 500-1000 yr (Ci m^{-3})	Maximum 1000-5000 yr (Ci m^{-3})	Maximum 5000-10,000 yr (Ci m^{-3})	Maximum 0-200,000 yr (Ci m^{-3})
H-3		9.0E-05	5.4E-08	5.6E-17	2.0E-39	0.0E+00	9.0E-05
C-14		1.5E-13	1.9E-10	1.3E-08	8.0E-07	1.1E-06	1.1E-06
C-14MF		6.8E-08	2.5E-08	4.5E-12	2.2E-20	7.5E-43	6.8E-08
Cl-36		1.3E-08	1.4E-08	1.1E-08	1.8E-09	4.8E-10	1.4E-08
I-129		1.4E-16	2.4E-13	1.8E-11	1.7E-09	3.2E-09	3.2E-09
I-129MF		1.0E-10	3.5E-11	5.6E-15	2.9E-23	1.6E-45	1.0E-10
Tc-99		2.2E-07	2.2E-07	1.8E-07	3.0E-08	7.9E-09	2.2E-07
U-238		5.7E-25	1.3E-21	3.5E-19	1.5E-15	4.0E-13	3.2E-08
	U-234	4.2E-28	2.3E-24	1.5E-21	3.0E-17	1.6E-14	1.5E-08
	Th-230	6.4E-38	1.5E-33	1.5E-29	1.0E-23	2.1E-20	1.2E-11
	Ra-226	1.4E-35	3.6E-31	3.8E-27	3.3E-21	5.6E-18	6.4E-10
	Pb-210	4.8E-38	1.2E-33	1.3E-29	1.1E-23	1.9E-20	2.2E-12
U-238MF		1.5E-08	4.6E-09	6.8E-13	3.5E-21	1.9E-43	1.5E-08
U-235		5.6E-26	2.5E-22	9.6E-20	5.5E-16	1.5E-13	2.9E-09
	Pa-231	1.2E-30	1.4E-26	3.6E-23	1.5E-18	7.8E-16	3.1E-10
	Ac-227	1.4E-34	2.0E-30	4.9E-27	2.0E-22	9.9E-20	3.9E-14
U-235MF		3.0E-10	9.2E-11	1.4E-14	7.0E-23	3.8E-45	3.0E-10
U-234		5.1E-25	2.3E-21	8.8E-19	5.0E-15	1.3E-12	2.2E-08
	Th-230	7.8E-35	1.6E-30	1.0E-26	2.2E-21	2.2E-18	1.7E-11
	Ra-226	1.8E-32	3.8E-28	2.7E-24	6.9E-19	5.7E-16	8.6E-10
	Pb-210	6.0E-35	1.3E-30	9.3E-27	2.4E-21	1.9E-18	2.9E-12
U-234MF		2.8E-09	8.4E-10	1.3E-13	6.4E-22	3.5E-44	2.8E-09
Th-230		4.0E-66	7.7E-62	3.0E-58	2.5E-53	3.9E-50	1.1E-37
	Ra-226	3.4E-42	8.1E-38	2.3E-34	2.2E-30	4.2E-28	3.5E-25
	Pb-210	1.2E-44	2.7E-40	7.8E-37	7.5E-33	1.4E-30	1.2E-27
Th-230MF		2.6E-13	8.7E-14	1.4E-17	6.9E-26	3.7E-48	2.6E-13
Ra-226		1.7E-37	1.3E-33	1.8E-30	6.5E-27	6.0E-25	1.9E-23

Table 16. Groundwater Concentrations for the Site Soils Cover for Closure in 2056

Radionuclide[a]	Progeny	Maximum 0-250 yr (Ci m^{-3})	Maximum 250-500 yr (Ci m^{-3})	Maximum 500-1000 yr (Ci m^{-3})	Maximum 1000-5000 yr (Ci m^{-3})	Maximum 5000-10,000 yr (Ci m^{-3})	Maximum 0-200,000 yr (Ci m^{-3})
	Pb-210	5.8E-40	4.6E-36	6.1E-33	2.2E-29	2.0E-27	6.4E-26
Ra-226MF		2.8E-11	9.8E-12	1.6E-15	6.8E-24	6.9E-47	2.8E-11
Pu-238		1.6E-51	1.5E-48	6.0E-47	4.7E-47	6.3E-56	6.0E-47
	U-234	9.7E-28	6.0E-24	3.5E-21	3.3E-17	1.2E-14	3.0E-10
	Th-230	1.4E-37	3.8E-33	3.6E-29	1.3E-23	1.8E-20	2.3E-13
	Ra-226	3.2E-35	9.2E-31	9.7E-27	4.2E-21	4.7E-18	1.1E-11
	Pb-210	1.1E-37	3.1E-33	3.3E-29	1.4E-23	1.6E-20	3.9E-14
Pu-238MF		4.9E-10	3.5E-11	5.3E-16	2.5E-26	5.9E-62	4.9E-10
	U-234MF	3.6E-13	8.6E-14	1.1E-17	5.2E-26	3.0E-48	3.6E-13
Pu-239		4.7E-51	3.1E-47	5.7E-44	2.6E-39	2.8E-36	2.9E-25
	U-235	1.5E-31	1.0E-27	7.2E-25	1.0E-20	5.8E-18	8.0E-12
	Pa-231	3.0E-36	5.3E-32	2.4E-28	2.5E-23	2.6E-20	1.1E-12
	Ac-227	3.6E-40	7.8E-36	3.3E-32	3.3E-27	3.4E-24	1.3E-16
Pu-239MF		5.7E-10	1.1E-10	1.1E-14	5.4E-23	2.7E-45	5.7E-10
Pu-240		2.0E-51	1.3E-47	2.3E-44	7.7E-40	5.8E-37	6.5E-29
	U-236	2.0E-30	1.4E-26	9.4E-24	1.3E-19	7.4E-17	4.4E-11
	Th-232	1.5E-45	4.4E-41	5.0E-37	2.6E-31	5.2E-28	2.6E-19
	Ra-228	5.9E-42	7.1E-38	1.4E-34	9.7E-30	9.5E-27	2.5E-19
	Th-228	1.8E-43	2.2E-39	4.2E-36	6.1E-32	1.0E-44	6.1E-32
Pu-240MF		2.4E-10	4.6E-11	4.8E-15	2.2E-23	7.9E-46	2.4E-10
Pu242		2.5E-52	1.6E-48	3.1E-45	1.6E-40	2.0E-37	2.2E-25
	U-238	1.5E-57	1.2E-53	1.1E-50	6.2E-46	9.7E-43	4.1E-30
	U-234	3.0E-38	5.7E-34	8.8E-31	3.2E-26	5.0E-23	1.2E-14
	Th-230	3.6E-48	2.7E-43	7.3E-39	9.7E-33	4.5E-29	4.5E-18
	Ra-226	8.1E-46	6.5E-41	1.9E-36	3.2E-30	1.3E-26	2.7E-16
	Pb-210	2.8E-48	2.2E-43	6.6E-39	1.1E-32	4.3E-29	9.2E-19
Pu-242MF		3.0E-11	5.7E-12	6.2E-16	3.0E-24	1.6E-46	3.0E-11
Th-232		5.0E-65	5.9E-61	2.1E-57	1.7E-52	2.7E-49	1.8E-36
	Ra-228	1.3E-47	1.1E-48	1.3E-48	1.6E-50	8.2E-48	3.3E-36
	Th-228	4.0E-49	3.2E-50	3.8E-50	1.3E-52	8.7E-66	4.0E-49
Th-232MF		1.5E-12	5.2E-13	9.2E-17	4.8E-25	2.6E-47	1.5E-12

a. The "MF" designation refers to mobile fraction

Table 17. Groundwater Concentrations for the Enhanced Cover for Closure in 2003

Radionuclide[a]	Progeny	Maximum 0-250 yr (Ci m^{-3})	Maximum 250-500 yr (Ci m^{-3})	Maximum 500-1000 yr (Ci m^{-3})	Maximum 1000-5000 yr (Ci m^{-3})	Maximum 5000-10,000 yr (Ci m^{-3})	Maximum 0-200,000 yr (Ci m^{-3})
H-3		8.0E-05	4.1E-10	2.3E-16	2.8E-29	0.0E+00	8.0E-05
C-14		2.4E-18	1.8E-18	5.4E-17	3.0E-08	6.0E-07	6.0E-07
C-14MF		4.7E-09	1.3E-09	9.6E-09	1.6E-08	4.3E-28	1.6E-08

Table 17. Groundwater Concentrations for the Enhanced Cover for Closure in 2003

Radionuclide[a]	Progeny	Maximum 0-250 yr (Ci m^{-3})	Maximum 250-500 yr (Ci m^{-3})	Maximum 500-1000 yr (Ci m^{-3})	Maximum 1000-5000 yr (Ci m^{-3})	Maximum 5000-10,000 yr (Ci m^{-3})	Maximum 0-200,000 yr (Ci m^{-3})
Cl-36		1.1E-10	5.6E-11	7.7E-10	3.4E-09	1.2E-09	3.4E-09
I-129		4.0E-22	3.7E-22	1.9E-20	7.4E-11	2.8E-09	3.0E-09
I-129MF		2.8E-12	1.5E-12	1.6E-11	2.7E-11	9.0E-31	2.7E-11
Tc-99		4.3E-09	1.5E-09	1.5E-08	5.2E-08	1.8E-08	5.2E-08
U-238		1.9E-29	1.6E-29	3.7E-28	3.1E-18	1.6E-14	3.1E-08
	U-234	1.0E-32	1.8E-32	1.0E-30	9.9E-20	1.3E-15	1.5E-08
	Th-230	3.5E-41	4.2E-40	1.1E-38	1.0E-26	8.8E-22	1.1E-11
	Ra-226	6.0E-39	9.7E-38	7.1E-36	3.7E-24	2.6E-19	6.1E-10
	Pb-210	2.1E-41	3.3E-40	2.4E-38	1.3E-26	8.8E-22	2.1E-12
U-238MF		9.3E-10	3.1E-10	2.5E-09	3.9E-09	1.1E-28	3.9E-09
U-235		7.6E-31	6.5E-31	1.8E-29	9.6E-19	6.0E-15	2.8E-09
	Pa-231	1.6E-34	5.0E-34	9.4E-33	1.4E-21	2.2E-17	3.1E-10
	Ac-227	2.1E-38	6.2E-38	1.7E-36	1.8E-25	2.8E-21	3.8E-14
U-235MF		1.9E-11	6.3E-12	5.1E-11	8.0E-11	2.2E-30	8.0E-11
U-234		6.9E-30	5.9E-30	1.6E-28	8.6E-18	5.3E-14	2.1E-08
	Th-230	3.6E-38	2.6E-37	2.9E-36	1.1E-24	4.4E-20	1.7E-11
	Ra-226	6.3E-36	5.8E-35	2.1E-33	3.8E-22	1.3E-17	8.4E-10
	Pb-210	2.1E-38	2.0E-37	7.2E-36	1.3E-24	4.3E-20	2.9E-12
U-234MF		1.7E-10	5.7E-11	4.6E-10	7.3E-10	2.0E-29	7.3E-10
Th-230		3.4E-70	1.1E-69	5.5E-69	1.1E-56	5.3E-52	5.1E-38
	Ra-226	3.7E-47	4.5E-47	4.2E-46	8.8E-33	5.1E-29	2.4E-25
	Pb-210	1.3E-49	1.5E-49	1.4E-48	3.0E-35	1.7E-31	8.1E-28
Th-230MF		8.1E-15	4.0E-15	4.0E-14	6.8E-14	2.1E-33	6.8E-14
Ra-226		9.8E-42	1.1E-41	7.6E-41	4.3E-30	9.7E-27	2.7E-24
	Pb-210	3.3E-44	3.7E-44	2.6E-43	1.5E-32	3.3E-29	9.2E-27
Ra-226MF		1.5E-12	4.8E-13	3.0E-12	4.8E-12	3.9E-32	4.8E-12
Pu-238		2.4E-55	2.3E-55	7.9E-56	3.2E-55	3.9E-59	3.2E-55
	U-234	9.1E-33	8.1E-33	2.5E-31	6.3E-20	5.5E-16	2.9E-10
	Th-230	4.7E-41	3.5E-40	4.1E-39	7.0E-27	4.2E-22	2.2E-13
	Ra-226	8.1E-39	7.9E-38	3.0E-36	2.5E-24	1.2E-19	1.1E-11
	Pb-210	2.8E-41	2.7E-40	1.0E-38	8.4E-27	4.2E-22	3.8E-14
Pu-238MF		1.6E-10	7.1E-12	5.8E-13	6.1E-14	3.4E-47	1.6E-10
	U-234MF	3.5E-14	1.7E-14	1.0E-13	1.3E-13	1.7E-33	1.3E-13
Pu-239		6.9E-55	1.8E-54	8.8E-54	1.4E-42	4.5E-38	1.4E-25
	U-235	1.4E-36	1.2E-36	3.8E-35	6.3E-23	9.0E-19	7.9E-12
	Pa-231	3.0E-40	9.5E-40	1.9E-38	7.8E-26	3.0E-21	1.0E-12
	Ac-227	3.9E-44	1.2E-43	3.3E-42	1.1E-29	3.9E-25	1.3E-16
Pu-239MF		1.0E-10	2.2E-11	1.1E-10	1.4E-10	1.5E-30	1.4E-10
Pu-240		2.9E-55	7.4E-55	3.5E-54	4.2E-43	9.0E-39	3.0E-29
	U-236	1.8E-35	1.6E-35	5.0E-34	7.8E-22	1.1E-17	4.3E-11
	Th-232	5.0E-49	3.7E-48	4.4E-47	4.2E-34	4.1E-29	2.5E-19

Table 17. Groundwater Concentrations for the Enhanced Cover for Closure in 2003

Radionuclide[a]	Progeny	Maximum 0-250 yr (Ci m^{-3})	Maximum 250-500 yr (Ci m^{-3})	Maximum 500-1000 yr (Ci m^{-3})	Maximum 1000-5000 yr (Ci m^{-3})	Maximum 5000-10,000 yr (Ci m^{-3})	Maximum 0-200,000 yr (Ci m^{-3})
	Ra-228	1.9E-46	4.4E-46	1.3E-44	3.3E-32	1.1E-27	2.5E-19
	Th-228	5.8E-48	1.3E-47	4.0E-46	5.4E-35	1.1E-45	5.4E-35
Pu-240MF		4.4E-11	9.5E-12	4.4E-11	5.5E-11	4.5E-31	5.5E-11
Pu242		3.7E-56	9.5E-56	4.8E-55	8.6E-44	3.1E-39	1.0E-25
	U-238	2.4E-62	4.3E-62	2.7E-60	6.0E-49	2.0E-44	1.9E-30
	U-234	1.2E-43	1.1E-43	4.0E-42	8.2E-28	1.9E-23	1.1E-14
	Th-230	6.0E-52	4.7E-51	5.8E-50	7.4E-35	1.2E-29	4.2E-18
	Ra-226	1.0E-49	1.1E-48	4.2E-47	2.7E-32	3.5E-27	2.5E-16
	Pb-210	3.5E-52	3.6E-51	1.4E-49	9.1E-35	1.2E-29	8.5E-19
Pu-242MF		5.5E-12	1.2E-12	6.0E-12	7.5E-12	9.2E-32	7.5E-12
Th-232		1.2E-68	3.6E-68	1.6E-67	7.1E-56	3.5E-51	7.7E-37
	Ra-228	9.8E-48	3.1E-56	5.4E-59	4.2E-53	1.9E-49	1.5E-36
	Th-228	3.0E-49	9.3E-58	1.6E-60	2.1E-55	2.0E-67	3.0E-49
Th-232MF		1.1E-13	3.1E-14	2.4E-13	3.9E-13	1.5E-32	3.9E-13

a. The "MF" designation refers to mobile fraction

Table 18. Groundwater Concentrations for the Enhanced Cover for Closure in 2056

Radionuclide[a]	Progeny	Maximum 0-250 yr (Ci m^{-3})	Maximum 250-500 yr (Ci m^{-3})	Maximum 500-1000 yr (Ci m^{-3})	Maximum 1000-5000 yr (Ci m^{-3})	Maximum 5000-10,000 yr (Ci m^{-3})	Maximum 0-200,000 yr (Ci m^{-3})
H-3		8.0E-05	4.1E-10	2.3E-16	3.6E-29	0.0E+00	8.0E-05
C-14		2.4E-18	1.8E-18	5.4E-17	3.5E-08	7.6E-07	7.6E-07
C-14MF		4.7E-09	1.3E-09	9.6E-09	1.6E-08	4.3E-28	1.6E-08
Cl-36		1.1E-10	5.6E-11	7.7E-10	3.5E-09	1.2E-09	3.5E-09
I-129		4.0E-22	3.7E-22	1.9E-20	7.7E-11	2.9E-09	3.2E-09
I-129MF		2.8E-12	1.5E-12	1.6E-11	2.7E-11	9.0E-31	2.7E-11
Tc-99		4.3E-09	1.5E-09	1.5E-08	5.7E-08	2.0E-08	5.7E-08
U-238		1.9E-29	1.6E-29	3.7E-28	3.1E-18	1.6E-14	3.1E-08
	U-234	1.0E-32	1.8E-32	1.0E-30	9.9E-20	1.3E-15	1.5E-08
	Th-230	3.5E-41	4.2E-40	1.1E-38	1.0E-26	8.8E-22	1.1E-11
	Ra-226	6.0E-39	9.7E-38	7.1E-36	3.7E-24	2.6E-19	6.1E-10
	Pb-210	2.1E-41	3.3E-40	2.4E-38	1.3E-26	8.8E-22	2.1E-12
U-238MF		9.3E-10	3.1E-10	2.5E-09	3.9E-09	1.1E-28	3.9E-09
U-235		7.6E-31	6.5E-31	1.8E-29	9.6E-19	6.0E-15	2.8E-09
	Pa-231	1.6E-34	5.0E-34	9.4E-33	1.4E-21	2.2E-17	3.1E-10
	Ac-227	2.1E-38	6.2E-38	1.7E-36	1.8E-25	2.8E-21	3.8E-14
U-235MF		1.9E-11	6.3E-12	5.1E-11	8.0E-11	2.2E-30	8.0E-11
U-234		6.9E-30	5.9E-30	1.6E-28	8.7E-18	5.4E-14	2.2E-08
	Th-230	3.6E-38	2.6E-37	2.9E-36	1.1E-24	4.4E-20	1.7E-11
	Ra-226	6.3E-36	5.8E-35	2.1E-33	3.8E-22	1.3E-17	8.4E-10

Table 18. Groundwater Concentrations for the Enhanced Cover for Closure in 2056

Radionuclide[a]	Progeny	Maximum 0-250 yr (Ci m^{-3})	Maximum 250-500 yr (Ci m^{-3})	Maximum 500-1000 yr (Ci m^{-3})	Maximum 1000-5000 yr (Ci m^{-3})	Maximum 5000-10,000 yr (Ci m^{-3})	Maximum 0-200,000 yr (Ci m^{-3})
	Pb-210	2.1E-38	2.0E-37	7.2E-36	1.3E-24	4.3E-20	2.9E-12
U-234MF		1.7E-10	5.7E-11	4.6E-10	7.3E-10	2.0E-29	7.3E-10
Th-230		3.4E-70	1.1E-69	5.5E-69	1.1E-56	5.3E-52	5.1E-38
	Ra-226	3.7E-47	4.5E-47	4.2E-46	8.8E-33	5.1E-29	2.4E-25
	Pb-210	1.3E-49	1.5E-49	1.4E-48	3.0E-35	1.7E-31	8.1E-28
Th-230MF		8.1E-15	4.0E-15	4.0E-14	6.8E-14	2.1E-33	6.8E-14
Ra-226		9.8E-42	1.1E-41	7.6E-41	5.1E-30	1.2E-26	3.7E-24
	Pb-210	3.3E-44	3.7E-44	2.6E-43	1.7E-32	4.2E-29	1.3E-26
Ra-226MF		1.5E-12	4.8E-13	3.0E-12	4.8E-12	3.9E-32	4.8E-12
Pu-238		2.4E-55	2.3E-55	7.9E-56	3.2E-55	3.9E-59	3.2E-55
	U-234	9.1E-33	8.1E-33	2.5E-31	6.3E-20	5.5E-16	2.9E-10
	Th-230	4.7E-41	3.5E-40	4.1E-39	7.0E-27	4.2E-22	2.2E-13
	Ra-226	8.1E-39	7.9E-38	3.0E-36	2.5E-24	1.2E-19	1.1E-11
	Pb-210	2.8E-41	2.7E-40	1.0E-38	8.4E-27	4.2E-22	3.8E-14
Pu-238MF		1.6E-10	7.1E-12	5.8E-13	6.1E-14	3.4E-47	1.6E-10
	U-234MF	3.5E-14	1.7E-14	1.0E-13	1.3E-13	1.7E-33	1.3E-13
Pu-239		6.9E-55	1.8E-54	8.8E-54	1.4E-42	4.5E-38	1.4E-25
	U-235	1.4E-36	1.2E-36	3.8E-35	6.3E-23	9.0E-19	7.9E-12
	Pa-231	3.0E-40	9.5E-40	1.9E-38	7.8E-26	3.0E-21	1.0E-12
	Ac-227	3.9E-44	1.2E-43	3.3E-42	1.1E-29	3.9E-25	1.3E-16
Pu-239MF		1.0E-10	2.2E-11	1.1E-10	1.4E-10	1.5E-30	1.4E-10
Pu-240		2.9E-55	7.4E-55	3.5E-54	4.2E-43	9.0E-39	3.0E-29
	U-236	1.8E-35	1.6E-35	5.0E-34	7.8E-22	1.1E-17	4.3E-11
	Th-232	5.0E-49	3.7E-48	4.4E-47	4.2E-34	4.1E-29	2.5E-19
	Ra-228	1.9E-46	4.4E-46	1.3E-44	3.3E-32	1.1E-27	2.5E-19
	Th-228	5.8E-48	1.3E-47	4.0E-46	5.4E-35	1.1E-45	5.4E-35
Pu-240MF		4.4E-11	9.5E-12	4.4E-11	5.5E-11	4.5E-31	5.5E-11
Pu242		3.7E-56	9.5E-56	4.8E-55	8.6E-44	3.1E-39	1.0E-25
	U-238	2.4E-62	4.3E-62	2.7E-60	6.0E-49	2.0E-44	1.9E-30
	U-234	1.2E-43	1.1E-43	4.0E-42	8.2E-28	1.9E-23	1.1E-14
	Th-230	6.0E-52	4.7E-51	5.8E-50	7.5E-35	1.2E-29	4.2E-18
	Ra-226	1.0E-49	1.1E-48	4.2E-47	2.7E-32	3.5E-27	2.5E-16
	Pb-210	3.5E-52	3.6E-51	1.4E-49	9.1E-35	1.2E-29	8.5E-19
Pu-242MF		5.5E-12	1.2E-12	6.0E-12	7.5E-12	9.2E-32	7.5E-12
Th-232		1.2E-68	3.6E-68	1.6E-67	7.3E-56	3.7E-51	8.0E-37
	Ra-228	9.8E-48	3.1E-56	5.5E-59	4.3E-53	2.0E-49	1.5E-36
	Th-228	3.0E-49	9.3E-58	1.7E-60	2.1E-55	2.1E-67	3.0E-49
Th-232MF		1.1E-13	3.1E-14	2.4E-13	3.9E-13	1.5E-32	3.9E-13

a. The "MF" designation refers to mobile fraction

Table 19. Groundwater Concentrations for the Enhanced Cover for Closure in 2215

Radionuclide[a]	Progeny	Maximum 0-250 yr (Ci m^{-3})	Maximum 250-500 yr (Ci m^{-3})	Maximum 500-1000 yr (Ci m^{-3})	Maximum 1000-5000 yr (Ci m^{-3})	Maximum 5000-10,000 yr (Ci m^{-3})	Maximum 0-200,000 yr (Ci m^{-3})
H-3		8.0E-05	4.1E-10	2.3E-16	4.0E-26	0.0E+00	8.0E-05
C-14		2.4E-18	1.8E-18	5.4E-17	5.1E-08	1.2E-06	1.2E-06
C-14MF		4.7E-09	1.3E-09	9.6E-09	1.6E-08	4.3E-28	1.6E-08
Cl-36		1.1E-10	5.6E-11	7.7E-10	3.8E-09	1.3E-09	3.8E-09
I-129		4.0E-22	3.7E-22	1.9E-20	8.5E-11	3.4E-09	3.7E-09
I-129MF		2.8E-12	1.5E-12	1.6E-11	2.7E-11	9.0E-31	2.7E-11
Tc-99		4.3E-09	1.5E-09	1.5E-08	7.2E-08	2.5E-08	7.2E-08
U-238		1.9E-29	1.6E-29	3.7E-28	3.1E-18	1.6E-14	3.1E-08
	U-234	1.0E-32	1.8E-32	1.0E-30	1.0E-19	1.3E-15	1.6E-08
	Th-230	3.5E-41	4.2E-40	1.1E-38	1.0E-26	8.8E-22	1.1E-11
	Ra-226	6.0E-39	9.7E-38	7.1E-36	3.7E-24	2.6E-19	6.2E-10
	Pb-210	2.1E-41	3.3E-40	2.4E-38	1.3E-26	8.8E-22	2.1E-12
U-238MF		9.3E-10	3.1E-10	2.5E-09	3.9E-09	1.1E-28	3.9E-09
U-235		7.6E-31	6.5E-31	1.8E-29	9.7E-19	6.1E-15	2.8E-09
	Pa-231	1.6E-34	5.0E-34	9.4E-33	1.4E-21	2.2E-17	3.1E-10
	Ac-227	2.1E-38	6.2E-38	1.7E-36	1.8E-25	2.9E-21	3.9E-14
U-235MF		1.9E-11	6.3E-12	5.1E-11	8.0E-11	2.2E-30	8.0E-11
U-234		6.9E-30	5.9E-30	1.6E-28	8.7E-18	5.4E-14	2.2E-08
	Th-230	3.6E-38	2.6E-37	2.9E-36	1.1E-24	4.4E-20	1.7E-11
	Ra-226	6.3E-36	5.8E-35	2.1E-33	3.8E-22	1.3E-17	8.5E-10
	Pb-210	2.1E-38	2.0E-37	7.2E-36	1.3E-24	4.3E-20	2.9E-12
U-234MF		1.7E-10	5.7E-11	4.6E-10	7.3E-10	2.0E-29	7.3E-10
Th-230		3.4E-70	1.1E-69	5.5E-69	1.1E-56	5.3E-52	5.1E-38
	Ra-226	3.7E-47	4.5E-47	4.2E-46	8.8E-33	5.1E-29	2.4E-25
	Pb-210	1.3E-49	1.5E-49	1.4E-48	3.0E-35	1.7E-31	8.1E-28
Th-230MF		8.1E-15	4.0E-15	4.0E-14	6.8E-14	2.1E-33	6.8E-14
Ra-226		9.8E-42	1.1E-41	7.6E-41	7.5E-30	2.1E-26	6.6E-24
	Pb-210	3.3E-44	3.7E-44	2.6E-43	2.6E-32	7.1E-29	2.3E-26
Ra-226MF		1.5E-12	4.8E-13	3.0E-12	4.8E-12	3.9E-32	4.8E-12
Pu-238		2.4E-55	2.3E-55	7.9E-56	3.2E-55	3.9E-59	3.2E-55
	U-234	9.1E-33	8.1E-33	2.5E-31	6.4E-20	5.5E-16	2.9E-10
	Th-230	4.7E-41	3.5E-40	4.1E-39	7.0E-27	4.3E-22	2.2E-13
	Ra-226	8.1E-39	7.9E-38	3.0E-36	2.5E-24	1.2E-19	1.1E-11
	Pb-210	2.8E-41	2.7E-40	1.0E-38	8.4E-27	4.2E-22	3.8E-14
Pu-238MF		1.6E-10	7.1E-12	5.8E-13	6.1E-14	3.4E-47	1.6E-10
	U-234MF	3.5E-14	1.7E-14	1.0E-13	1.3E-13	1.7E-33	1.3E-13
Pu-239		6.9E-55	1.8E-54	8.8E-54	1.4E-42	4.5E-38	1.4E-25
	U-235	1.4E-36	1.2E-36	3.8E-35	6.3E-23	9.0E-19	8.0E-12
	Pa-231	3.0E-40	9.5E-40	1.9E-38	7.9E-26	3.0E-21	1.0E-12
	Ac-227	3.9E-44	1.2E-43	3.3E-42	1.1E-29	3.9E-25	1.3E-16

Table 19. Groundwater Concentrations for the Enhanced Cover for Closure in 2215

Radionuclide[a]	Progeny	Maximum 0-250 yr (Ci m^{-3})	Maximum 250-500 yr (Ci m^{-3})	Maximum 500-1000 yr (Ci m^{-3})	Maximum 1000-5000 yr (Ci m^{-3})	Maximum 5000-10,000 yr (Ci m^{-3})	Maximum 0-200,000 yr (Ci m^{-3})
Pu-239MF		1.0E-10	2.2E-11	1.1E-10	1.4E-10	1.5E-30	1.4E-10
Pu-240		2.9E-55	7.4E-55	3.5E-54	4.2E-43	9.0E-39	3.0E-29
	U-236	1.8E-35	1.6E-35	5.0E-34	7.8E-22	1.1E-17	4.3E-11
	Th-232	5.0E-49	3.7E-48	4.4E-47	4.2E-34	4.1E-29	2.5E-19
	Ra-228	1.9E-46	4.4E-46	1.3E-44	3.3E-32	1.1E-27	2.5E-19
	Th-228	5.8E-48	1.3E-47	4.0E-46	5.4E-35	1.1E-45	5.4E-35
Pu-240MF		4.4E-11	9.5E-12	4.4E-11	5.5E-11	4.5E-31	5.5E-11
Pu242		3.7E-56	9.5E-56	4.8E-55	8.6E-44	3.1E-39	1.0E-25
	U-238	2.4E-62	4.3E-62	2.7E-60	6.0E-49	2.0E-44	1.9E-30
	U-234	1.2E-43	1.1E-43	4.0E-42	8.2E-28	1.9E-23	1.1E-14
	Th-230	6.0E-52	4.7E-51	5.8E-50	7.5E-35	1.2E-29	4.2E-18
	Ra-226	1.0E-49	1.1E-48	4.2E-47	2.7E-32	3.5E-27	2.5E-16
	Pb-210	3.5E-52	3.6E-51	1.4E-49	9.1E-35	1.2E-29	8.6E-19
Pu-242MF		5.5E-12	1.2E-12	6.0E-12	7.5E-12	9.2E-32	7.5E-12
Th-232		1.2E-68	3.6E-68	1.6E-67	7.6E-56	4.0E-51	9.1E-37
	Ra-228	9.8E-48	3.1E-56	5.8E-59	4.7E-53	2.2E-49	1.7E-36
	Th-228	3.0E-49	9.3E-58	1.8E-60	2.3E-55	2.3E-67	3.0E-49
Th-232MF		1.1E-13	3.1E-14	2.4E-13	3.9E-13	1.5E-32	3.9E-13

a. The "MF" designation refers to mobile fraction

Table 20. Groundwater Concentrations for the Proposed Cover for Closure in 2056

Radionuclide[a]	Progeny	Maximum 0-250 yr (Ci m^{-3})	Maximum 250-500 yr (Ci m^{-3})	Maximum 500-1000 yr (Ci m^{-3})	Maximum 1000-5000 yr (Ci m^{-3})	Maximum 5000-10,000 yr (Ci m^{-3})	Maximum 0-200,000 yr (Ci m^{-3})
H-3		8.0E-05	7.9E-10	1.4E-15	6.6E-29	0.0E+00	8.0E-05
C-14		3.6E-18	1.6E-17	1.3E-15	5.2E-08	7.8E-07	7.8E-07
C-14MF		4.7E-09	4.3E-09	1.3E-08	1.1E-08	1.9E-29	1.3E-08
Cl-36		1.1E-10	2.8E-10	2.3E-09	3.5E-09	1.1E-09	3.5E-09
I-129		7.6E-22	4.6E-21	7.6E-19	1.1E-10	3.0E-09	3.2E-09
I-129MF		2.9E-12	6.3E-12	2.3E-11	1.9E-11	4.0E-32	2.3E-11
Tc-99		4.3E-09	5.9E-09	3.9E-08	5.7E-08	1.8E-08	5.7E-08
U-238		2.8E-29	1.2E-28	8.2E-27	5.8E-18	2.2E-14	3.2E-08
	U-234	1.8E-32	1.6E-31	2.3E-29	1.6E-19	1.5E-15	1.5E-08
	Th-230	4.4E-41	1.3E-39	1.6E-37	1.9E-26	1.1E-21	1.1E-11
	Ra-226	8.4E-39	3.9E-37	6.5E-35	6.5E-24	3.2E-19	6.2E-10
	Pb-210	2.9E-41	1.3E-39	2.2E-37	2.2E-26	1.1E-21	2.1E-12
U-238MF		9.4E-10	1.1E-09	3.1E-09	2.4E-09	4.9E-30	3.1E-09
U-235		1.2E-30	5.6E-30	5.4E-28	1.8E-18	8.1E-15	2.8E-09
	Pa-231	2.2E-34	2.3E-33	1.5E-31	2.7E-21	3.1E-17	3.1E-10
	Ac-227	3.1E-38	3.3E-37	2.4E-35	3.6E-25	3.9E-21	3.8E-14

Table 20. Groundwater Concentrations for the Proposed Cover for Closure in 2056

Radionuclide[a]	Progeny	Maximum 0-250 yr (Ci m^{-3})	Maximum 250-500 yr (Ci m^{-3})	Maximum 500-1000 yr (Ci m^{-3})	Maximum 1000-5000 yr (Ci m^{-3})	Maximum 5000-10,000 yr (Ci m^{-3})	Maximum 0-200,000 yr (Ci m^{-3})
U-235MF		1.9E-11	2.2E-11	6.2E-11	4.9E-11	9.8E-32	6.2E-11
U-234		1.1E-29	5.1E-29	4.9E-27	1.6E-17	7.2E-14	2.2E-08
	Th-230	4.5E-38	7.1E-37	4.1E-35	2.3E-24	6.2E-20	1.7E-11
	Ra-226	8.6E-36	2.2E-34	1.8E-32	8.0E-22	1.8E-17	8.4E-10
	Pb-210	2.9E-38	7.4E-37	6.0E-35	2.7E-24	6.1E-20	2.9E-12
U-234MF		1.7E-10	2.0E-10	5.7E-10	4.5E-10	8.9E-31	5.7E-10
Th-230		4.1E-70	3.0E-69	2.0E-67	2.2E-56	7.7E-52	5.5E-38
	Ra-226	4.9E-47	2.5E-46	2.7E-44	1.3E-32	5.8E-29	2.5E-25
	Pb-210	1.7E-49	8.7E-49	9.2E-47	4.3E-35	2.0E-31	8.4E-28
Th-230MF		8.3E-15	1.6E-14	5.6E-14	4.6E-14	9.4E-35	5.6E-14
Ra-226		1.3E-41	5.1E-41	2.8E-39	1.0E-29	1.8E-26	4.2E-24
	Pb-210	4.3E-44	1.7E-43	9.6E-42	3.5E-32	6.0E-29	1.4E-26
Ra-226MF		1.5E-12	1.6E-12	4.3E-12	3.5E-12	1.8E-33	4.3E-12
Pu-238		2.9E-55	2.9E-55	2.3E-55	2.0E-54	8.0E-59	2.0E-54
	U-234	1.5E-32	7.5E-32	8.4E-30	1.2E-19	7.3E-16	2.9E-10
	Th-230	5.9E-41	9.9E-40	6.4E-38	1.5E-26	5.9E-22	2.2E-13
	Ra-226	1.1E-38	3.0E-37	2.7E-35	5.1E-24	1.7E-19	1.1E-11
	Pb-210	3.8E-41	1.0E-39	9.4E-38	1.7E-26	5.8E-22	3.8E-14
Pu-238MF		1.6E-10	1.2E-11	2.5E-12	2.7E-14	1.5E-48	1.6E-10
	U-234MF	3.5E-14	4.9E-14	8.7E-14	5.7E-14	7.7E-35	8.7E-14
Pu-239		8.5E-55	4.9E-54	2.2E-52	3.0E-42	6.5E-38	1.5E-25
	U-235	2.2E-36	1.2E-35	1.3E-33	9.0E-23	1.0E-18	8.0E-12
	Pa-231	4.1E-40	4.5E-39	3.5E-37	1.2E-25	3.5E-21	1.0E-12
	Ac-227	5.8E-44	6.6E-43	5.4E-41	1.6E-29	4.5E-25	1.3E-16
Pu-239MF		1.0E-10	5.5E-11	9.3E-11	6.0E-11	6.8E-32	1.0E-10
Pu-240		3.6E-55	2.0E-54	9.0E-53	8.8E-43	1.3E-38	3.2E-29
	U-236	2.9E-35	1.5E-34	1.7E-32	1.1E-21	1.2E-17	4.4E-11
	Th-232	6.2E-49	1.1E-47	6.9E-46	6.6E-34	4.8E-29	2.5E-19
	Ra-228	3.2E-46	2.8E-45	2.4E-43	4.9E-32	1.2E-27	2.5E-19
	Th-228	9.8E-48	8.5E-47	7.2E-45	9.2E-35	1.3E-45	9.2E-35
Pu-240MF		4.5E-11	2.3E-11	3.8E-11	2.4E-11	2.0E-32	4.5E-11
Pu242		4.6E-56	2.6E-55	1.2E-53	1.8E-43	4.5E-39	1.1E-25
	U-238	4.2E-62	4.2E-61	7.3E-59	1.2E-48	2.8E-44	2.1E-30
	U-234	2.0E-43	1.2E-42	1.8E-40	1.0E-27	2.1E-23	1.1E-14
	Th-230	7.5E-52	1.4E-50	1.1E-48	9.6E-35	1.3E-29	4.2E-18
	Ra-226	1.4E-49	4.2E-48	4.6E-46	3.4E-32	3.8E-27	2.5E-16
	Pb-210	4.9E-52	1.4E-50	1.6E-48	1.2E-34	1.3E-29	8.6E-19
Pu-242MF		5.5E-12	2.9E-12	5.1E-12	3.3E-12	4.1E-33	5.5E-12
Th-232		1.4E-68	8.9E-68	3.9E-66	1.5E-55	5.4E-51	8.6E-37
	Ra-228	9.9E-48	4.3E-56	5.7E-58	7.4E-53	2.7E-49	1.6E-36
	Th-228	3.0E-49	1.3E-57	1.7E-59	3.8E-55	2.9E-67	3.0E-49

Table 20. Groundwater Concentrations for the Proposed Cover for Closure in 2056

Radionuclide[a]	Progeny	Maximum 0-250 yr ($Ci\ m^{-3}$)	Maximum 250-500 yr ($Ci\ m^{-3}$)	Maximum 500-1000 yr ($Ci\ m^{-3}$)	Maximum 1000-5000 yr ($Ci\ m^{-3}$)	Maximum 5000-10,000 yr ($Ci\ m^{-3}$)	Maximum 0-200,000 yr ($Ci\ m^{-3}$)
Th-232MF		1.1E-13	1.0E-13	3.2E-13	2.7E-13	6.8E-34	3.2E-13

a. The "MF" designation refers to mobile fraction

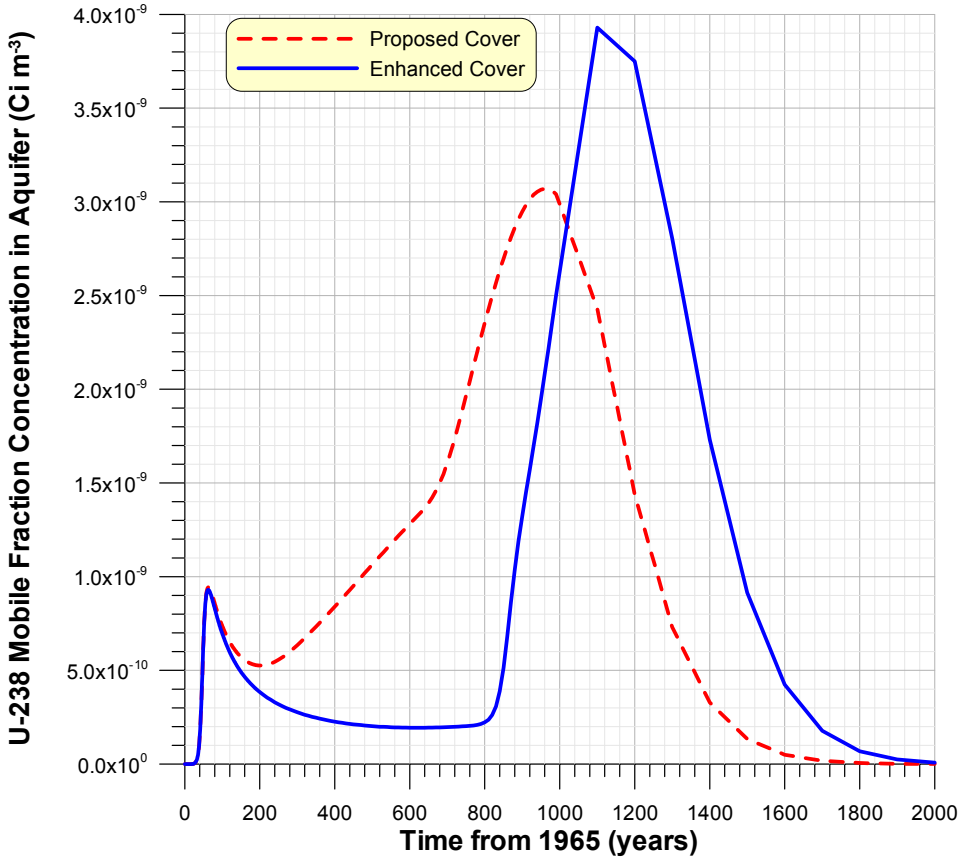

Figure 18. Graph showing U-238 mobile fraction aquifer concentrations for the enhanced and proposed covers. Concentrations while the cover remains intact are lower for the enhanced cover but are higher after cover failure. The area under the two curves is the same.

Drinking water doses as a function of time are presented in Figures 19 through 23. Doses from actinides include doses from all radioactive progeny that form during transport. Dominant dose contributors during specific time periods can be summarized as follows:

- For the 0–100-year time frame, H-3 is the major dose contributor.
- For the 100–1,000 year time frame, U-238 and Tc-99 are the major dose contributors.

- For the 1,000–10,000 year time frame, I-129, C-14, and U-238 are the major dose contributors.

Immobile fraction plutonium and thorium isotopes do not reach their maximum concentration in groundwater until well after 10,000 years.

Total dose as a function of time is presented in Figure 24 for each of the five closure scenarios. This figure illustrates the relative merits of each of the closure options. The site soils cover provides the least amount of protection however, doses are still predicted to be less than 5 mrem yr^{-1} while the cover is intact. Estimated doses while the enhanced and proposed cover are intact are generally less than 1 mrem yr^{-1}. After cover failure, doses from the immobile actinide fraction, C-14, and I-129 are about the same for all closure options. Maximum doses in the 1000–10,000-year time frame are less than 3-mrem yr^{-1} and are driven mainly by U-238, C-14, and I-129.

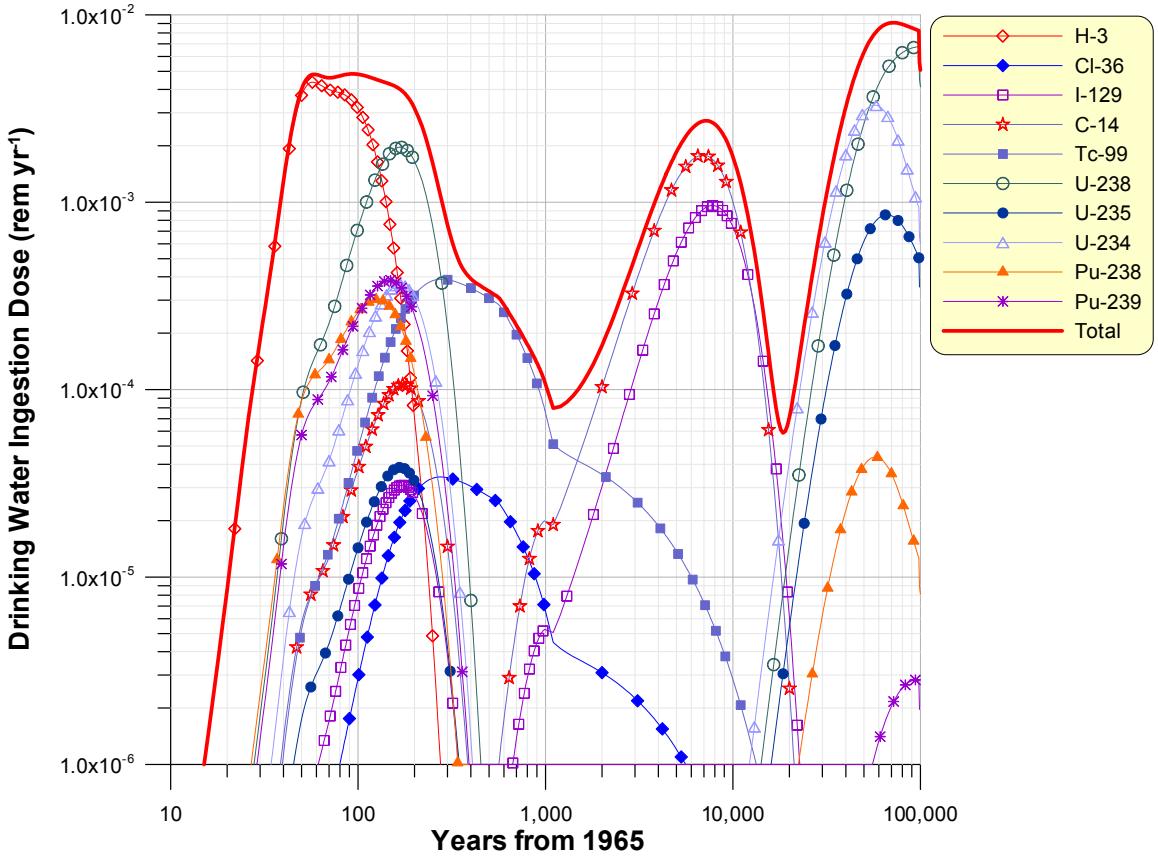

Figure 19. Groundwater ingestion dose as a function of time for the site soils cover for closure in 2056.

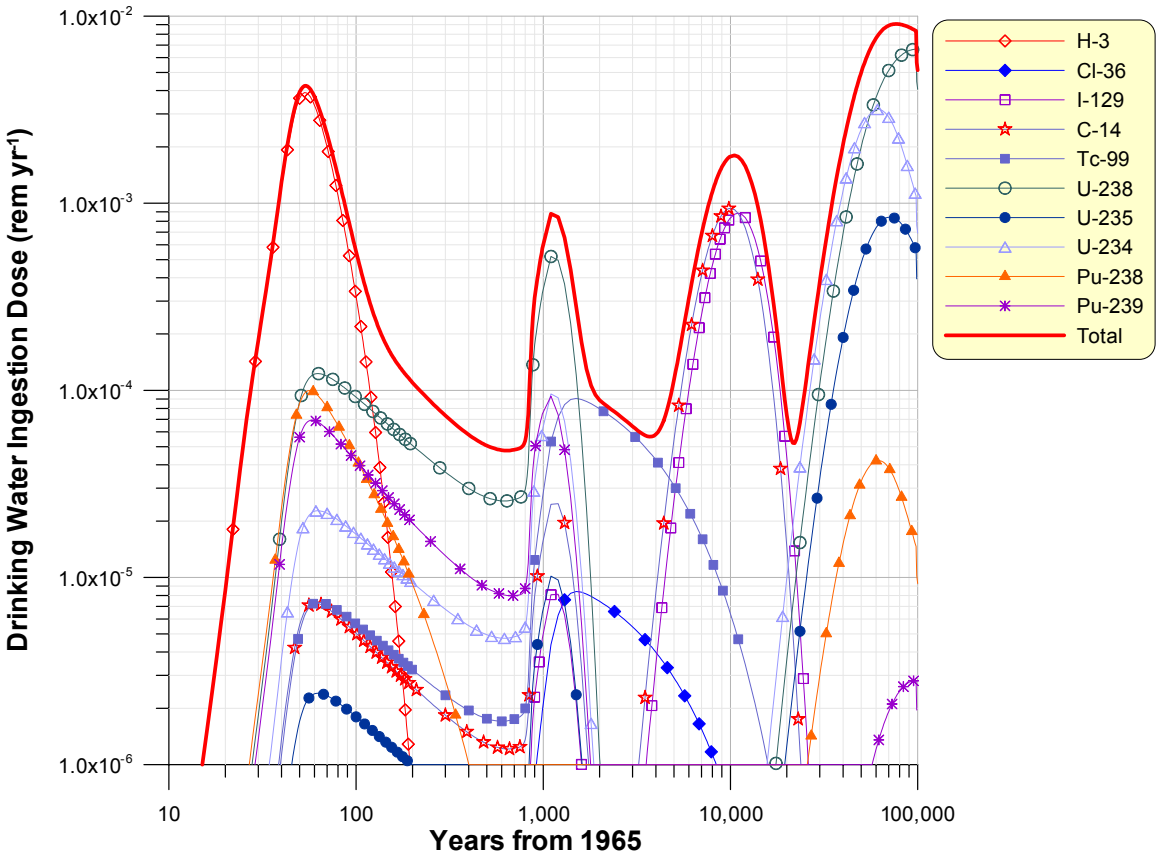

Figure 20. Groundwater ingestion doses as a function of time for the enhanced cover for closure in 2003.

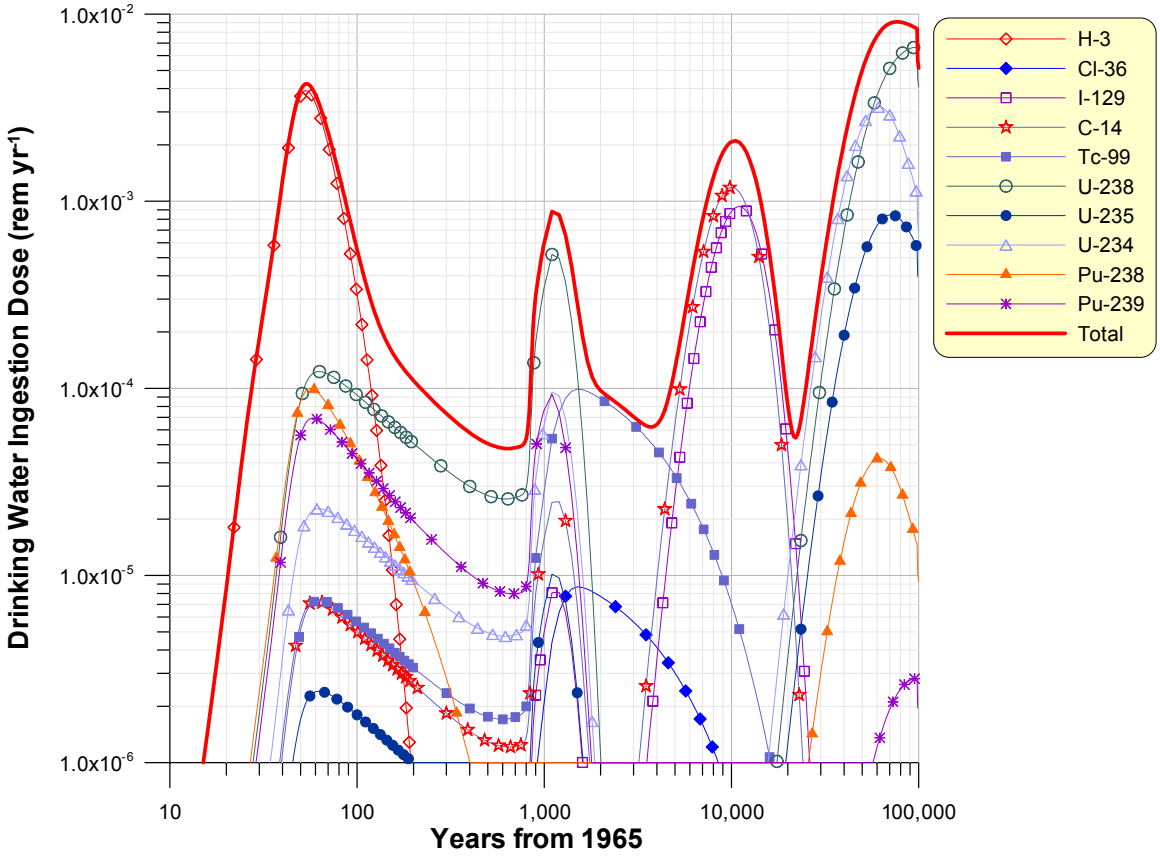

Figure 21. Groundwater ingestion doses as a function of time for the enhanced cover for closure in 2056.

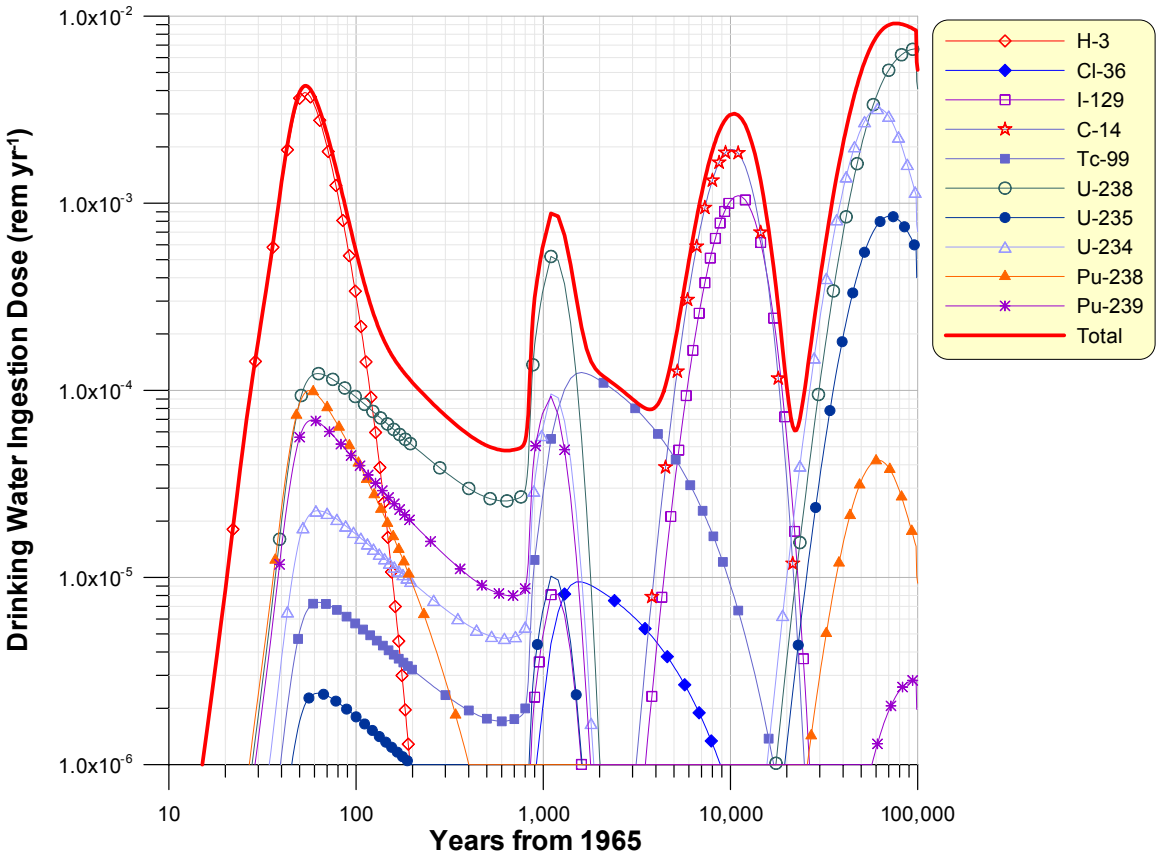

Figure 22. Groundwater ingestion doses as a function of time for the enhanced cover for closure in 2215.

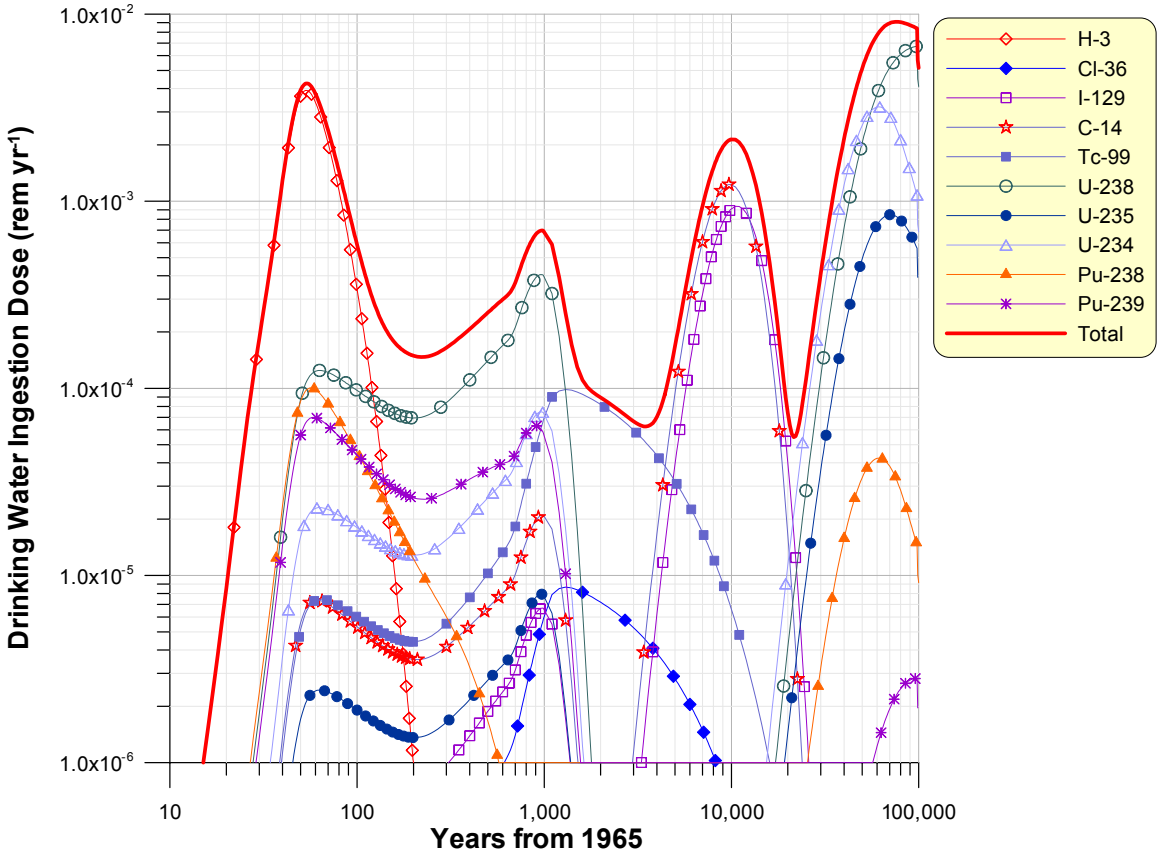

Figure 23. Groundwater ingestion dose as a function of time for the US Ecology proposed cover for closure in 2056.

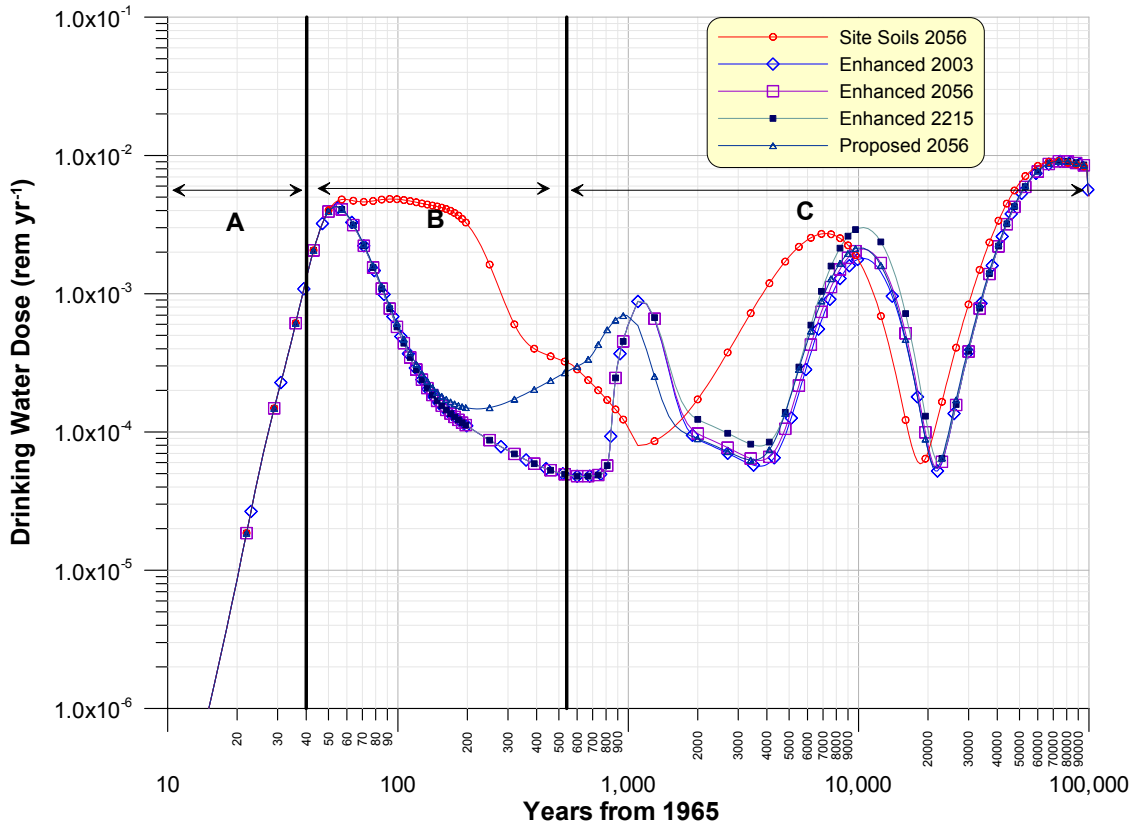

Figure 24. Total drinking water dose as a function of time for the five closure options. Three time periods of interest are shown: A = pre-cover period (year 1965–2005); B = cover period (year 2005–2505); and post cover period (year 2505–100,000).

Comparison With Original DEIS Results

Groundwater concentrations for the original DEIS (Dunkelman 2000) were reported for five of the 15 radionuclides analyzed in this assessment; Cl-36, I-129, Tc-99, U-235, and U-238. There were major differences in the conceptual model for fate and transport, radionuclide inventories, partition coefficients, and assumptions about cover lifetime. Maximum groundwater concentrations in this assessment were in some cases higher and in others, lower than those in the original DEIS (Table 21) for several reasons.

First, the waste disposal history was accounted for in this assessment but was not accounted for in the original DEIS analysis. During active waste disposal in this assessment, infiltration was enhanced due to the presence of open trenches and disturbed soil, resulting in migration of radionuclides from the trenches and into the unsaturated zone before placement of the cover. In the original DEIS, no radionuclide migration was assumed before placement of the cover.

Second, the cover was assumed to only last 500 years (and degrade to natural infiltration over the next 500 years) in this assessment compared to an infinite cover lifetime in the original DEIS. The results of this current assessment show that choice cover design has little impact on the maximum concentration during the 0-10,000 year time of compliance. However, cover design makes a large impact on groundwater concentrations during the time the cover remains intact.

Table 21. Maximum 0–10,000 year Concentrations from the Original DEIS and those from this Assessment for Closure in 2056

			Original DEIS results[a]			Results of this assessment		
Radionuclide	Original DEIS Inventory (Ci)[b]	Inventory used in this assessment (Ci)	Enhanced Cover (pCi L^{-1})	Proposed Cover (pCi L^{-1})	Site Soils Cover (pCi L^{-1})	Enhanced Cover (pCi L^{-1})	Proposed Cover (pCi L^{-1})	Site Soils Cover (pCi L^{-1})
Cl-36	4.910E+00	3.229E+00	2.0E+01	3.6E+01	4.6E+01	3.5E+00	3.5E+00	1.4E+01
I-129	6.010E+00	5.977E+00	1.9E+00	3.9E+00	4.9E+00	2.9E+00	3.2E+00	3.2E+00
Tc-99	6.710E+01	5.510E+01	2.7E+02	4.9E+02	6.3E+02	5.7E+01	5.7E+01	2.2E+02
U-235	1.467E+04	3.058E+01	5.7E-02	2.3E-01	2.3E+00	8.0E-02	6.2E-02	3.0E-01
U-238	2.227E+04	1.510E+03	8.9E-03	3.6E-02	3.6E-01	3.9E+00	3.1E+00	1.5E+01

a. From Section 3.0 of the groundwater pathway analysis for the DEIS (Dunkelman 2000).
b. From Table 8 of the groundwater pathway analysis for the DEIS (Dunkelman 2000).

Third, the cover in this assessment affects infiltration throughout the unsaturated zone whereas, in the original DEIS, it only restricted infiltration through the waste. That is, water fluxes in the unsaturated zone below the waste in the original DEIS were assumed to be the same as natural recharge.

Fourth, in the case of Cl-36 and Tc-99, a calibrated partition coefficient of 0.75 mg L^{-1} was used in the waste whereas in the original DEIS, a partition coefficient of zero was assumed for the waste. This difference is thought to be the major reason why the Cl-36 and Tc-99 concentrations in this assessment are about a factor of 6 lower than those in the original DEIS.

Finally, the maximum uranium isotope concentrations in this assessment during the 0-10,000 year time frame are driven by the mobile fraction of uranium; the immobile fraction peaks after 10,000 years. A mobile fraction was not included in the original DEIS calculations. If we ignore the mobile fraction, uranium isotope concentrations calculated in this assessment during the 0 to 10,000 year time frame are substantially less than those in the original DEIS because disposal inventories were substantially smaller in this assessment compared to those in the original DEIS (500 times smaller for U-235 and 15 times smaller for U-238).

Several other points should be made concerning the uranium isotopes. In the original DEIS, a uranium solubility of 1 mg L^{-1} was used whereas in this assessment, a solubility of 25 mg L^{-1} was used (which was the median estimated value used in the stochastic simulation in Rood 2000). Uranium solubility only affects the U-238 concentration because solubility limited releases are mass (not activity) limited. Also, partition coefficients used in this assessment were corrected for the percent gravel content whereas in the original DEIS, gravel content was not correct for. Gravel-content corrected partition coefficients were about a factor of 2 less than their nominal values.

The transport model used in the original DEIS should not be faulted as being "non-conservative". The difference between the results of this analysis and those in the original DEIS are driven mainly by the assumption of cover lifetime and inclusion of a fraction of the radionuclide inventory that was mobile, and not model formulation. If cover lifetime were assumed to be infinite as was assumed in the original DEIS analysis, then radionuclide concentrations of immobile radionuclides would be lower than the concentrations reported in Tables 16–20.

PARAMETER UNCERTAINTY ANALYSIS

This section presents the methodology and results of the parameter uncertainty and sensitivity analysis performed for the US Ecology Site. An overall uncertainty analysis evaluates the precision and accuracy of the model. Sensitivity analysis evaluates the sensitivity of model output to variability in model input. Uncertainty in models arises because a) errors in model formulation and b) errors (or uncertainty) in model input parameters (parametric uncertainty). Model formulation errors are inherent in mathematical modeling because environmental models are only simplified representations of complex environmental systems. Errors in model parameterization occur because lack of knowledge about a parameter's true, but unknown value. Ideally, site-specific parameter values should be derived and used in the simulation. In practice, parameter values are often inferred from limited measured data or derived from the literature. Additionally, model parameters may represent time and space scales that differ greatly from what can be measured in the field or laboratory. Natural variability also contributes to parameter uncertainty. The choice of a deterministic parameter value or its distribution is ultimately determined by the judgment of the analyst, and is therefore considered to have an element of subjectivity. A distribution selected in this manner is essentially a statement of the analyst's belief that the parameter's true but unknown value lies within the stated distribution.

Uncertainty in model formulation can only be evaluated through model validation. Model validation answers the question "Does the model accurately simulate the behavior of the system?". To demonstrate a model is valid, an independent data set is required. Often times, adequate independent data sets are not available and the analyst resorts to model calibration. In model calibration, parameter values are adjusted (within reason) so that model predictions match the field observations as close as possible.

Because this assessment addresses impacts that occur far into the future, it is impossible to validate the model application for future predictions because measurements are unavailable (much in the same way Einstein's theory of the speed of gravity was only recently validated because we lacked the means to measure the necessary quantities). Therefore, model uncertainty is only qualitatively addressed through the calibration procedure discussed earlier in this report. Model calibration only provides a measure of what the model can accurately simulate in the environment for the current time frame. The use of the model for forecasting the release and transport of radionuclides far into the future can never really be truly validated.

A parametric uncertainty analysis quantifies the variability in model output resulting from variability in the model parameters. It is a measure of the precision of the model and cannot address the overall accuracy of the predictions. Numerous synonyms exist in the literature for this type of analysis including error propagation (Gardner et al. 1980), impression analysis (Schwarz and Hoffman 1981), and statistical sensitivity analysis (Shaeffer 1980). The terminology adopted by Hoffman and Gandner (1983) is used in this document. As defined in Hoffman and Gardner (1983), a parametric uncertainty analysis is applicable when the structure of the model is relatively unbiased. While the overall structure of the model presented here is believed to be unbiased, the choice of some of the deterministic input parameters (which were also held constant in the parametric uncertainty analysis) were intentionally biased high (because of lack of information about the parameter), most notably, the fractional release rate from waste to soil . Therefore, the output distribution was considered to have the potential for positive bias.

Parametric uncertainty was evaluated using Monte Carlo simulation combined with simple random sampling techniques. Uncertainty is expressed in terms of a probability density function of the output variable. Information provided by the uncertainty analysis was also used to do the sensitivity analysis. Model sensitivity was evaluated by calculating the rank correlation between the distribution of the output variable and each of the distributions of the input parameters.

Parametric uncertainty analysis uses an estimated frequency distribution of values for each model parameter considered to be uncertain and produces a frequency distribution of model predictions. In Monte Carlo simulation, parameter values are randomly sampled from distributions developed by the analyst. The model is then run and the output variable stored. The process is repeated for multiple model realizations (typically greater than 100) resulting in an empirical distribution of the output variable. A Perl[4] script was used as the Monte Carlo driver for the simulation and performed the following functions for each Monte Carlo trial:

- sampled parameter values from assigned distributions
- wrote FOLAT and GWSCREEN input files for each of the radionuclides
- executed FOLAT and GWSCREEN models for each radionuclide
- extracted and stored concentrations and doses at specific times from the GWSCREEN output.

The number of radionuclides evaluated in the uncertainty analysis was limited to the primary dose contributors of the deterministic simulation. These radionuclides were H-3, Tc-99, I-129, C-14, U-238, U-238MF, and Pu-239MF. Radioactive progeny from the decay of the immobile U-238 fraction were included in the analysis. The enhanced cover for closure in the year 2056 was the only cover/closure scenario evaluated.

One of the major limitations of this parametric uncertainty analysis is that radionuclide inventories, mobile release fractions, and waste-soil fractional release rates were treated deterministically. Analysis of the mobile release fractions would require an estimate of uncertainty in the source term. Derivation of source term uncertainty was beyond the scope of this project. However, the Perl script written for the uncertainty analysis is certainly amenable to inclusion of this uncertainty in the future. Uncertainty was also not evaluated for the exposure scenario (drinking water ingestion rate) or dose conversion factors.

Infiltration from 1965 to 2005 was not considered stochastically along with the calibrated source K_d value for Tc-99. Because these values are correlated, the calibration procedure used to develop the source K_d value would have to be modified to incorporate uncertainty in these parameters. Additionally, infiltration through the engineered cover while it remained intact was also treated as a fixed value.

The parametric uncertainty analysis presented here was not intended to be comprehensive because time and resources limited what could be accomplished in an uncertainty analysis for this project. Nevertheless, the analysis lays the framework for uncertainty analysis that can be refined later with revised parameter distributions and assumptions.

Parameter distributions used in the uncertainty analysis are presented in Table 22. In general, parameter distributions were constructed by the analyst from relevant site-specific or literature data. If relevant data were not available (such as the case with the cover integrity), then a

[4] Perl (Practical Extraction Reporting Language) is a scripting language available on most Unix workstations and recently made available for Microsoft Windows-based machines

distribution was assumed. The distributions represent the analyst belief that the true, but unknown value of the parameter lies within the distribution. Material properties and natural infiltration rates were largely taken from Rood (2000a) and used without modification. Distributions of partition coefficients were based on the data in Kincaid et al. (1998). Because partition coefficient values often times span an order of magnitude or more, log-triangular distributions were assumed. The mode of the distribution was taken to be the "best estimate" K_d value reported in Kincaid et al. (2000) which was also used in the deterministic simulations. The minimum K_d was taken to be the conservative estimate of the K_d as reported in Kincaid et al. (2000). This value was used in the Phase II screening described earlier in this report. The maximum of the distribution was taken to be the highest value reported in the range of possible K_d values in Kincaid et al. (1998). No distribution was assigned to the mobile fraction actinide K_d or the Tc-99 K_d (deterministic value of zero).

Uncertainty was also considered in the longevity of cover integrity. That is, the time in which the cover remains an effective infiltration barrier. The deterministic value for this parameter was assumed to be 500 years. The distribution used in the stochastic simulation was assumed and was not based on engineering studies of the cover. The time over which the cover degraded was assumed to be equivalent to the time the cover remained intact. For example, if the cover remains intact for 300 years, then it degrades to natural infiltration in the next 300 years.

Table 22. Definition of Parameter Distributions used in the Uncertainty Analysis

Parameter	Distribution	Comments/Reference
Background infiltration (m y^{-1})	Triangular: minimum 0.0025; mode 0.005, maximum 0.01	Rood (2000a)
Longevity of cover integrity (yr)	Triangular: minimum 250, mode 500, maximum 750	Assumed
Longitudinal dispersivity in aquifer (m)	Triangular: minimum 13.75, mode 27.5, maximum 41.25	Rood (2000a)
Transverse dispersivity in aquifer (m)	Triangular: minimum 2.5, mode 5.0, maximum 7.5	Rood (2000a)
Darcy velocity in aquifer (m yr^{-1})	Truncated Lognormal: GM 32.9, GSD 2.33, minimum 3.0, maximum 250	Rood (2000a)
Bulk density, source unsaturated zone and aquifer (g cm^{-3})	Triangular: minimum 1.58, mode 1.97, maximum 2.36	Nominal values based on Kincaid et al (1998). Distribution based on Rood (2000a)
Aquifer porosity (m^3 m^{-3})	Triangular: minimum 0.097, mode 0.10, maximum 0.103	Rood (2000a)
Uranium K_d (mL g^{-1})	Log triangular: minimum 0.6, mode 3.0, maximum 79	Kincaid et al. (1998)
Thorium K_d (mL g^{-1})	Log triangular: minimum 40, mode 1000, maximum 2000	Kincaid et al. (1998)
Radium K_d (mL g^{-1})	Log triangular: minimum 8, mode 20, maximum 173	Kincaid et al. (1998)
Lead K_d (mL g^{-1})	Log triangular: minimum 2000, mode 6000, maximum 7900	Kincaid et al. (1998)
Carbon K_d (mL g^{-1})	Log triangular: minimum 0.25, mode 0.5, maximum 5.0	Kincaid et al. (1998)
Iodine K_d layers 5–13 (mL g^{-1})	Log triangular: minimum 0.3, mode 0.5, maximum 15	Kincaid et al. (1998)
Uranium solubility (mg L^{-1})	Triangular: minimum 1.0, mode 25,	Rood (2000a)

Table 22. Definition of Parameter Distributions used in the Uncertainty Analysis

Parameter	Distribution	Comments/Reference
	maximum 50	

The output variable presented in this report is the total drinking water dose at specific times after 1965. Output distributions of individual radionuclide concentrations and individual radionuclide doses are available electronically.

Distributions of model output were developed from 500 model realizations. The decision to use this number was based more on computer run time and disk storage considerations than statistical considerations. Although adding more realizations would result in greater confidence in the output distribution, the real question is what confidence do we have in any given percentile of the overall distribution. A confidence interval around percentiles of the output distribution was defined using a distribution-free approach developed in Hahn and Meeker (1991). The approach developed by Hahn and Meeker uses ordered statistics to define an interval where the true value of a given percentile lies at a specified level of confidence. In this way, confidence for any given percentile within the distribution could be defined. Of particular interest are the tails of the distribution, because values at the tails (i.e., top and bottom) of the distribution change more with the number of model realizations; central values are more stable. The ordered statistics for the 5th and 95th percentiles for 500 model realizations are 25 and 475, respectively. That is, if the output values for 500 realizations are sorted in acceding order, the 5th percentile represents the 25th highest value; the 95th percentile represents the 475th highest value. The 95% confidence interval around the 5th percentile in terms of the ordered statistics is 15 and 35. The 95% confidence interval around the 95th percentile in terms of the ordered statistics is 465 and 485. We interpret this to mean we are 95% percent confident that 90% of the model output lies between the ordered statistics 15 and 485. The range of *values* represented by these ordered statistics will vary depending on the distribution.

Uncertainty Analysis Results

A summary of the sampled parameters (Table 23) shows that median values of the assigned distributions were well represented by the sampled distributions. However, the tails of the distributions for some of the parameters were not well represented by the sampling. For example, the lower tail of the sampled distribution of uranium solubility was 2.85 mg L^{-1} but the assigned distribution had a minimum value of 1 mg L^{-1}. A greater number of model realizations and/or alternate distributions combined with Latin-Hypercube sampling may alleviate some of these sampling problems. Nevertheless, application of non-parametric confidence limits on the output distributions does account for some of the sampling error noted above and changes to the sampling scheme and assigned parameter distributions is left to a future iteration of this work.

Table 23. Statistics of the Sampled Parameter Distributions for 500 Model Realizations

Parameter	Minimum	Maximum	Mean	Median
Natural infiltration (m yr^{-1})	1.39E-03	1.91E-02	8.41E-03	7.88E-03
Cover longevity (years)	2.78E+02	7.37E+02	4.97E+02	4.99E+02
Longitudinal dispersivity (m)	1.58E+01	4.07E+01	2.77E+01	2.79E+01
Transverse dispersivity (m)	2.71E+00	7.44E+00	5.04E+00	5.02E+00
Darcy velocity in aquifer (m yr^{-1})	2.74E+00	2.25E+02	4.26E+01	3.21E+01
Bulk density (g cm^{-3})	1.61E+00	2.33E+00	1.96E+00	1.96E+00
Aquifer porosity (m3 m^{-3})	9.71E-02	1.03E-01	1.00E-01	1.00E-01
Uranium K_d , unsaturated layer 1 (mL g^{-1})[a]	8.63E-02	6.06E+01	5.91E+00	2.23E+00
Uranium K_d , unsaturated layer 2-13 (mL g^{-1})[a]	6.08E-02	4.27E+01	4.16E+00	1.58E+00
Thorium K_d , unsaturated layer 1 (mL g^{-1}) [a]	3.99E+01	1.55E+03	4.62E+02	3.79E+02
Thorium K_d , unsaturated layer 2–13 (mL g^{-1})[a]	2.81E+01	1.09E+03	3.26E+02	2.67E+02
Radium K_d , unsaturated layer 1 (mL g^{-1})[a]	4.40E+00	1.34E+02	2.88E+01	2.11E+01
Radium K_d , unsaturated layer 2–13 (mL g^{-1})[a]	3.10E+00	9.43E+01	2.03E+01	1.49E+01
Lead K_d , aquifer (mL g^{-1})[a]	2.18E+03	9.68E+03	5.41E+03	5.27E+03
Iodine K_d , unsaturated layer 1 (mL g^{-1})[a]	1.71E-01	1.17E+01	1.61E+00	8.25E-01
Iodine K_d , unsaturated layer 2–13 (mL g^{-1})[a]	1.21E-01	8.24E+00	1.13E+00	5.81E-01
Carbon K_d , unsaturated layer 1 (mL g^{-1})[a]	2.30E-01	3.50E+00	8.73E-01	6.66E-01
Carbon K_d , unsaturated layer 2–13 (mL g^{-1})[a]	1.62E-01	2.47E+00	6.16E-01	4.69E-01
Uranium solubility (mg L^{-1})	2.85E+00	4.92E+01	2.54E+01	2.55E+01

[a.] Sampled K_d value has been corrected for the percent gravel content in unsaturated layer 1 (17.3%) and unsaturated layers 2–13 (41.7%). Partition coefficients in the aquifer and source were assumed to be the same as in unsaturated layers 2–13.

Distributions of radionuclide concentrations at four output times (60 yrs, 800 yrs, 2000 yrs, and 10,000 yrs after 1965) are summarized in terms of four percentile values; 5th, 25th, 50th, and 95th percentile (Tables 24 and 25). Detailed output containing distributions of radionuclide concentrations for 28 separate output times are found in the ASCII files that accompany this report. The percentiles in Tables 24 and 25 do not include the 95% confidence intervals. The interval between the 5th and 95th percentiles spans upwards of 20 orders of magnitude or greater in some cases. Note that the span of the concentration distributions in year 60 for all mobile radionuclides (H-3, Tc-99, U-238MF, U-234MF, and Pu-239MF) were substantially smaller compared to other years of output. This difference is because the infiltration through the trenches and the cover was not considered stochastically and the radionuclides that dominate the dose at this time have K_d values fixed at zero.

Table 24. Percentiles of the Distribution of Groundwater Concentrations at 60 and 800 years from the Simulation Start Time (1965)

	Percentile, time = 60 years (Ci m^{-3})					Percentile, time = 800 years (Ci m^{-3})				
Radio-nuclide	5th	25th	50th	75th	95th	5th	25th	50th	75th	95th
H-3	2.00E-05	4.23E-05	7.02E-05	1.21E-04	2.71E-04	7.27E-24	1.95E-23	6.19E-23	3.52E-22	2.53E-21
C-14	7.07E-29	6.75E-25	1.19E-21	4.29E-19	1.20E-16	1.17E-27	2.25E-23	2.39E-20	4.47E-18	1.73E-15
I-129	2.77E-39	5.00E-32	5.93E-27	2.68E-23	2.89E-20	6.35E-37	1.58E-30	2.70E-25	1.45E-21	2.48E-18
Tc-99	1.24E-09	2.55E-09	4.37E-09	7.37E-09	1.71E-08	3.90E-10	1.09E-09	3.39E-09	1.86E-08	1.35E-07
U-238	1.29E-45	4.23E-37	7.64E-30	3.09E-24	3.95E-16	3.68E-43	7.13E-35	1.40E-28	2.75E-23	1.59E-15
U-234	1.84E-49	6.00E-41	1.16E-33	5.34E-28	1.02E-19	7.60E-46	1.52E-37	3.13E-31	6.27E-26	5.04E-18
Th-230	3.72E-57	2.24E-50	1.59E-44	3.18E-39	4.94E-32	9.63E-51	1.03E-43	4.33E-38	3.10E-33	4.39E-26
Ra-226	2.13E-54	1.35E-48	7.56E-43	5.21E-38	2.68E-31	1.62E-48	2.70E-42	1.80E-36	9.99E-32	7.06E-25
Pb-210	2.98E-57	2.43E-51	1.81E-45	9.55E-41	9.01E-34	3.59E-51	8.08E-45	4.86E-39	2.63E-34	1.88E-27
U-238MF	2.69E-10	5.66E-10	9.43E-10	1.64E-09	3.76E-09	7.65E-11	2.05E-10	6.41E-10	2.76E-09	1.23E-08
U-234MF	4.97E-11	1.05E-10	1.75E-10	3.03E-10	6.95E-10	1.42E-11	3.79E-11	1.18E-10	5.28E-10	2.26E-09
Pu-239MF	2.96E-11	6.28E-11	1.05E-10	1.83E-10	4.28E-10	4.45E-12	1.18E-11	3.56E-11	1.27E-10	4.57E-10

Table 25. Percentiles of the Distribution of Groundwater Concentrations at 2000 and 10,000 years from the Simulation Start Time (1965)

	Percentile, time = 2000 years (Ci m^{-3})					Percentile, time = 10,000 years (Ci m^{-3})				
Radio-nuclide	5th	25th	50th	75th	95th	5th	25th	50th	75th	95th
H-3	7.27E-24	1.95E-23	6.19E-23	3.52E-22	2.53E-21	0.00E+00	0.00E+00	0.00E+00	0.00E+00	0.00E+00
C-14	1.17E-27	2.25E-23	2.39E-20	4.47E-18	1.73E-15	2.65E-14	3.28E-10	4.92E-08	4.17E-07	1.58E-06
I-129	6.35E-37	1.58E-30	2.70E-25	1.45E-21	2.48E-18	2.30E-21	1.25E-14	2.10E-11	1.03E-09	5.00E-09
Tc-99	3.90E-10	1.09E-09	3.39E-09	1.86E-08	1.35E-07	5.56E-11	5.41E-10	2.50E-09	5.76E-09	1.73E-08
U-238	3.68E-43	7.13E-35	1.40E-28	2.75E-23	1.59E-15	5.81E-28	8.77E-19	8.52E-14	1.60E-09	8.19E-08
U-234	7.60E-46	1.52E-37	3.13E-31	6.27E-26	5.04E-18	1.97E-29	4.69E-20	7.55E-15	3.55E-10	2.67E-08
Th-230	9.63E-51	1.03E-43	4.33E-38	3.10E-33	4.39E-26	8.08E-34	1.33E-25	2.24E-20	7.77E-16	2.66E-13
Ra-226	1.62E-48	2.70E-42	1.80E-36	9.99E-32	7.06E-25	1.57E-30	9.89E-24	1.74E-18	3.05E-14	6.82E-12
Pb-210	3.59E-51	8.08E-45	4.86E-39	2.63E-34	1.88E-27	2.74E-33	5.08E-26	3.25E-21	8.14E-17	1.51E-14
U-238MF	7.65E-11	2.05E-10	6.41E-10	2.76E-09	1.23E-08	0.00E+00	2.02E-94	1.72E-66	1.03E-45	8.96E-16
U-234MF	1.42E-11	3.79E-11	1.18E-10	5.28E-10	2.26E-09	0.00E+00	3.64E-95	3.09E-67	1.85E-46	1.61E-16
Pu-239MF	4.45E-12	1.18E-11	3.56E-11	1.27E-10	4.57E-10	0.00E+00	2.48E-94	1.56E-67	3.56E-46	3.83E-16

Distribution of the total drinking water dose as a function of time (Figure 25) shows the uncertainty bounds increasing with increasing time. The uncertainty bounds (shaded area on Figure 25) represent the 5th and 95th percentiles with 95% confidence. Maximum doses during the 0–100 year time frame span about a factor of 25 between the 5th (<0.1 mrem yr^{-1}) and 95th (~ 2.5 mrem yr^{-1}) percentiles. Deterministic doses during the 0–100 year time frame are less than 5 mrem yr^{-1} and follow the median (50th percentile) of the distribution of predicted doses. Beyond 1000 years, the median estimate of the dose distribution does not exactly follow the deterministic value and the span of the 5th and 95th percentile values increase to over three orders of magnitude

at 10,000 years. Divergence of the median value from the deterministic dose estimate after 100 years is due to the increasing importance cover failure time and doses from sorbing radionuclides.

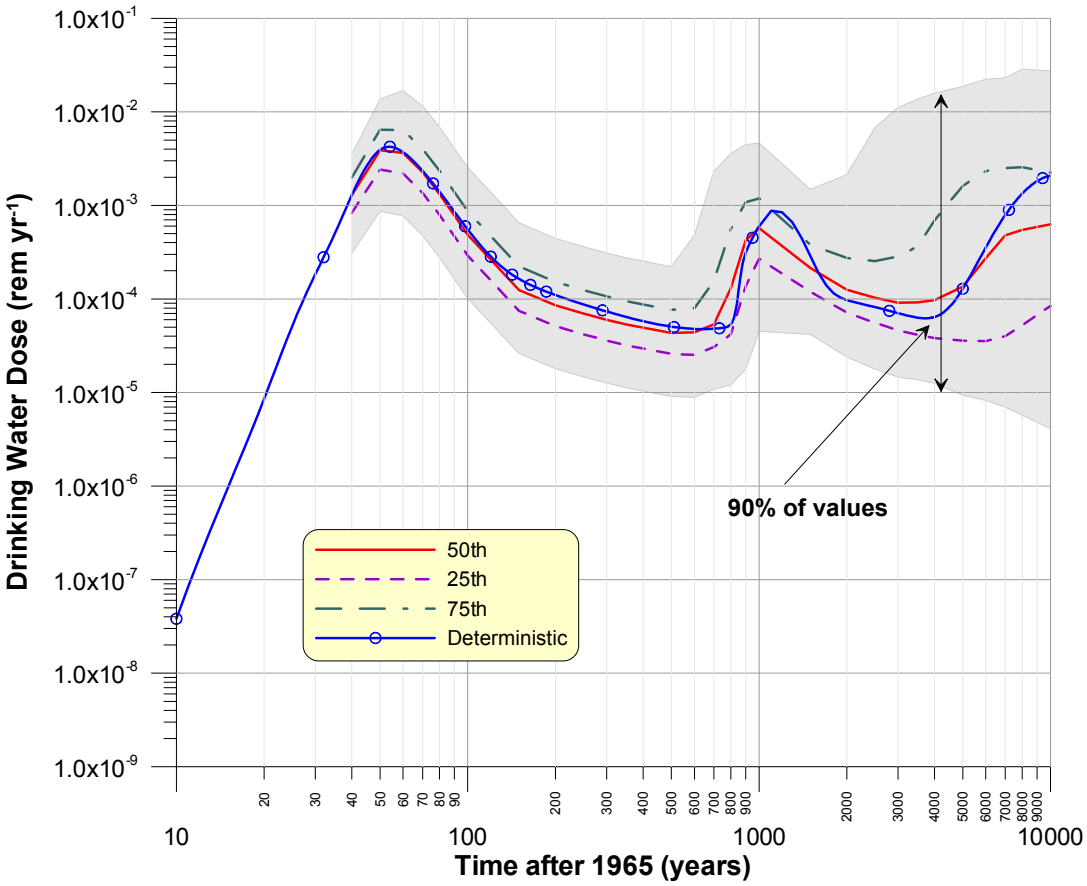

Figure 25. Stochastic simulation of the enhanced cover for closure in 2056 showing the distribution of total dose as a function of time. The shaded area represents the area between the 5th and 95th percentiles of the distribution (with 95% confidence). Also shown are the 25th, 50th and 75th percentiles of the distribution, and the deterministic results.

The results presented here indicate the variability of the model-predicted total drinking water dose is roughly a factor of 25 at times less than 100 years, and increases to over three orders-of-magnitude for times greater than 100 years. The distribution of total doses are summarized in Table 26. Note that the distributions of doses only relate to the variability in predicted doses and not to any real or actual doses.

Table 26 Summary of Distributions of Predicted Total Drinking Water Dose at the Receptor Well for the Enhanced Cover for Closure in year 2056

	Year of dose (years from start of simulation in 1965)				
	Year 2,025 (60 years)	Year 2,465 (500 years)	Year 2,965 (1,000 years)	Year 4,465 (2,500 years)	Year 9,965 (8,000 years)
Percentile	Dose (mrem)	Dose (mrem)	Dose (mrem)	Dose (mrem)	Dose (mrem)
2.5^{th}	0.77	0.0091	0.045	0.018	0.0057
5^{th}	1.0	0.012	0.066	0.024	0.0095
25^{th}	2.2	0.026	0.27	0.056	0.052
50^{th}	3.6	0.043	0.57	0.10	0.55
75^{th}	6.4	0.077	1.2	0.25	2.6
95^{th}	14	0.18	3.6	2.8	13
97.5^{th}	17	0.22	4.6	6.8	28

Sensitivity Analysis

A quantitative sensitivity analysis was performed using the data generated during the uncertainty analysis. In the approach presented here, the Monte Carlo sampling techniques described earlier were used to propagate input parameter uncertainty into the predicted dose estimates. Then, using regression techniques, rank correlation coefficients were calculated between each parameter and the corresponding predicted dose. Parameter sensitivities are then established by the degree of correlation between the parameter and the output variable (predicted dose).

The methods used to evaluate parameter sensitivity are described in Crystal Ball software package (Decisioneering Inc. 2000). The rank correlation coefficients provide a quantitative measure of the sensitivity of the predicted dose to variations in the input parameters. Rank correlation replaces each input parameter and endpoint value pair, with its ranking within the distribution. Linear correlation of the rankings is then performed. Consider a simulation of n Monte Carlo trials where the parameters, a, b, and c are defined stochastically. The output variable defined as y, is calculated n times during the simulation. The results may be tabulated as follows:

$a_1 \quad b_1 \; c_1 \quad \Rightarrow \quad y_1$
$a_2 \quad b_2 \; c_2 \quad \Rightarrow \quad y_2$
$a_3 \quad b_3 \; c_3 \quad \Rightarrow \quad y_3$
.
.
.
$a_n \quad b_n \; c_n \quad \Rightarrow \quad y_n$

The subscript 1, 2, 3, ...n refer to the Monte Carlo trial number. To calculate the rank correlation coefficient, the values of a_i, b_i, c_i, and y_i are replaced by their ranking within the distribution of values. For example, suppose for the third Monte Carlo trial, the values a_3, b_3, c_3, are selected

yielding an output value of y_3. Suppose 500 trials are performed and the value of a_3 was ranked at 23; –that is, it is the 23rd highest value within the distribution 500 values of a. The value of a_3 is replaced by 23. Likewise, the values of b_3, c_3, and y_3 are replaced by their respective ranks. Linear correlation is then performed between the ranks of each of the parameters and output variable, y.

The advantage of rank correlation over simple liner correlation is that it is nonparameteric. That is, it is not dependent on the underlying distribution of either the input or output variables. The rank correlation coefficient is given by (Press et al. 1992)

$$r_s = \frac{\sum_i \left(R_i - \overline{R}\right)\left(S_i - \overline{S}\right)}{\sqrt{\sum_i \left(R_i - \overline{R}\right)^2}\sqrt{\sum_i \left(S_i - \overline{S}\right)^2}} \tag{17}$$

where

r_s = the rank correlation coefficient
R_i = the rank of the input parameter value
S_i = the rank of the corresponding output value.

The advantage of using Monte Carlo techniques over that of a one-factor-at-a-time approach is that interactions between parameters are included in the analysis. For example, the sensitivity of the dose due to parameter *Y* may depend on the value chosen for parameter *X*. Rank correlation coefficients provides a meaningful measure of the degree to which parameters and the endpoint (drinking water dose) *change together*. The rank correlation coefficient takes on a value between –1 and +1. Perfect correlation is achieved when the absolute value of the correlation coefficient equals 1. Degree of correlation (and thereby degree of sensitivity), decreases with a decrease in the absolute value of the correlation coefficient. A positive correlation coefficient indicates that an increase in the value of the parameter results in an increase in the computational endpoint. A negative correlation coefficient indicates that an increase in the value of the parameter results in a decrease in the computational endpoint.

Another way to visualize the sensitivity analysis results is to compute the percent contribution each parameter has to the total variance. The contribution to the total variance was *approximated* using a simple technique described in the Crystal Ball® software (Decisioneering Inc. 2000) where the rank correlation coefficient for each parameter is squared and normalized to 100%. The output variable for this analysis is total (all nuclides) drinking water dose at specific times. Based on the results of the uncertainty analysis, four time-periods were chosen: 60, 800, 2000, and 10,000 years. These time periods correspond roughly to the times of maximum dose in the 0–10,000-year time frame.

Sensitivity Analysis Results

Results of the sensitivity analysis (Table 27) indicate that the sensitivity of a given parameter is time dependent. At 60 years after the start of operations, drinking water doses were most sensitive to Darcy velocity in the aquifer and to aquifer porosity. Correlation coefficients for most other parameters (excluding Darcy velocity and porosity) were not statistically significant, indicating there was no correlation between the drinking water dose and the parameter. Doses at 60 years were dominated by H-3.

At 800 years, drinking water doses were most sensitive to cover longevity, Darcy velocity in the aquifer, and background infiltration. The mean cover failure time was 500 years after installation of the cover in the year 2005 and therefore, failure would have a substantial impact on non-sorbing radionuclides. Doses at 800 years were dominated by the mobile fraction of the uranium and plutonium isotopes and to a minor extent, Tc-99.

At 2000 years, drinking water doses were most sensitive to Darcy velocity in the aquifer and to background infiltration. Drinking water doses also show some sensitivity to the iodine and uranium K_d values as well as the uranium solubility. Doses at 2000 years were dominated by Tc-99, I-129, and U-238.

At 10,000 years, drinking water doses were most sensitive to uranium K_d values, background infiltration, Darcy velocity in the aquifer, and carbon and iodine K_d values. Doses at 10,000 years were dominated by U-238 and C-14.

Table 27. Rank Correlation Coefficient (RCC) and Percent Contribution to Variance for the Enhanced Cover with Closure in Year 2056

	60 years		800 years		2000 years		10,000 years	
Parameter	RCC	Percent variance	RCC	Percent variance	RCC	Percent variance	RCC	Percent variance
Background infiltration	1.54E-02	0.02%	3.27E-01	12.13%	1.58E-01	2.93%	4.09E-01	19.96%
Cover longevity	8.26E-03	0.01%	-7.03E-01	56.12%	2.46E-02	0.07%	-2.54E-01	7.69%
Longitudinal dispersivity	-8.62E-03	0.01%	1.31E-02	0.02%	-4.52E-02	0.24%	5.75E-02	0.39%
Transverse dispersivity	-2.41E-02	0.06%	6.42E-03	0.01%	-9.61E-03	0.01%	-1.73E-02	0.04%
Darcy velocity	-1.00E+00	94.59%	-5.01E-01	28.49%	-8.54E-01	85.64%	-3.48E-01	14.41%
Bulk density-source	2.98E-02	0.08%	-1.79E-02	0.04%	-3.72E-02	0.16%	8.55E-02	0.87%
Bulk density-unsat and aquifer	-9.97E-03	0.01%	1.71E-02	0.03%	6.84E-03	0.01%	3.58E-02	0.15%
Aquifer porosity	-1.07E-01	1.09%	-7.22E-02	0.59%	-7.48E-02	0.66%	-8.23E-02	0.81%
Uranium Kd, Unsat layers 1	-2.65E-02	0.07%	4.13E-03	0.00%	-9.75E-02	1.12%	-4.17E-01	20.70%
Uranium Kd, Unsat layer 2-13	-2.65E-02	0.07%	4.09E-03	0.00%	-9.74E-02	1.12%	-4.17E-01	20.70%
Thorium Kd, Unsat layers 1	6.75E-02	0.43%	-3.76E-02	0.16%	5.81E-02	0.40%	2.34E-02	0.07%
Thorium Kd, Unsat layers 2-13	6.75E-02	0.43%	-3.76E-02	0.16%	5.82E-02	0.40%	2.34E-02	0.07%
Radium Kd, Unsat layers 1	5.28E-02	0.26%	2.50E-02	0.07%	6.50E-02	0.50%	2.49E-02	0.07%
Radium Kd, Unsat layers 2-13	5.27E-02	0.26%	2.50E-02	0.07%	6.50E-02	0.50%	2.49E-02	0.07%
Lead Kd, aquifer	5.78E-02	0.32%	8.66E-02	0.85%	5.31E-02	0.33%	5.12E-02	0.31%
Iodine Kd, Unsat layers 1	-8.50E-02	0.68%	-6.61E-02	0.50%	-1.05E-01	1.30%	-1.72E-01	3.53%
Iodine Kd, Unsat layers 2-13	-8.50E-02	0.68%	-6.62E-02	0.50%	-1.05E-01	1.30%	-1.72E-01	3.53%
Carbon Kd, Unsat layers 1	-4.62E-03	0.00%	-2.02E-02	0.05%	-7.01E-02	0.58%	-1.66E-01	3.28%
Carbon Kd, Unsat layers 2-13	-4.57E-03	0.00%	-2.02E-02	0.05%	-7.01E-02	0.58%	-1.66E-01	3.27%
Uranium solubility	9.94E-02	0.93%	3.91E-02	0.17%	1.36E-01	2.18%	2.51E-02	0.08%

SUMMARY AND CONCLUSIONS

The analysis documented in this report was performed in response to the WDOH request to reconcile measured concentrations of radionuclides in the unsaturated zone with model-estimated values. Borehole measurements below trench 5 showed detectable concentrations of radionuclides. Evaluation of concentrations in the unsaturated zone required a new conceptual

and mathematical model of waste disposal and radionuclide transport in the unsaturated zone. The conceptual and mathematical models incorporated into this assessment more accurately reflect the waste disposal history at the US Ecology site, time-variable infiltration as a consequence of pre- and post-cover disposals, and radionuclide transport in the unsaturated zone. Three cover designs were evaluated; a site soils cover, an enhanced cover, and the US Ecology proposed cover. The benefit of installing an engineered cover as opposed to the site soils cover is a reduction of the predicted doses during the 100 to 600 year time period; the time the cover is assumed to remain intact. Doses after about 1,000 years are essentially the same for each cover design.

In addition to calculating aquifer concentrations and drinking water ingestion doses with estimates of uncertainty, the entire radionuclide inventory was re-examined for potential impacts to the groundwater pathway using a two-phase screening methodology. The screening results showed 15 radionuclides (C-14, Cl-36, H-3, I-129, Pu-238,-239,-240,-242, Ra-226, Tc-99, Th-230, Th-232, U-234, U-235, and U-238) were important to the groundwater pathway compared to the five radionuclides considered in the original DEIS (I-129, Tc-99, Cl-36, U-235, and U-238). However, the deterministic simulation results indicated only eight radionuclides contribute significantly to the drinking water ingestion dose for the 0 to 10,000-year time period. These radionuclides included four of the five radionuclides considered in the original DEIS plus H-3, C-14, U-234MF, and Pu-239MF. The immobile fractions of the actinides were estimated to arrive at the aquifer well after 10,000 years. Although Ni-63 and Sr-90 were screened from the initial radionuclide inventory, these radionuclides were detected in borehole samples and were therefore considered in the model calibration procedure. Conservative estimates of the drinking water dose estimates for Ni-63 and Sr-90 mobile fractions were less than 4 mrem yr^{-1}, and therefore these radionuclides did not warrant further consideration beyond model calibration. Tritium was shown to be the major dose contributor in the 0 to 100 year time period; however, deterministic doses were less than one 5 mrem yr^{-1}. Carbon-14 concentrations and doses were highest around 10,000 years but doses were less than a mrem yr^{-1}. With the possible exception of C-14 and H-3, the radionuclide screening performed in the original DEIS appears to have correctly chosen the major dose contributors.

Aquifer concentrations for these analyses were higher in some cases and lower in others compared to those reported in the original DEIS. The higher concentrations were mainly attributed to the assumed lifetime of the cover and inclusion of a mobile actinide fraction. In the original DEIS, the cover was assumed to last for infinity. This assumption is difficult to defend given that manmade disturbance could compromise the integrity of the cover anytime after institutional control. If cover integrity is assumed to be infinite, then estimated doses would be substantially lower. It is impossible to know how the cover will perform over long periods of time with no periodic maintenance or monitoring. For these reasons, a 500-year cover lifetime was assumed in the calculations.

Uranium-238 aquifer concentrations were higher in this assessment compared to the original DEIS despite the fact that the U-238 inventory in the original DEIS was more than an order of magnitude higher than in this analysis. This apparent discrepancy was attributed to the uranium solubility value, cover lifetime, and the mobile fraction of uranium. The solubility value used in the original deterministic DEIS calculations (1 mg L^{-1}) was on the lower end of the distribution of uranium solubility limits (~1 to 50 mg L^{-1}). If the original deterministic DEIS uranium solubility value (1 mg L^{-1}) were to be used with the current transport model, and the mobile fraction

ignored, then U-238 concentrations would be about an order of magnitude lower than the values reported in this document.

Ancillary calculations using the HYDRUS code indicated that over time, the infiltration shadow beneath the cover would extend all the way to the aquifer. This is an important finding and differs from the conservative assumption used in the original DEIS that the infiltration shadow only extended a minor distance below the bottom of the trench.

Uncertainty analysis indicated that the distribution of model-predicted doses spanned about a factor of 25 for times less than 100 years (5^{th} and 95^{th} percentiles). The span of the dose distribution increased to about three orders of magnitude at 10,000 years. The uncertainty analysis provides a measure of the precision of the model and should not be interpreted as the probability of any real or actual exposure occurring. It is simply a measure of the precision by which the model can estimate concentrations and doses far into the future.

The sensitivity analysis showed the cover lifetime to be a particularly sensitive parameter at 800 years from the start of the simulation in 1965. Doses were not particularly sensitive to its value at output times less than 200 years or greater than 2000 years.

Overall, the assessment integrates natural processes that govern the transport radionuclides in the subsurface, with known waste disposal histories, past operational practices, and future closure plans of the site into a transport model that estimates both past and future radionuclide migration from the US Ecology low-level radioactive waste site. Conservative assumptions were made where uncertainty exists and therefore, these results should be viewed as conservative estimates of radionuclide concentrations and drinking water doses.

REFERENCES

Baes, C.F. III and R.D. Sharp, 1983. "A Proposal for Estimation of Soil Leaching and Leaching Constants for Use in Assessment Models" *Journal of Environmental Quality* 12(1): pp 17-28.

Bowman, S.M., and T. Suto, 1996. *Scale-4 Analysis of Pressurized Water Reactor Critical Configurations: Volume 5–North Anna Unit 1 Cycle 5*. ORLN/TM-12294/V5. Oak Ridge National Laboratory, Oak Ridge Tennessee.

Cox, W.M. and J.A. Tikvart. 1990. "A Statistical Procedure for Determining the Best Performing Air Quality Simulation Model." *Atmospheric Environment* 24A: 2387–2395.

DOE (U.S. Department of Energy), 1994, *Track 2 Sites: Guidance for Assessing Low Probability Hazard Sites at the INEL,* DOE/ID-10389, U.S. Department of Energy Idaho Operations Office, Idaho Falls, ID, January 1994.

EPA (U.S. Environmental Protection Agency). 1988. *Procedures for Determining the Best Performing Model*. Office of Air Quality Planning and Standards, Research Triangle Park, NC.

Fox, D.G. 1981. "Judging Air Quality Model Performance–A Review of the Woods Hole Workshop." *Bull. Am. Meteorol. Soc*. 62: 599–602.

Decisioneering Inc. 2000. *Crystal Ball 2000; Forecasting and Risk Analysis for Spreadsheet Users*. Decisioneering Inc., Denver Colorado.

Dunkelman, M., 2000. *Groundwater Pathway Analysis for the Commercial Low-Level Radioactive Waste Disposal Site, Richland Washington*. Washington State Department of Health, Division of Radiation Protection, Olympia, Washington.

Gee, G.W., M.J. Fayer, M.L. Rockhold, and M.D. Campbell, 1992. "Variations in Recharge at the Hanford Site." *Northwest Science*, vol 61, pp237–250.

Hahn, G.J. and W.Q. Meeker. 1991. *Statistical Intervals: A Guide for Practitioners*. New York: John Wiley & Sons Incorporated.

Hoffman, F.O., and R.H. Gardner, 1983. "Evaluation of Uncertainties in Radiological Assessment Models" In: *Radiological Assessment*, J.E. Till and H.R. Meyer eds. NUREG CR-3332. U.S. Nuclear Regulatory Commission, Washington, DC.

International Commission on Radiation Protection (ICRP), 1958. *Recommendations of the International Commission on Radiation Protection, Report to the Committee on Permissible Dose for Internal Radiation–1958 Revision*. Pergamon Press, London England.

ICRP 1993. *Age-dependent Doses to Members of the Public from Intake of Radionuclides: Part 2, Ingestion Dose Coefficients*. ICRP Publication 67. Annals of the ICRP 23(3/4). Elsevier Science Ltd., Oxford, England.

ICRP 1998. *The ICRP Database of Dose Coefficients: Workers and Members of the Public*. Elsevier Science Ltd., Oxford, England.

Kincaid, C.T., M.P. Bergeron, C.R. Cole, M.D. Freshley, N.L. Hassig, V.G. Johnson, D.I. Kaplan, R.J. Serne et al., 1998. *Composite Analysis for Low-Level Waste Disposal in the 200 Area Plateau of the Hanford Site*. PNNL-11800, Pacific Northwest Laboratories, Richland, Washington.

Lyman, W.J., W.F. Reehl, and D.H. Rosenblatt. 1990. *Handbook of Chemical Property Estimation Methods.* American Chemical Society, Washington, DC.

Minor, D.A., 2001. *Data Evaluation: Facility Investigation Data: US Ecology Inc Data: Washing State Department of Health Data*. Prepared for the Washington State Department of Health by Doris A. Minor, Nuclear and Environmental Consultant, August 1999.

Press, W.H., B.P. Flannery, S.A. Teukolsky, and W.T. Vetterling, 1992. *Numerical Recipes: The Art of Scientific Computing.* Cambridge: Cambridge University Press.

Rood, A. S., 1999. *GWSCREEN: A Semi-Analytical Model for Assessment of the Groundwater pathway from Surface or Buried Contamination, Theory and User's Manual Version 2.5*. INEEL/EXT-98-00750, Rev 1 February, Idaho National Engineering and Environmental Laboratory, Idaho Falls, Idaho.

Rood, A.S., 2000a. *Groundwater Pathway Uncertainty Analysis in Support of the Performance Assessment for the US Ecology Low-Level Radioactive Waste Facility*. K-Spar Inc., Rigby, Idaho, Originally published September 16, 1999, Revised May 24, 2000.

Rood, A.S., 2000b. *Further Evaluation of Groundwater Concentrations for Different Covers at the US Ecology Low-Level Waste Disposal Site, Hanford Washington using GWSCREEN 2.5 and Minimizing the Cover's Effect at Depth*. K-Spar Inc, Rigby, Idaho, May 10,2000.

Rood, A.S., 2003. *FOLAT: A Model for Assessment of Leaching and Transport of Radionuclides in Unsaturated Porous Media*. K-Spar Inc., Rigby Idaho, December, 2002.

Scott, S.J., and D.M. Hetrick, 1994. *The New SESOIL User's Guide*. PUBL-SW-200-94. Science & Technology Management Inc., Brookfield, WI. Distributed by the Radiation Safety Information Computational Center, Oak Ridge National Laboratory, Oak Ridge, Tennessee.

Sheppard, M.E. and D.H. Thibault. 1990. "Default Soil Solid/liquid Partition Coefficients, k_ds, for Four Major Soil Types: A Compendium." *Health Phys.* 59 (4): 471–482.

Simunek, J, M. Sejna, and M. Th. Van Genuchten, 1999, *HYDRUS-2D/MESHGEN-2D Simulating Water Flow and solute Transport in Two-Dimensional Variably Saturated Media*, IGWMC-TPS 53C, Version 2.0, International Ground Water Modeling Center, Colorado School of Mines, Golden, Colorado.

Schwarz, G. and F.O. Hoffman, 1981. "Imprecision of Dose Predictions for Radionuclides Released to the Environment: An Application of a Monte Carlo Simulation Technique." *Environment International* 4, 289–97.

Shaeffer, D.L., 1980. "A Model Evaluation Methodology Applicable to Environment Assessment Models." *Ecol. Modeling* 8, 275–95.

Sullivan, T.M., 1996. *DUST Disposal Unit Source Term, Data Input Guide.* NUREG/CR-6041, BNL-NUREG-52375. Brookhaven National Laboratory, Upton, New York.

Tuli, J.K., 1990. *Nuclear Wallet Cards*. National Nuclear Data Center, Brookhaven National Laboratory, Upton, NY.

US Ecology 1999. *Comprehensive Facility Investigation Richland LLRW Disposal Facility Richland, Washington Phase 1 and 2 Report*. US Ecology, Richland Washington.

US Ecology 1994. *Site Stabilization and Closure Plan for the Low-Level Radioactive Waste Management Facility*. US Ecology Inc., Richland, Washington.

APPENDIX A

SUMMARY OF RADIONUCLIDE CONCENTRATIONS IN BORE HOLE SAMPLES

APPENDIX A: SUMMARY OF RADIONUCLIDE CONCENTRATIONS IN BORE HOLE SAMPLES

Table A-1 Summary of Measured Concentrations of Radionuclides in Boreholes Beneath Trench 5 (from US Ecology 1999, Appendix A)

Borehole	Depth (m)	U-238 (pCi/g)	U-235 (pCi/g)	U-234 (pCi/g)	Pu-239 (pCi/g)	Pu-238 (pCi/g)	Sr-90 (pCi/g)	Ni-63 (pCi/g)	Tc-99 (pCi/g)	Th-232 (pCi/g)	Ra-226 (pCi/g)
A	0.0	2.2E-01	1.3E-02	2.6E-01	<MDC	<MDC	3.0E-01	<MDC	<MDC	2.9E-01	2.9E-01
	3.0	3.2E-01	5.1E-02	4.6E-01	<MDC	<MDC	5.2E-01	5.0E+00	<MDC	5.3E-01	5.6E-01
	5.5	3.0E-01	3.4E-02	3.1E-01	<MDC	3.7E-02	2.3E-01	5.8E+00	<MDC	5.7E-01	5.0E-01
	8.2	3.0E-01	4.1E-02	3.3E-01	1.9E-02	<MDC	3.6E-01	2.9E+00	6.1E-01	1.2E+00	4.3E-01
	13.4	4.0E-01	4.5E-02	3.7E-01	1.9E-02	<MDC	3.5E-01	5.1E+00	<MDC	6.1E-01	5.4E-01
	16.2	3.1E-01	2.9E-02	3.7E-01	<MDC	<MDC	5.1E-01	6.1E+00	<MDC	7.1E-01	7.3E-01
	18.6	3.9E-01	2.4E-02	4.4E-01	3.6E-02	<MDC	1.4E-01	5.1E+00	<MDC	8.8E-01	5.1E-01
	21.3	4.1E-01	5.2E-02	3.9E-01	2.6E-02	<MDC	6.1E-01	3.5E+00	<MDC	5.4E-01	5.0E-01
B	0.0	3.8E-02	1.9E-02	3.2E-02	<MDC	<MDC	3.7E-01	2.0E+00	5.8E-01	2.3E-01	7.5E-01
	2.4	3.5E-02	mdc	2.6E-02	1.9E-02	<MDC	4.0E-01	5.0E+00	<MDC	6.1E-01	6.4E-01
	5.2	4.1E-02	1.9E-02	4.4E-02	1.9E-02	2.0E-02	6.0E-01	1.2E+00	<MDC	7.2E-01	5.2E-01
	7.9	4.0E-02	2.2E-02	6.4E-02	1.9E-02	<MDC	4.4E-01	4.5E+00	7.2E-01	5.5E-01	3.9E-01
	10.7	5.3E-02	2.9E-02	5.7E-02	1.9E-02	<MDC	8.4E-01	5.0E+00	<MDC	6.7E-01	4.9E-01
	13.1	6.8E-02	1.5E-02	9.7E-02	<MDC	2.0E-02	6.5E-01	4.5E+00	<MDC	7.2E-01	6.7E-01
	15.8	4.9E-02	7.0E-03	4.0E-02	<MDC	<MDC	1.1E+00	1.7E+00	<MDC	5.7E-01	2.9E-01
	18.3	4.8E-02	2.0E-02	1.0E-01	1.9E-02	<MDC	6.8E-01	1.5E+00	<MDC	5.4E-01	5.1E-01
	21.0	6.0E-02	1.4E-02	6.5E-02	<MDC	<MDC	3.4E-01	4.0E+00	<MDC	6.3E-01	6.4E-01
C	0.0	1.8E-01	1.1E-01	1.7E-01	<MDC	<MDC	2.1E-01	1.0E+01	<MDC	8.6E-02	5.0E-01
	3.0	1.5E-01	4.6E-02	1.7E-01	<MDC	<MDC	2.2E-01	3.7E+00	<MDC	1.4E-01	9.3E-01
	6.1	1.1E-01	3.7E-02	1.1E-01	<MDC	<MDC		3.9E+00	<MDC	2.8E-01	8.3E-01
	8.2	1.7E-01	2.4E-02	1.8E-01	<MDC	<MDC	1.2E-01	5.8E+00	6.9E-01	1.7E-01	5.9E-01
	11.0	1.8E-01	mdc	1.6E-01	<MDC	<MDC	8.9E-02	3.3E+00	<MDC	2.2E-01	8.5E-01
	13.4	2.9E-01	4.1E-02	2.7E-01	<MDC	<MDC		4.3E+00	<MDC	1.8E-01	7.2E-01
	16.2	2.0E-01	2.3E-02	1.9E-01	<MDC	<MDC	3.1E-01	5.3E+00	<MDC	1.7E-01	4.5E-01
	18.9	1.6E-01	mdc	2.1E-01	<MDC	<MDC		5.6E+00	<MDC	1.3E-01	6.6E-01
	21.3	2.0E-01	mdc	2.0E-01	<MDC	<MDC		4.3E+00	<MDC	2.3E-01	6.6E-01
	21.3	1.9E-01	2.4E-02	1.8E-01	<MDC	<MDC	7.2E-02	6.1E+00	<MDC	1.4E-01	3.3E-01
D	0.0	1.6E-01	5.2E-02	2.0E-01	<MDC	<MDC	1.6E-01	6.7E+00	<MDC	2.2E-01	5.3E-01
	2.4	1.2E-01	2.5E-02	1.3E-01	<MDC	<MDC	8.0E-02	4.2E+00	<MDC	2.2E-01	4.9E-01
	5.2	1.3E-01	mdc	1.5E-01	<MDC	<MDC	2.9E-01	4.1E+00	<MDC	1.8E-01	6.4E-01
	7.9	1.1E-01	mdc	1.5E-01	<MDC	<MDC	4.9E-02	6.4E+00	<MDC	2.4E-01	5.2E-01
	10.7	9.2E-02	mdc	1.4E-01	<MDC	<MDC	9.0E-02	3.4E+00	6.2E-01	1.7E-01	8.9E-01
	13.4	1.2E-01	mdc	1.3E-01	<MDC	<MDC	1.4E-01	6.7E+00	<MDC	1.6E-01	7.0E-01
	15.8	1.0E-01	mdc	1.5E-01	<MDC	<MDC	2.0E-01	6.5E+00	<MDC	7.2E-01	1.0E+00
	18.6	2.1E-01	mdc	3.3E-01	<MDC	<MDC	2.8E-01	4.0E+00	<MDC	2.4E-01	5.7E-01
	21.3	1.1E-01	mdc	2.3E-01	<MDC	<MDC	2.9E-01	5.7E+00	<MDC	2.4E-01	4.9E-01
	21.3	1.8E-01	2.8E-02	1.7E-01	<MDC	<MDC	3.2E-01	7.2E+00	<MDC	2.3E-01	6.4E-01

Table A-2 Mass of Uranium Isotopes in Bore Hole Samples and Computed Weight Percents

		Mass of isotope in 1 g of soil				Weight percent		
Borehole	Depth (m)	U-238	U-235	U-234	Total	U-238	U-235	U-234
A	0.0	6.53E-07	6.83E-09	4.12E-11	6.60E-07	98.9591%	1.0347%	0.0062%
	3.0	9.61E-07	2.68E-08	7.29E-11	9.88E-07	97.2788%	2.7138%	0.0074%
	5.5	8.86E-07	1.79E-08	4.88E-11	9.04E-07	98.0182%	1.9764%	0.0054%
	8.2	8.95E-07	2.15E-08	5.32E-11	9.17E-07	97.6437%	2.3505%	0.0058%
	13.4	1.18E-06	2.36E-08	5.86E-11	1.21E-06	98.0330%	1.9622%	0.0049%
	16.2	9.25E-07	1.52E-08	5.99E-11	9.40E-07	98.3727%	1.6209%	0.0064%
	18.6	1.18E-06	1.26E-08	6.97E-11	1.19E-06	98.9327%	1.0615%	0.0059%
	21.3	1.21E-06	2.73E-08	6.29E-11	1.24E-06	97.7942%	2.2008%	0.0051%
B	0.0	1.13E-07	9.98E-09	5.12E-12	1.23E-07	91.9022%	8.0937%	0.0042%
	2.4	1.04E-07		4.16E-12				
	5.2	1.22E-07	9.98E-09	7.05E-12	1.32E-07	92.4486%	7.5460%	0.0053%
	7.9	1.19E-07	1.16E-08	1.02E-11	1.31E-07	91.1610%	8.8312%	0.0078%
	10.7	1.58E-07	1.52E-08	9.13E-12	1.73E-07	91.2047%	8.7900%	0.0053%
	13.1	2.03E-07	7.88E-09	1.55E-11	2.11E-07	96.2529%	3.7398%	0.0074%
	15.8	1.46E-07	3.68E-09	6.41E-12	1.50E-07	97.5414%	2.4544%	0.0043%
	18.3	1.43E-07	1.05E-08	1.63E-11	1.54E-07	93.1529%	6.8365%	0.0106%
	21.0	1.79E-07	7.36E-09	1.04E-11	1.86E-07	96.0470%	3.9474%	0.0056%
C	0.0	5.34E-07	5.73E-08	2.79E-11	5.91E-07	90.3091%	9.6862%	0.0047%
	3.0	4.53E-07	2.42E-08	2.72E-11	4.78E-07	94.9339%	5.0604%	0.0057%
	6.1	3.34E-07	1.94E-08	1.76E-11	3.54E-07	94.4965%	5.4986%	0.0050%
	8.2	5.07E-07	1.26E-08	2.82E-11	5.20E-07	97.5684%	2.4262%	0.0054%
	11.0	5.43E-07		2.63E-11				
	13.4	8.65E-07	2.15E-08	4.29E-11	8.87E-07	97.5656%	2.4296%	0.0048%
	16.2	6E-07	1.21E-08	2.98E-11	6.12E-07	98.0196%	1.9756%	0.0049%
	18.9	4.65E-07		3.4E-11				
	21.3	6.09E-07		3.12E-11				
	21.3	5.76E-07	1.26E-08	2.82E-11	5.88E-07	97.8520%	2.1432%	0.0048%
D	0.0	4.86E-07	2.73E-08	3.16E-11	5.14E-07	94.6741%	5.3198%	0.0061%
	2.4	3.64E-07	1.31E-08	2E-11	3.77E-07	96.5113%	3.4834%	0.0053%
	5.2	3.88E-07		2.4E-11				
	7.9	3.4E-07		2.37E-11				
	10.7	2.74E-07		2.16E-11				
	13.4	3.55E-07		2.15E-11				
	15.8	3.04E-07		2.35E-11				
	18.6	6.38E-07		5.25E-11				
	21.3	3.34E-07		3.7E-11				
	21.3	5.25E-07	1.47E-08	2.71E-11	5.40E-07	97.2693%	2.7257%	0.0050%